VGV optimization for performance

Sara Ling and Ted Sönne

Thesis for the Degree of Master of Science

Division of Thermal Power Engineering
Department of Energy Sciences
Faculty of Engineering, LTH
Lund University
P.O. Box 118
SE-221 00 Lund
Sweden

VGV optimization for performance

Thesis for the Degree of Master of Science

Division of Thermal Power Engineering

Department of Energy Sciences
By

Sara Ling
Ted Sönne

LUND
UNIVERSITY

May 2014
Master Thesis
Department of Energy Sciences
Lund Institute of Technology
Lund University, Sweden

Abstract

Today's market for gas turbines is very competitive and it is important to constantly improve the performance of the engines. It is commonly known that gas turbines have better performance at low ambient temperatures than at high ambient temperatures. One way to counteract the negative influence of a high ambient temperature is to use variable compressor guide vanes. The aim of this thesis is to evaluate the potential of using another way to control these variable guide vanes to enhance the performance of gas turbines at high ambient temperatures. This is done by modelling and calculations complemented with interviews and discussions with employees at Siemens Industrial Turbomachinery.

This master thesis consists of several studies that together form a foundation to build an improved control algorithm from. In the first study of this thesis the compressor turbine performance at different physical shaft-speeds is evaluated. The second study shows how the gas turbines react when the ambient temperature is varied. In the third study the variable guide vanes are altered to find the most suitable way to control them. The fourth study studies the most promising positions, from the third study, with consideration to the effects from the secondary air system. The fifth study shows how the engine would react to a more opened position of the variable guide vanes when running at part load. In the final study of this thesis, separate controlling of the inlet guide vane and the first stator is evaluated to see if it could increase the performance for SGT-700. In this thesis the effects on surge margin and engine lifespan, as the variable guide vane positions are altered, are also evaluated.

Based on the results in this master thesis SGT-700 is concluded to be running at optimal variable guide vane settings at the tested ambient temperatures. The test of using separate actuators for the inlet guide vane and stator 1 did not result in any improved performance.

The results show that SGT-750 could gain from a more opened position at high ambient temperatures when running on full load. The most promising case at 30°C is an opening of the inlet guide vane of 2.5° relative to today's existing position. This results in an increase in shaft power of 0.5% and an increase in thermal efficiency of 0.1%. The most promising case at 45°C is an opening of the inlet guide vane of 4° relative to today's existing position. This results in an increase in shaft power of nearly 2.9% and an increase in thermal efficiency of 1.1%.

At part load the results show that SGT-750 will benefit from running at a more opened position as long as the aerodynamic shaft-speed is low. As the aerodynamic shaft-speed is increased, the part load performance does no longer benefit from running at a more opened position of the variable guide vanes.

Using these new variable guide vane positions will lead to a decreased surge margin but the decrease in surge margin is considered acceptable. The proposed changes will lead to lower physical shaft-speeds thus lowering the centrifugal stresses. The lowered stresses are positive but will not result in longer service intervals.

Based on the results in this master thesis the recommendation is that further time and resources are devoted to find an improved control algorithm for SGT-750. The biggest potential of improvement is found for engines running at full load at high ambient temperatures. It is also recommended that further investigation is done into the possibility to use a more opened position at part load.

Acknowledgments

This master thesis has been performed at Siemens Industrial Turbomachinery AB in Finspång. It marks the end of our five year education in mechanical engineering at Lunds University.

We would especially like to thank our supervisor at Siemens, Kerstin Tageman, for all help and guidance throughout our work with this thesis. It has been nice to have someone that can answer all questions, from the trickiest to the silliest ones. We would also like to thank our group manager, Lennart Näs who gave us the opportunity to do this study, and the entire RPP department for giving us such a warm welcome. Many employees at Siemens have helped us during this thesis and we thank them all. An extra thank to Sven Axelsson and Ken Flydalen for all the time they have devoted to helping us and explaining this difficult topic.

We would also like to thank our supervisor at Lunds University, Magnus Genrup, who came up with the idea behind this master thesis and helped us with the first contact with Siemens. He is also the person who introduced us to the interesting world of gas turbines and gave us the tools to be a part of it. We would also like to thank Marcus Thern for his help with the structure and design of our report. During our education we have had the pleasure to meet many good teachers and we would like to thank them all.

A final thank to our families and loved ones for all support.

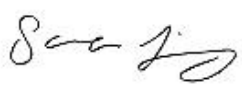

Sara Ling

Ted Sönne

Finspång 2014-04-09

Contents

Nomenclature

Abbreviations

CT	Compressor turbine
IGV	Inlet guide vane
PT	Power turbine
S1	First stator
SAS	Secondary air system
SIT	Siemens Industrial Turbomachinery
STAL	Svenska Turbinfabriksaktiebolaget Ljungström
TIT	Turbine inlet temperature
VGV	Variable guide vane

Latin

A	Area
c_p	Specific heat capacity at constant pressure
c_v	Specific heat capacity at constant volume
C	Absolute velocity
h	Enthalpy
i	Incidence
m	Mass flow
N	Rotational speed
p	Pressure
PR	Pressure ratio
R	Gas constant
RH	Relative humidity
SM	Surge margin

T	Temperature
U	Blade velocity
W	Relative velocity

Greek

α	Absolute flow angle
α'	Absolute blade angle
β	Relative flow angle
γ	Ratio of specific heats
η	Efficiency
ρ	Density
υ	Specific volume

Subscripts

0	Stagnation
1, 2, 3, etc.	Reference planes
a	Ambient
c	Compressor
CT	Compressor turbine
g	Gas (out of the combustion chamber)
m	Mechanical
op	Operational point
S	Surge

1 Introduction

1.1 Siemens Industrial Turbomachinery AB

In 1913 the two brothers Birger and Fredrik Ljungström founded the company Svenska Turbinfabriksaktiebolaget Ljungström (STAL) in Finspång. Already during their first year they received an order for a steam turbine from London. About 40 years later STAL manufactured their first gas turbine (Siemens Industrial Turbomachinery AB, 2013).

In the late 1950s STAL merged with AB de Laval Ångturbin, who had been manufacturing turbines since the late 1900s and held a lot of patents, forming STAL-LAVAL Turbin AB. During the following years the company changed owner and name several times until 2003 when Siemens acquired the company and formed Siemens Industrial Turbomachinery (SIT) AB (Siemens Industrial Turbomachinery AB, 2013). Today SIT employs about 2800 persons (Siemens Industrial Turbomachinery AB, 2009).

The gas turbines designed in Finspång are SGT-500, SGT-600, SGT-700, SGT-750 and SGT-800 (Siemens AG, 2013). SGT-750 is the newest gas turbine designed in Finspång, launched officially in November 2010 (Siemens AG, 2014). Gas turbines made in Finspång can be found in over 100 different countries all over the world (Siemens Industrial Turbomachinery AB, 2013).

1.2 Background

Gas turbines consist primarily of three parts; a compressor, a combustion chamber, also referred to as a combustor, and a turbine. Air enters the compressor where the pressure is increased. After the compression the air is mixed with fuel in the combustion chamber and lightened before it continues into the turbine where the released energy is used to create a shaft work, see Fig. 1-1. The excess energy that is not required to drive the compressor can be used for power generation or propulsion through a shaft.

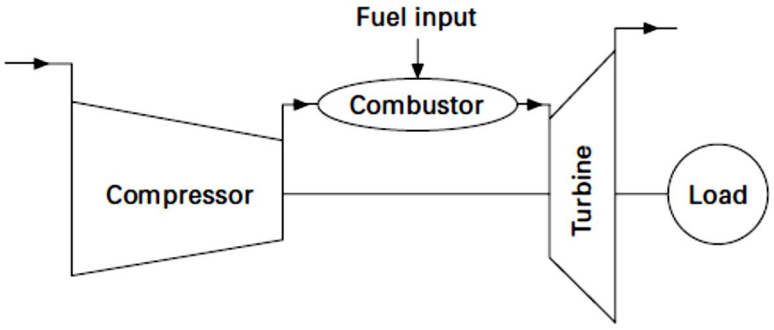

Fig. 1-1 Schematic layout of a single-shaft gas turbine (Razak, 2007, p. 2)

The performance of a gas turbine is dependent on the properties of the ambient air that is drawn into the compressor. When designing a gas turbine the ambient conditions must be estimated. Whenever the gas turbine runs on conditions not matching the design conditions it is said to be running off-design. A gas turbine running off-design often lacks in performance compared to when running under design conditions.

SIT sells gas turbines all over the world and the conditions on site vary from place to place, especially the ambient temperature. High ambient temperature will lead to a decrease in efficiency and power output of the engine (Brun & Kurz, 2000, p. II-2-8). A way to compensate for the loss in efficiency would be desirable, not only for the economical aspect but also for the sake of our environment. An increase in thermal efficiency will lead to lower emissions of carbon dioxide which is important to reduce global warming.

When the ambient temperature increases the compressor aerodynamic shaft-speed will decrease, thereby disturbing the flow in both the compressor and the turbine. One way to control the shaft-speed is by using variable guide vanes (VGVs) to control the intake area and air velocity.

The VGVs consist of several rows, starting with the inlet guide vanes (IGVs) and thereafter continuing with variable stators in the first stages of the compressor. The rows are often controlled by one single armature but it may also be possible to control each row separately to achieve an even better performance.

1.3 Objectives

The purpose of this thesis is to analyse the potential of having a more advanced control algorithm of the VGVs to obtain an enhanced gas turbine performance. The focus will be on improvements at SIT's gas turbines SGT-700 and SGT-750 at high ambient temperatures.

1.3.1 Problem definition

The following questions will be analysed and answered in this thesis:

- Is there a potential for enhanced performance when altering the VGVs at high ambient temperatures? What will be the impact on SGT-700 and SGT-750?

If there is a potential improvement the following question will be investigated:

- What will be needed to assure surge margin?

If there is no potential improvement the following question will be investigated:

- Is there a potential for enhanced performance by having different actuators for the different VGVs?

1.4 Limitations

Many parameters are affected in the gas turbine when the position of the VGVs is altered. To investigate them all would be too extensive for this thesis and therefore some limitations are established. The following areas will not be investigated:

- Emission tuning with VGV
- Lifing detailed analysis
- Detailed control description
- Transient analysis
- Other gas turbine models than SGT-700 and SGT-750
- Arctic and normal matched gas turbines

1.5 Methodology

The methodology chosen for this thesis is modelling since there is not enough published material to only do a mapping of existing knowledge. In addition the resources and time are not sufficient to support experimental studies. Gathered information from a literature survey along with interviews with employees at SIT has been used as a complement and validation of the results. Several in-house programs have been used for the modelling.

GTPerform is used to model the performance of the complete gas turbine. Since the compressor characteristic is sensitive to VGV-position, GTPerform is not sufficient to model the compressor if the VGV-position is altered. The same applies for the turbines if the ratios of the secondary air system (SAS) flow are altered.

HT0300 is used to model the compressor. HT0300 does not have the ability to estimate the impact on the complete cycle. Therefore an iterative process is needed using GTPerform to estimate the behaviour of the complete cycle and thereafter transferring the data as input to HT0300, where the compressor behaviour can be estimated. The results are then taken back to GTPerform to correct the behaviour of the compressor and rerun the evaluation of the cycle. This sequence will be continued until convergence is reached resulting in a good estimate of the compressor behaviour and the performance of the total cycle.

Merlin is used as a user interface coupling and handling the data transfer between 2ndFlow and MAC 1/Beta2. 2ndFlow is used to calculate the behaviour of the SAS as the pressure in the compressor changes due to different VGV-positions. MAC 1/Beta 2 is used to calculate the flow in the compressor turbine (CT) and power turbine (PT). The difference between the two programs is that MAC1 performs mean line calculations while Beta2 performs the calculations in two dimensions. Beta2 is more accurate but the calculation time is larger compared to using MAC1. Merlin is used to scale the parameters correctly between 2ndFlow and MAC1/Beta2 and combining them into an iterative loop. The iteration loop using MAC1 is shown in Fig. 1-2.

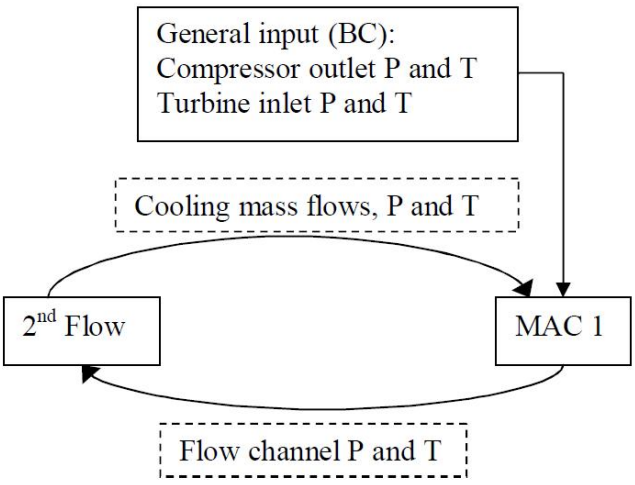

Fig. 1-2 Description of the iteration loop between MAC 1 and 2ndFlow. Merlin works as a user interface between the two programs, scaling, handling data and presenting the results in a user friendly way (Flydalen, 2011, p. 44)

This thesis will be focusing on two hypotheses:

- An opening of the VGVs is a suitable way to reduce physical shaft-speed and enhance compressor efficiency without having a clearly negative impact on the total gas turbine performance or loosing sufficient surge margin
- A closing of the VGVs is a suitable way to enhance CT efficiency without having a clearly negative impact on the total gas turbine performance or endangering the lifespan of the gas turbine

The hypotheses will be tried by testing and modelling in several programs provided by SIT. Four cases will be analysed for each gas turbine. The cases are full load and part load, at 75% of full load, at ambient temperatures of 30 and 45°C. As soon as one hypothesis can be proven false for one case, the hypothesis will no longer be tested for that case. Table 1-1 shows a hypothesis matrix that will be updated at the end of every chapter, starting from chapter 4, until all hypotheses are proven either true or false. The aim with this hypothesis matrix is to get a quick overview of the status of each hypothesis. As a hypothesis is proven false or true it is denoted with an F for false or a T for true. Hypothesis still under investigation will be denoted with the notation u.i.

Table 1-1 Hypothesis matrix showing the progress for each hypothesis. A hypothesis proven true will be denoted by a T and a hypothesis proven false will be denoted by an F. Hypothesis under investigation will be denoted u.i.

	30°C/100%	45°C/100%	30°C/75%	45°C/75%
SGT-750/Open	u.i.	u.i.	u.i.	u.i.
SGT-750/Close	u.i.	u.i.	u.i.	u.i.
SGT-700/Open	u.i.	u.i.	u.i.	u.i.
SGT-700/Close	u.i.	u.i.	u.i.	u.i.

1.6 Outline of the thesis

Chapter 2 covers the theory needed to understand the results presented in latter chapters. The reader is assumed to have basic knowledge of thermodynamics, aerodynamics and gas turbine performance. The most basic theory is therefore explained shortly or excluded.

Chapter 3 gives a description of the two gas turbines this thesis focuses on, SGT-700 and SGT-750. Here the specific models are described briefly to give the reader a basic understanding of how these gas turbines are designed.

Starting from chapter 4 and ending at chapter 8 the chapters follow the same structure. Each chapter starts with a general introduction to the analysis and is thereafter divided into three sections. The first section presents the results for SGT-700, the second section presents the results for SGT-750 and the third section contains a summary and a comparison of the results from the two earlier sections.

Chapter 4 contains a mapping of the CT efficiency as a function of physical shaft-speed for the two engines. The mapping is done using GTPerform. Since the VGV-position is controlled by the aerodynamic shaft-speed in GTPerform, which is coupled to the physical shaft-speed, this mapping can be seen as a mapping of the CT efficiency as a function of VGV-position. The sections presenting the results for each gas turbine model are further divided into two parts, one for each temperature.

Chapter 5 contains an evaluation of how the ambient temperature affects the gas turbine performance. Since the two gas turbines control the VGV-position as a function of aerodynamic shaft-speed it is important to distinguish the effects that occur due to pure physics from those occurring due to the control of the VGVs. In this evaluation GTPerform and HT0300 are used in an iterative process to evaluate the performance at different operating conditions as the VGVs are kept at a fixed position.

In chapter 6 several different VGV-positions are tested for ambient temperatures of 30 and 45°C. Both opening and closing relative to today's existing position is tested to distinguish the cases with potential. In this analysis GTPerform and HT0300 are used in an iterative process.

Chapter 7 contains an analysis of how the physical shaft-speed affects the lifespan of the two gas turbine models. The conclusions are drawn based on interviews with employees at SIT.

Chapter 8 contains an analysis of how the SAS flow is affected by the new VGV-positions and how the new SAS flow affects the gas turbine performance. In this analysis GTPerform and Merlin are used in an iterative process. The results are then verified by running HT0300.

Chapter 9 contains an analysis of how the surge margin is affected by the new VGV-positions. HT0300 is used to estimate the numerical surge margin and to estimate the pressure ratios in the compressor stages.

In chapter 10 the proposed VGV-positions are tested at part load. This gives the possibility to see if the proposed control algorithm can be used with the aerodynamic shaft-speed as the only input. This study is performed through an iterative process between GTPerform and Merlin.

Chapter 11 contains an analysis of how separate controlling of the IGV and stator 1 (S1) affects the performance for SGT-700 at 30°C. The chapter is divided into two sections. In the first section several combinations of angles are tested using HT0300 and GTPerform without considering the effects from SAS. In the second section the most promising combinations are evaluated using Merlin and GTPerform to catch the effects from SAS.

Chapter 12 contains conclusions and recommendations. Chapter 13 contains some guidelines for future work at SIT. The bibliography is presented in chapter 14.

This master thesis contains three appendixes. Appendix A contains a discussion about new ways to measure surge margin during operation. Appendix B contains three suggestions for an improved control algorithm based on the results in this master thesis. Appendix C discusses how the CT efficiency is evaluated in GTPerform and Merlin as the ambient temperature and physical shaft-speed is altered.

2 Theory

2.1 Gas turbine configuration

The gas turbine configuration varies depending on the application of the gas turbine. The components it consist of, how they are linked together and number of shafts all varies. In chapter 1.2 on p. 1 the components; compressor, combustions chamber and turbine were mentioned. These components are always present and together they form the gas generator. An additional PT as well as other components such as heat-exchangers, intercoolers and reheaters could also be added to improve performance.

2.1.1 Single-shaft and twin-shaft engines

A single-shaft gas turbine was shown in Fig. 1-1 on p. 1. It consists of a compressor, a combustion chamber and a turbine. The single-shaft gas turbine is best suited for applications with fixed shaft-speed. The single-shaft configuration also gives a protection against over-speeding because of the drag of the compressor that gives a high inertia (Saravanamuttoo, et al., 2009, pp. 5-6). Another configuration that is common in the industry is the twin-shaft gas turbine. Here the turbine has been divided into two parts. The first turbine, the CT, drives the compressor and the second turbine, the PT, drives the load. Twin-shaft gas turbines are best suited for varied speed or load (Saravanamuttoo, et al., 2009, p. 6). A twin-shaft gas turbine is also easier to start since only the shaft with compressor and CT needs to be turned and not the PT and generator (Saravanamuttoo, et al., 2009, p. 7). A twin-shaft configuration is shown in Fig. 2-1. Since both the SGT-700 and SGT-750 are twin-shaft engines this configuration will be assumed in the following chapters unless otherwise noted.

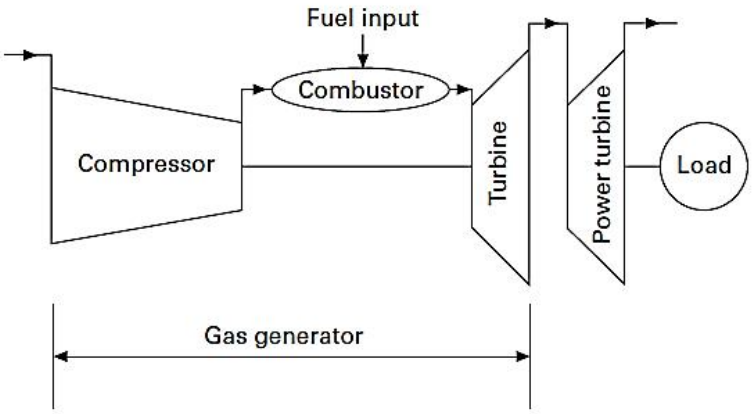

Fig. 2-1 Schematic layout of a twin-shaft gas turbine (Razak, 2007, p. 4)

2.2 Velocity triangles

A common way to describe the flow in a gas turbine is to use velocity triangles. The notations differs in literature but in this master thesis the absolute velocity is denoted by C, the relative velocity is denoted by W and the blade speed is denoted by U. Absolute angles are denoted by α

and relative angles by β. Fig. 2-2 shows the flow through a stage in a compressor and the representative velocity triangles.

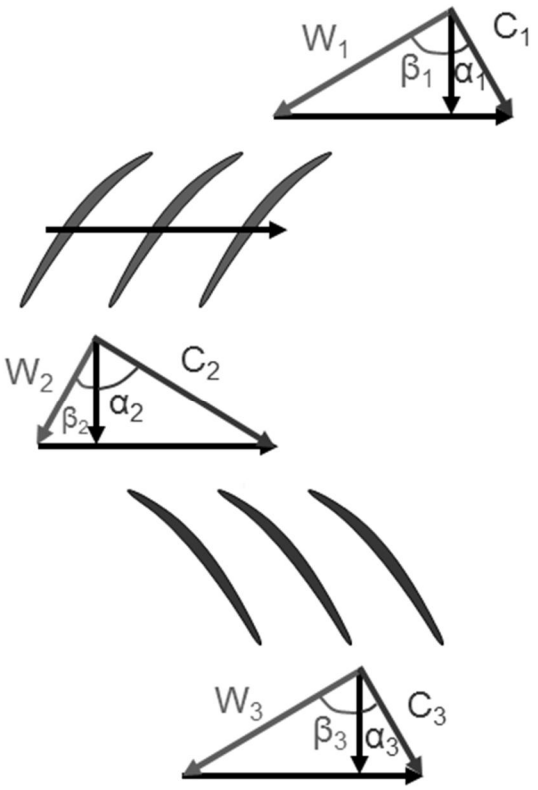

Fig. 2-2 The flow through a compressor stage with representative velocity triangles (Courtesy to Magnus Genrup)

The velocity triangles show the relationship between the flow angles, flow speed and the blade speed. If non-dimensional parameters are used the velocity triangles can be expressed as Mach numbers, coupling the velocity triangles to the characteristics of the components.

2.3 Incidence

A fluid approaches a blade with an inlet angle (α_1). When it passes by the blade it gets deflected and leaves with an exit angle (α_2) as previously shown in Fig. 2-2. The deflection of the fluid is the way to transfer energy between the fluid and the blade. The blade has an inlet angle (α_1'). The difference between the two inlet angles is called incidence (i) (Moustapha, et al., 2003, p. 13), see Equ. (2-1) .

$$i = \alpha_1 - \alpha_1' \qquad (2\text{-}1)$$

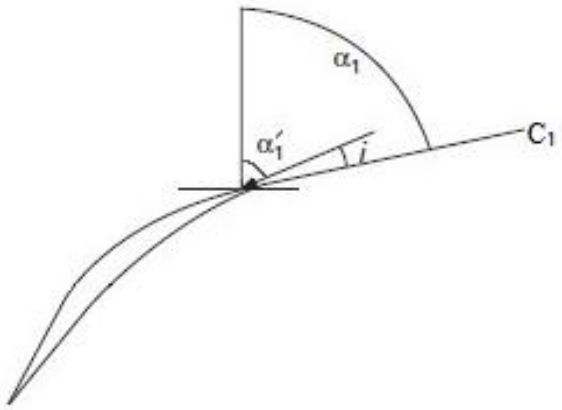

Fig. 2-3 Schematic sketch of the definition of incidence

Fig. 2-3 shows a schematic sketch of the definition of incidence. If the incidence differs from the design value it might lead to separation in the boundary layers of the blades and in the worst case cause stall or surge. It is therefore crucial to keep the incidence within acceptable levels. A rotating blade will not see the actual velocity but the relative velocity. Here the incidence is defined as the difference in relative flow angle (β_1) and α_1' (Moustapha, et al., 2003, p. 13). The rotational speed is affecting the velocity angles and thereby the performance of the engine.

The angle of the fluid is determined by the ratio between the axial component and the swirl component of the fluid. As the shaft-speed varies the swirl component of the relative velocity will vary as well. One way to counteract this is to vary the VGV-position thereby adding or removing swirl, keeping the incidence at design level. With the VGVs it is also possible to affect the shaft-speed thus counteracting the influence of other parameters, for example the ambient temperature. The velocity profile will vary over the height of the blade leading to a variation of α_1 along the blade height. The blades are twisted along the height to compensate for this and keep the incidence at acceptable levels at all radii.

Another phenomenon that affects the losses due to incidence is the Mach number. The relation between the Mach number and the incidence interval that the compressor can work in without too big losses is shown in Fig. 2-4. As can be seen in this figure the incidence interval that gives a predefined loss coefficient gets smaller and the minimum loss increases as the Mach number increases. The Mach number decreases as the temperature rises due to the increase in speed of sound. This implies that the last stages of a compressor have lower Mach number and therefore a bigger incidence interval to work in than the first stages (Saravanamuttoo, et al., 2009, pp. 254-255).

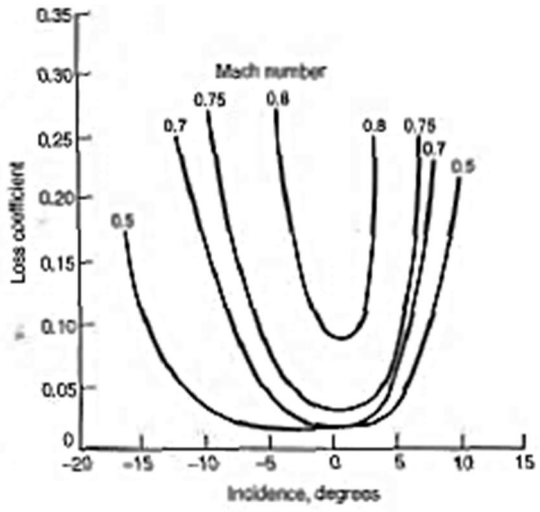

Fig. 2-4 Loss coefficient as a function of incidence angle and Mach number. The values on the axes are only representable for the particular measurement but the trends are valid for all compressors (Saravanamuttoo, et al., 2009, p. 255)

For rotating parts the Mach number will increase with radius since the blade speed, and thereby the relative velocity of the fluid, increases along with the radius, see Fig. 2-5. This implies that the tip of a rotor blade has a narrower incidence interval to work in than the hub of the same blade. For the stator it is the hub that encounters the highest Mach number, under the assumption that the enthalpy rise is constant over the blade radius, since the tangential velocity is larger here due to the need of higher deflection in the hub to satisfy the constant work assumption. The Mach numbers in the stator are usually low compared to those in the rotor (Saravanamuttoo, et al., 2009, pp. 255-256).

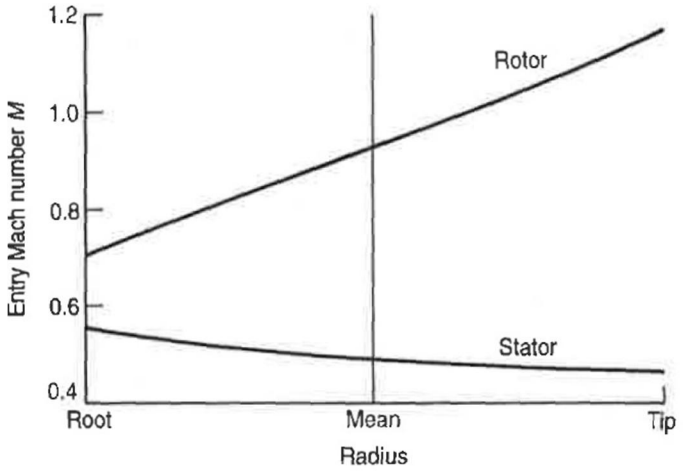

Fig. 2-5 Typical Mach numbers at different radii of the stator and the rotor (Saravanamuttoo, et al., 2009, p. 255)

2.4 Dimensionless parameters

Non-dimensional parameters can be used to describe the performance of a gas turbine. The parameters are formed into so called dimensionless groups even though the groups usually are not truly dimensionless. In literature there is no definite way to form these dimensionless groups and the formation varies from case to case. The name of these groups also varies in literature. Aerodynamic-, non-dimensional- and corrected parameters are all common names of these groups.

At SIT the standard is to correct the values according to ISO values (Tageman, 2014). In this thesis, the corrected values will be referred to as aerodynamic shaft-speed and corrected parameters and should not be confused with the dimensionless groups used in literature. In the theory part of this thesis, these groups will be referred to as non-dimensional parameters.

2.5 Stagnation properties

In gas turbine calculations it is common to use stagnation properties. If stagnation properties are used, it simplifies the calculations since they consider both the change in static enthalpy and the change in velocity and thereby change in kinetic energy. The speed alteration in a gas turbine is major and the kinetic energy alteration is therefore too big to neglect.

2.5.1 Stagnation enthalpy

Stagnation enthalpy is the total enthalpy a fluid would have if it, adiabatically and without work transfer, was brought to zero speed. If a steady flow is considered to go through a nozzle adiabatically without any losses in potential energy the energy equation would become as in Equ. (2-2) where h_0 is the stagnation enthalpy, h is the static enthalpy and C the velocity before the deceleration (Saravanamuttoo, et al., 2009, p. 55).

$$(h_0 - h) + \frac{1}{2}(0 - C^2) = 0 \qquad (2\text{-}2)$$

Thus the stagnation enthalpy is the sum of the static enthalpy and the kinetic energy ($C^2/2$) as can be seen in Equ. (2-3) (Saravanamuttoo, et al., 2009, p. 55).

$$h_0 = h + C^2/2 \qquad (2\text{-}3)$$

2.5.2 Stagnation temperature

If the fluid is considered to be a perfect gas the relationship between enthalpy and temperature can be described as in Equ. (2-4) (Saravanamuttoo, et al., 2009, p. 55).

$$h = c_p T \quad (2\text{-}4)$$

Thus, using Equ. (2-3), the stagnation temperature (T_0) can be expressed as in Equ. (2-5) where the first term is called static temperature (T) and the second term is called dynamic temperature ($C^2/2c_p$) (Saravanamuttoo, et al., 2009, p. 55).

$$T_0 = T + C^2/2c_p \quad (2\text{-}5)$$

2.5.3 Stagnation pressure

If the deceleration of the fluid is also reversible, i.e. the deceleration is isentropic, the stagnation pressure (p_0) is defined by the relationship in Equ. (2-6) (Saravanamuttoo, et al., 2009, p. 56) where the ratio of specific heat (γ) is defined as the ratio between c_p and c_v.

$$\frac{p_0}{p} = \left(\frac{T_0}{T}\right)^{\gamma/(\gamma-1)} \quad (2\text{-}6)$$

2.6 Compressor characteristic

The behaviour of the compressor is explained and described by a compressor characteristic, sometimes also referred to as a compressor map. The compressor characteristic is a chart where pressure ratio and compressor efficiency are plotted as a function of mass flow. Points with the same aerodynamic shaft-speed are then formed together to lines, so called constant speed lines.

To enable application to all inlet conditions mass flow, pressure ratio and shaft-speed must be geometrically non-dimensional. This will make every point in the compressor map fixed. For a given corrected mass flow and pressure ratio only one aerodynamic shaft-speed and one compressor isentropic efficiency is possible. This is achieved when (Sjödin, 2013, p. 43):

1) The Mach numbers are identical
2) The velocity triangles are identical
3) The Reynolds numbers are identical

Fig. 2-6 shows an example of a compressor characteristic. Here the vertical lines are constant speed lines and the dotted lines form so called efficiency islands. The isentropic efficiency is constant along the border of an efficiency island. In this figure the surge line is plotted. Surge is further described in section 2.10 on p. 24. The compressor characteristic varies for different compressors and geometries. It is also common to have non-dimensional mass flow on the abscissa instead of non-dimensional flow. Stagnation properties can also be used.

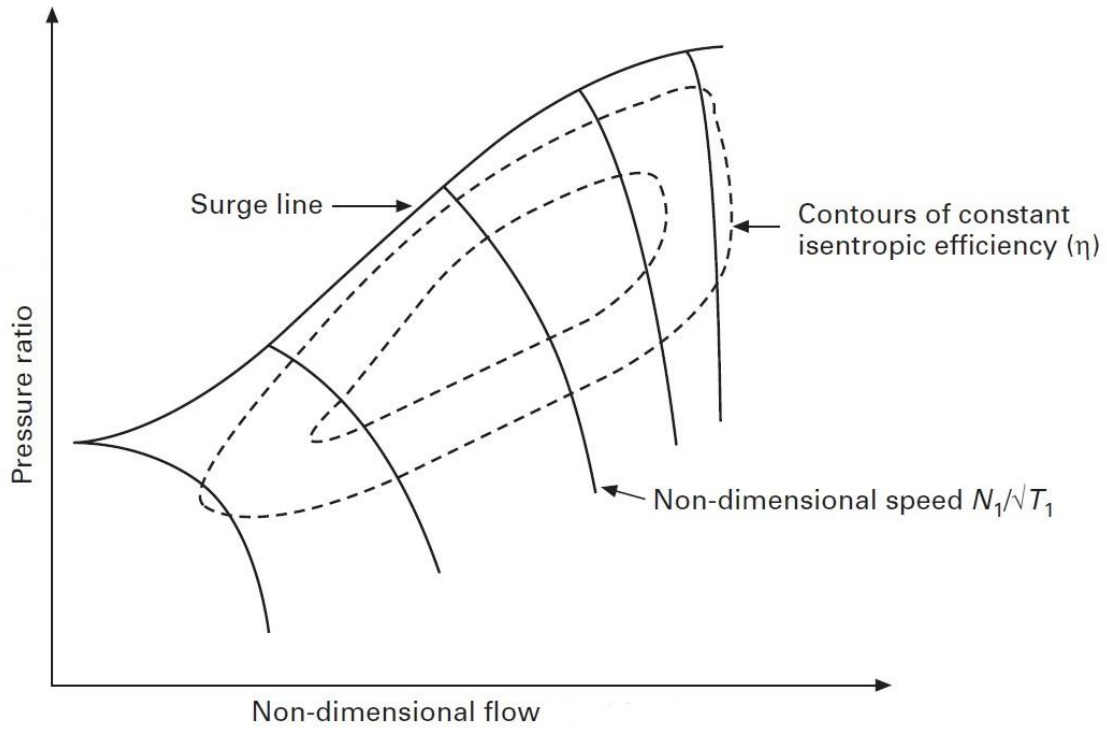

Fig. 2-6 Compressor characteristic. The vertical lines are constant speed lines and the dotted lines form efficiency islands. The surge line marks the limit where the compressor runs into surge (Razak, 2007, p. 175)

Due to the small influence and great theoretical complexity, the effect of the Reynolds number is neglected. By assuming that γ is constant the influence of the Mach number can be ignored (Sjödin, 2013, p. 45). The effects of an increase in ambient conditions are minor and therefore the results can be trusted even though the ambient conditions changes. If the medium would be changed, the impact of the errors would be large and the results would not be trustable (Sjödin, 2014).

The compressor characteristic is unique for a fixed geometry. If the VGV-position is altered the characteristic will no longer be valid since the intake area of the engine has changed, thereby changing the geometry of the engine (Walsh & Fletcher, 2004, p. 172). There are two ways to deal with this problem. Either separate characteristics are made for different VGV-positions or a scaling factor is used to scale the map when the VGV-positions are changed (Sjödin, 2013, p. 50). Using a scaling factor will be cheaper and less time consuming but might not be as accurate as making separate characteristics (Tageman, 2014).

SIT uses different approaches for different gas turbines. For single-shaft engines several characteristics are made for different VGV-positions. For twin-shaft engines the VGV-position is controlled as a function of aerodynamic shaft-speed, i.e. for one given aerodynamic shaft-speed only one VGV-position is used. It is therefore unnecessary to make more characteristics for

different VGV-positions since the control system will prevent them from occurring. If the control algorithms were to be changed new compressor characteristic would have to be generated (Tageman, 2014).

A compressor can operate anywhere in the compressor map but when it is connected to a turbine it will be restricted due to the influence of the turbine. The interaction between the components is described in the following section.

2.7 Component matching

The compressor, CT and PT interacts with each other and the reaction of one component, for example to higher ambient temperature, will also affect the other components. All off-design conditions will affect the components and thereby the interaction in different ways. The components therefore needs to be matched together and the interaction between the components is referred to as component matching (Razak, 2007, pp. 174-175).

The compressor and the CT have a mechanical coupling i.e. the shaft-speed is the same for the two components. The PT does not have a mechanical coupling with the two other components but the mass flow from the CT goes into the PT and therefore the PT and CT is said to have an aerodynamically coupling (Razak, 2007, p. 181). The pressure ratio that is available to the PT also depends on the pressure ratios of the CT and compressor (Saravanamuttoo, et al., 2009, p. 466).

To visualize the area in which the gas turbine operates, the characteristic of the compressor and turbines are normally plotted on a non-dimensional basis with non-dimensional shaft-speed, non-dimensional mass flow, pressure ratio and isentropic efficiency (Razak, 2007, p. 176).

The matching process is normally calculated by computers (Razak, 2007, p. 185) but Saravanamuttoo et al. (2009, pp. 463-469) describes how the calculation could be done by hand. Assumptions of turbines in series are presented in section 2.7.1 on p. 15. Thereafter the calculations are reproduced, first for a gas turbine with unchoked PT in section 2.7.2 on p. 17 and then for a gas turbine with choked PT in section 2.7.3 on p. 20. The numbering of the gas turbine sections used in this chapter is shown in Fig. 2-7.

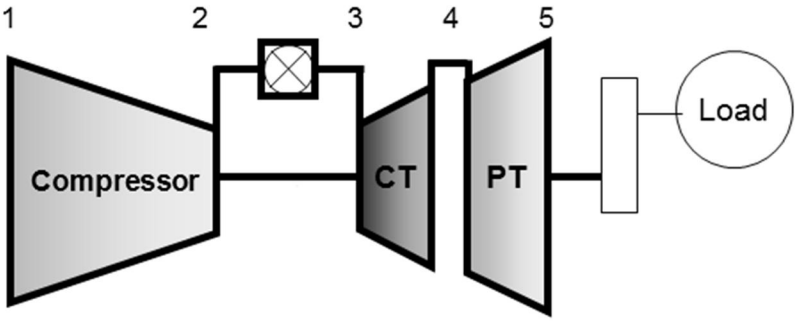

Fig. 2-7 Numbering of the sections in a twin-shaft gas turbine. 1 refers to the intake of the compressor, 2 to the outlet of the compressor, 3 to the intake of the CT, 4 to the intake of the PT and 5 to the exhaust of the PT (Courtesy to Magnus Genrup)

In these calculations the ambient conditions have been assumed known and the inlet and exhaust losses have been assumed negligible. The combustion chamber pressure loss has been assumed a fixed percentage of the compressor delivery pressure. The mass flow through the engine is assumed constant.

2.7.1 Assumptions of turbines in series

Turbines normally experience merely minor changes in non-dimensional mass flow ($\frac{m\sqrt{T_0}}{p_0}$) when the non-dimensional shaft-speed ($\frac{N}{\sqrt{T_0}}$) is altered. In general other components restrict the area in which the turbine could operate. If these assumptions are made the mass flow function could be assumed as a single line in the turbine characteristic as seen in Fig. 2-8 (Saravanamuttoo, et al., 2009, p. 456) instead of several lines as in Fig. 2-12 on p. 23. At SIT $\frac{m\sqrt{T_0}}{p_0}$ is referred to as flow number.

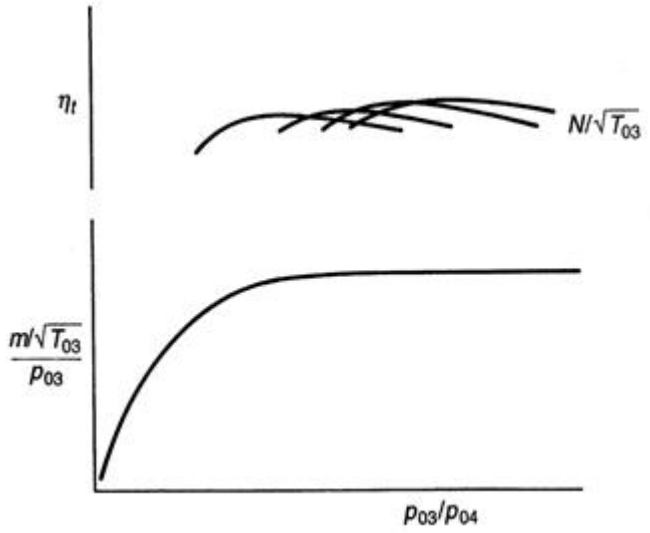

Fig. 2-8 Turbine characteristics. The top chart shows the isentropic efficiency (η_t) as a function of pressure ratio ($\frac{p_{03}}{p_{04}}$) and relative non-dimensional shaft-speed ($\frac{N}{\sqrt{T_{03}}}$). The bottom chart shows the non-dimensional mass flow ($\frac{m\sqrt{T_{03}}}{p_{03}}$), assumed to be independent of $\frac{N}{\sqrt{T_{03}}}$, as a function of $\frac{p_{03}}{p_{04}}$ (Saravanamuttoo, et al., 2009, p. 457)

In Fig. 2-8 the variation in CT efficiency at a given pressure ratio is minor. If the efficiency is assumed to be a mean value at any given pressure ratio, $m\sqrt{T_{04}}/p_{04}$ becomes a function of only $m\sqrt{T_{03}}/p_{03}$ and p_{03}/p_{04} according to Equ. (2-7) where $\sqrt{\frac{T_{04}}{T_{03}}} = \sqrt{1-\frac{\Delta T_{034}}{T_{03}}}$ and $\frac{\Delta T_{034}}{T_{03}} = \eta_t\left[1-\left(\frac{1}{p_{03}/p_{04}}\right)^{(\gamma-1)/\gamma}\right]$.

$$\frac{m\sqrt{T_{04}}}{p_{04}} = \frac{m\sqrt{T_{03}}}{p_{03}} * \frac{p_{03}}{p_{04}} * \sqrt{\frac{T_{04}}{T_{03}}} \qquad (2\text{-}7)$$

If this calculation is performed for all points on the line in the CT characteristic a new line can be added that illustrates $m\sqrt{T_{04}/p_{04}}$ as a function of $m\sqrt{T_{03}/p_{03}}$ and p_{03}/p_{04} (Saravanamuttoo, et al., 2009, p. 468). This line is illustrated in Fig. 2-9.

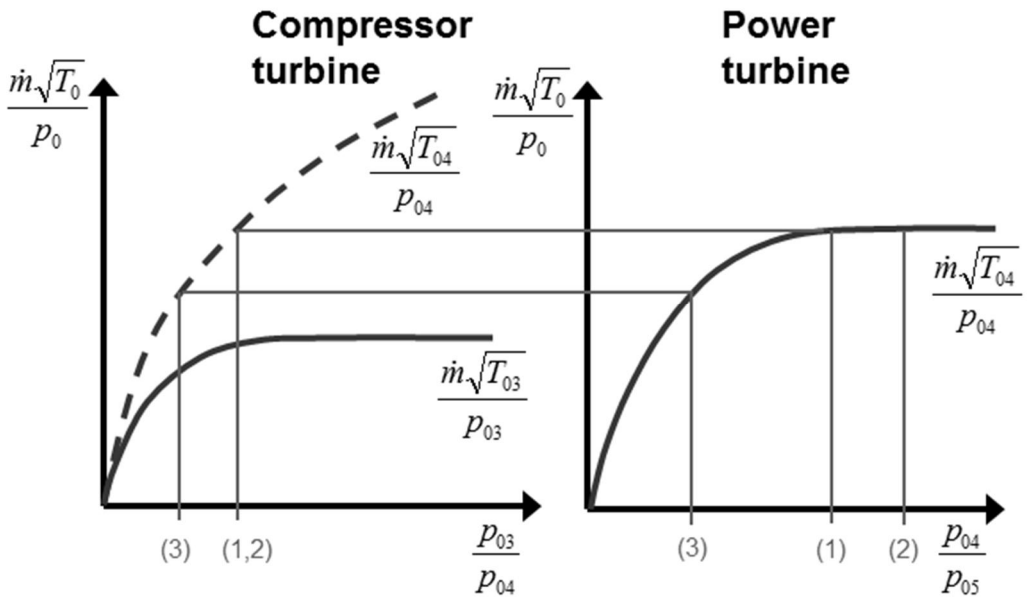

Fig. 2-9 The left turbine characteristics illustrates non-dimensional mass flow into the CT ($\frac{\mathrm{m}\sqrt{\mathrm{T}_{03}}}{\mathrm{p}_{03}}$) and out of the CT ($\frac{m\sqrt{T_{04}}}{p_{04}}$) as functions of CT pressure ratio ($\frac{\mathrm{p}_{03}}{\mathrm{p}_{04}}$). The right turbine characteristic illustrates $\frac{m\sqrt{T_{04}}}{p_{04}}$ as function of PT pressure ratio ($\frac{\mathrm{p}_{04}}{\mathrm{p}_{05}}$). The dashed lines illustrate how the aerodynamic coupling affects the interaction between the two components and how the swallowing capacity of the PT restricts the non-dimensional mass flow through the CT (Courtesy to Magnus Genrup)

Fig. 2-9 illustrates how the aerodynamic coupling between the CT and PT affects the interaction between the components. In points (1) and (2) the PT is choked which causes the CT to operate on a fixed non-dimensional point even if the pressure ratio over the PT is raised (Saravanamuttoo, et al., 2009, pp. 468-469).

When the PT is unchoked the CT will operate with a fixed non-dimensional outlet mass flow and pressure ratio for each PT pressure ratio. This is illustrated by point (3). Therefore the CT outlet pressure, and as a result also the non-dimensional mass flow, always depends on the PT's swallowing capacity (Saravanamuttoo, et al., 2009, pp. 468-469).

2.7.2 Calculations for twin-shaft gas turbine with unchoked PT

In this section calculation for a gas turbine with unchoked PT is reproduced from Saravanamuttoo et al. (2009, pp. 463-467).

1. The first step is to choose a constant non-dimensional shaft-speed line in the compressor characteristic which the calculations should be executed for. Thereafter a point on that line is chosen which will give the pressure rise over the compressor ($p_{02}\ /p_{01}$), the

compressor non-dimensional mass flow ($m\sqrt{T_{01}}/p_{01}$) and the compressor efficiency (η_c). An example of a compressor characteristic is shown in Fig. 2-10

2. The non-dimensional compressor temperature rise ($\Delta T_{012}/T_{01}$) can then by calculated from Equ. (2-8)

$$\Delta T_{012} = \frac{T_{01}}{\eta_c}\left[\left(\frac{p_{02}}{p_{01}}\right)^{(\gamma-1)/\gamma} - 1\right] \qquad (2\text{-}8)$$

3. The next step is to guess the value of the pressure ratio for the CT (p_{03}/p_{04}) so that the value of CT non-dimensional mass flow ($m\sqrt{T_{03}}/p_{03}$) can be obtained from the CT characteristic. Under the assumption that the non-dimensional mass flow is independent of the non-dimensional shaft-speed, Fig. 2-8 can be used as turbine characteristic

4. The equation for flow compatibility between the compressor and CT can then be used to obtain the temperature rise over compressor and combustion chamber ($T_{03}\ /T_{01}$), see Equ. (2-9)

$$\frac{m\sqrt{T_{03}}}{p_{03}} = \frac{m\sqrt{T_{01}}}{p_{01}} * \frac{p_{01}}{p_{02}} * \frac{p_{02}}{p_{03}} * \sqrt{\frac{T_{03}}{T_{01}}} \qquad (2\text{-}9)$$

5. When $T_{03}\ /T_{01}$is known, the equation for compatibility of shaft-speed for the CT and compressor can be used to calculate the CT non-dimensional shaft-speed ($N\ /\sqrt{T_{03}}$), see Equ. (2-10)

$$\frac{N}{\sqrt{T_{03}}} = \frac{N}{\sqrt{T_{01}}} * \sqrt{\frac{T_{01}}{T_{03}}} \qquad (2\text{-}10)$$

6. When $N\ /\sqrt{T_{03}}$ have been obtained the CT characteristic can be used again to get a value for CT isentropic efficiency (η_{CT})

7. The next step is to calculate the non-dimensional temperature drop over the CT ($\Delta T_{034}/T_{03}$) from Equ. (2-11)

$$\Delta T_{034} = \eta_{CT} T_{03}\left[1 - \left(\frac{1}{p_{03}/p_{04}}\right)^{(\gamma-1)/\gamma}\right] \qquad (2\text{-}11)$$

8. A new value for T_{01}/T_{03} can then be calculated from Equ. (2-12) where η_m is the mechanical efficiency

$$\frac{\Delta T_{034}}{T_{03}} = \frac{\Delta T_{012}}{T_{01}} * \frac{T_{01}}{T_{03}} * \frac{c_{pa}}{c_{pg}\eta_m} \qquad (2\text{-}12)$$

9. If the new value for T_{01}/T_{03} does not agree with the value calculated in step 4, P_{03}/P_{04} needs to be modified and the equations recalculated from step 3 in an iterative process until the values converge

10. When the values are equal, the non-dimensional mass flow out of the CT ($m\sqrt{T_{04}}/p_{04}$) can be calculated from Equ. (2-7)

11. The pressure ratio over the PT (p_{04}/p_a) can then be calculated from Equ. (2-13)

$$\frac{p_{04}}{p_a} = \frac{p_{02}}{p_{01}} * \frac{p_{03}}{p_{02}} * \frac{p_{04}}{p_{03}} \qquad (2\text{-}13)$$

12. p_{04}/p_a can then be used to get a new value for $m\sqrt{T_{04}}/p_{04}$ from the PT characteristic which will have the same shape as the CT characteristics in Fig. 2-8 but with different parameters and values at the axes

13. If the new value for $m\sqrt{T_{04}}/p_{04}$ does not match the value calculated in step 10 a new compressor operating point needs to be selected and the calculation repeated from step 2 until the flows from the two turbines converge

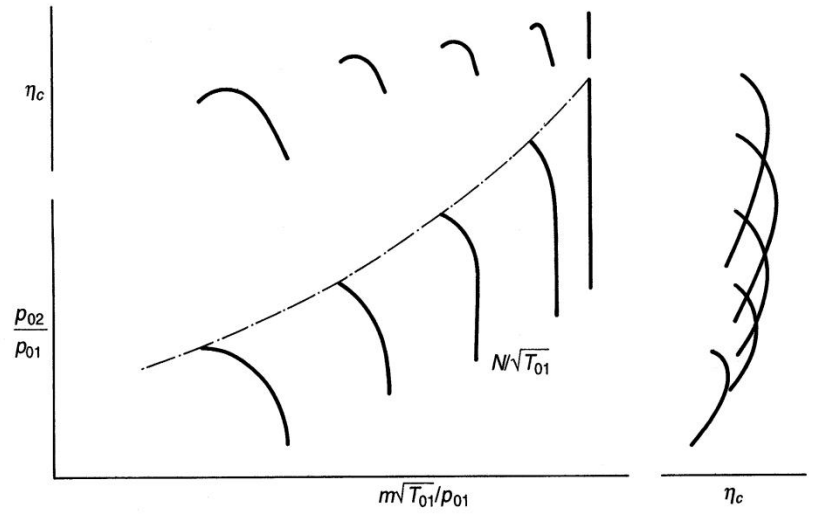

Fig. 2-10 Compressor characteristic. The top chart shows the isentropic efficiency (η_c) as a function of non-dimensional mass flow ($\frac{m\sqrt{T_{01}}}{p_{01}}$). The right chart shows η_c as a function of pressure ratio ($\frac{p_{02}}{p_{01}}$). The left bottom chart shows $\frac{p_{02}}{p_{01}}$ as a function of $\frac{m\sqrt{T_{01}}}{p_{01}}$ and the non-dimensional shaft-speed ($\frac{N}{\sqrt{T_{01}}}$) (Saravanamuttoo, et al., 2009, p. 456)

2.7.3 Calculations for twin-shaft gas turbine with choked PT

In this section calculation for a gas turbine with choked PT is reproduced from (2009, pp. 468-469)

1. When the PT is chocked the CT pressure ratio and the non-dimensional mass flow through CT and PT is known, see. Fig. 2-9

2. If the calculations are performed for a constant non-dimensional shaft-speed line the compressor pressure ratio can be obtained from the compressor characteristic, see Fig. 2-10

3. The next step is to calculate the PT pressure ratio from Equ. (2-13)

For a gas turbine with a choked PT all parameters can be calculated by a single iteration.

2.7.4 Running line

There will be only one point on the constant speed line, on the compressor characteristic, that will fulfil both the aerodynamic coupling between the PT and CT and the mechanical coupling between the compressor and CT. If the calculations are performed for all constant speed lines a line could be drawn between the emerged points, called a running line. This running line will be independent of load and instead decided by the swallowing capacity of the PT. The gas turbine

will always run on this line since it is the only path that fulfils both the aerodynamic and mechanical couplings between the components (Saravanamuttoo, et al., 2009, p. 467).

2.8 Variable PT geometry

One way to increase the swallowing capacity of the PT is to increase the inlet area using variable geometry or refitting the PT with a new first stator row with different angles. In theory the mass flow and aerodynamic shaft-speed are assumed to be constant. When the PT intake area is increased, the CT pressure ratio is also increased, as shown in Fig. 2-11 (Saravanamuttoo, et al., 2009, p. 487).

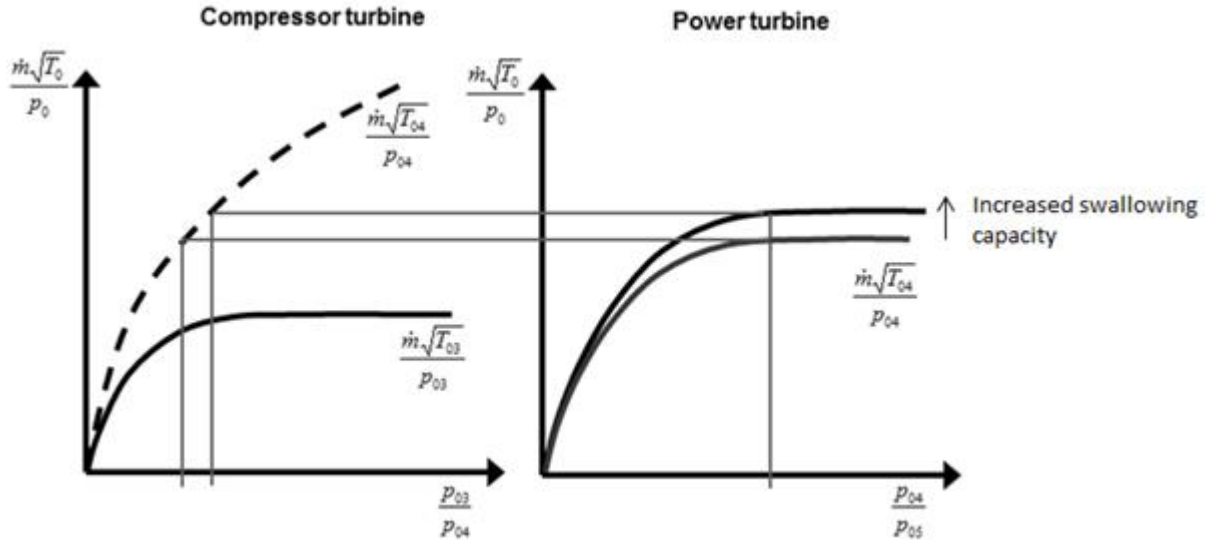

Fig. 2-11 Turbine characteristic illustrating the effects of increasing PT intake area. An increase in PT intake area will lead to higher CT pressure ratio (Courtesy to Magnus Genrup)

In practice the higher pressure drop in the CT along with higher mass flow will lead to an increase in aerodynamic shaft-speed. The power output will increase due to higher mass flow through the engine (Tageman, 2014).

When the ambient temperature is above design level the mass flow and the shaft-speed is lower than at design level. If the PT intake area is increased, the shaft-speed will increase along with the mass flow thus bringing the engine closer to the design case. This enables the engine to run at better efficiency and forces a higher mass flow through the engine thus increasing power output and counteracting the influence of the high ambient temperature. A gas turbine with these modifications is referred to as a tropical matched turbine (Tageman, 2014).

If the PT swallowing capacity is decreased by reducing the PT intake area the opposite behaviour will occur. A closed PT is referred to as an arctic matched turbine and can be used to counteract

the influence of cold ambient temperatures. If no modifications are made to the PT the gas turbine is referred to as a normal matched turbine (Tageman, 2014).

2.9 Correlation between gas turbine parameters

2.9.1 Gas turbine performance predictions from characteristics

In section 2.7 on p. 14 it was shown how the operation area of a gas turbine is reduced down to a single line when the compressor and turbines operates together. Thus the performance of the gas turbine could be gained from compressor and turbines characteristics. In the compressor characteristics in Fig. 2-10 it could be seen that if the non-dimensional shaft-speed is altered it will affect compressor pressure ratio, efficiency and non-dimensional mass flow. If the non-dimensional shaft-speed is reduced both compressor pressure ratio and non-dimensional mass flow will decrease and contrariwise. From the same figure it can be seen that the compressor efficiency depends on both pressure ratio and dimensionless mass flow.

According to the turbine characteristics, as seen in Fig. 2-12, the CT pressure ratio and the non-dimensional mass flow are nearly independent of the non-dimensional shaft-speed. When the turbine is unchoked, the non-dimensional mass flow decreases when the pressure ratio decreases. The turbine efficiency depends on all three parameters; non-dimensional shaft-speed, non-dimensional mass flow and pressure ratio.

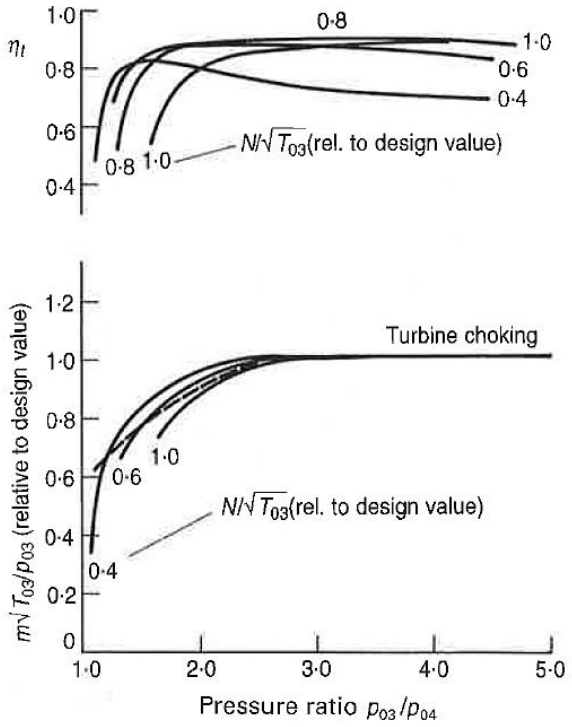

Fig. 2-12 Turbine characteristic. The top chart shows the isentropic efficiency (η_t) as a function of pressure ratio ($\frac{p_{03}}{p_{04}}$) and relative non-dimensional shaft-speed ($\frac{N}{\sqrt{T_{03}}}$). The bottom chart shows non dimensional mass flow ($\frac{m\sqrt{T_{03}}}{p_{03}}$) as a function of $\frac{p_{03}}{p_{04}}$ and $\frac{N}{\sqrt{T_{03}}}$ (Saravanamuttoo, et al., 2009, p. 365)

2.9.2 Humidity's effect on density and mass flow

The mass flow through the gas turbine depends on the intake area (A), the density (ρ) and the velocity according to Equ. (2-14).

$$m = \rho A C \qquad (2\text{-}14)$$

Thus if the density, the intake area or velocity changes, this will impact the mass flow.

Humidity is a measurement of the amount of water in the air. The relative humidity is defined as the ratio between the amount of water the air holds and the maximum amount it could hold at that temperature and pressure. The air density is affected when the humidity changes. Water vapour is lighter than air thus an increase in relative humidity will decrease the air density, thereby lowering the mass flow at the compressor inlet (Brun & Kurz, 2000, p. Part II-2-9).

The amount of water air can hold is less at low temperatures than at high temperatures. High relative humidity at low temperatures does therefore not affect the density as much as a high

relative humidity at high temperatures. Thus the gas turbine performance is more affected by a change in relative humidity at high ambient temperatures (Brun & Kurz, 2000, p. Part II-2-9).

2.9.3 Temperature's effect on density

A change in temperature also affects the density. If the air is considered to be an ideal gas the relationship could be received from the ideal gas law, see Equ. (2-15).

$$pv = RT \leftrightarrow p = \rho RT \qquad (2\text{-}15)$$

Thus if the temperature increases the density will decrease.

2.9.4 Physical shaft-speed's effects on lifespan

The maximum centrifugal stresses occur in the root of the blade. The centrifugal stresses in a rotor blade are proportional to the annulus area and to the square of the physical shaft-speed (Saravanamuttoo, et al., 2009, pp. 346-347, 354), commonly referred to as AN^2. For an existing gas turbine the annulus area is already set. The only thing that is left for the engineer to control the stress levels with, is the physical shaft-speed. Since the centrifugal stresses are proportional to the square of the physical shaft-speed there is a great potential to enhance the lifespan of the engine if the physical shaft-speed can be reduced.

2.10 Surge margin

One of the most severe problems that can occur in a gas turbine is surge. Surge occurs when the compressor is unable to build up enough pressure, resulting in a turn of the flow which can lead to great dynamical damages (Razak, 2007, p. 111). Altering the VGVs will affect the surge margin. If the VGVs are closed the non-dimensional flow will decrease thus improving the surge margin (Razak, 2007, p. 246). If a more opened VGV-position is used the surge line may drift towards the running line thereby increasing the risk of surge (Razak, 2007, p. 248). The concept of the running line was explained in section 2.7.4 on p. 20. If the running line is plotted into Fig. 2-6 on p. 13 the circumstances that lead to surge for that particular compressor can be detected. The vertical distance from the operating point to the surge line is called surge margin and is measured as percentage of the operating pressure ratio (Walsh & Fletcher, 2004, p. 472), see Equ. (2-16).

$$SM = \frac{PR_S}{PR_{op}} - 1 \qquad (2\text{-}16)$$

At SIT the surge margin is defined as the distance from the operating point to the surge line, following the constant speed line. The surge margin (SM) is then calculated according to Equ. (2-17) using the pressure ratio (PR) and the corrected mass flow (m) (Axelsson, 2014).

$$SM = \frac{PR_S}{PR_{op}} * \frac{m_{op}}{m_S} - 1 \qquad (2\text{-}17)$$

The surge margin is needed to ensure that the gas turbine never encounters surge even as the running conditions changes. The surge margin needs to take the fouling of the compressor into

account along with the possibility of rapidly increasing the load and the transient behaviour of the gas turbine. Some extra margin is always taken to be able to handle manufacturing differences and other parameters that may vary from engine to engine (Walsh & Fletcher, 2004, p. 459).

Calculations made by SIT shows that the risk of surge due to rapid load increase is very small for their twin-shaft engines. The rapid response of the gas generator makes it very unlikely to encounter surge since the sudden increase in pressure ratio is quickly met by a higher aerodynamic shaft-speed. In a theoretical world the pressure ratio could reach about 10% higher than the running line at a sudden increase in load. The mechanical limitations make this impossible since it is impossible to inject the needed fuel so quickly. Thus the actual pressure rise is even lower (Axelsson, 2014).

The most accurate way to measure the surge margin is to do experimental tests but since surge may damage the engine severely, these tests are rarely made for full size engines at full load. One common way to test is to use a smaller scaled version and then interpret the results. The problem with this method is that some of the phenomena are hard to scale. One example is the effects of the Reynolds number. Another example is the gap between the casing and the rotor tip. As the engine is scaled down some tolerances are still needed to ensure that the rotor does not hit the casing. It may be hard to scale down this gap as much as the rest of the engine. Thus a smaller engine often encounters higher gap-losses (Axelsson, 2014).

At SIT experimental surge margin tests have been performed at a full size engine running at full load but at lowered intake pressure to minimize the forces and thus the potential of damages. Using this method there are no scaling effects affecting the results but the risks are higher since the full size engine is much more expensive than a smaller prototype (Axelsson, 2014).

2.11 SAS

SAS is a commonly used term for all the air that is extracted from the compressor to be used as cooling or as a pressure barrier. In advanced gas turbines up to 25% of the intake air may be used as SAS (Walsh & Fletcher, 2004, p. 226). The air is extracted from different stages in the compressor. If the extraction is at the early stages less work have been used to compress the air thus the performance loss will be lower than if air is extracted from the final stages. The extraction point must be of sufficient pressure to ensure sufficient flow through the extraction even when losses, from extraction and transportation, are considered (Walsh & Fletcher, 2004, p. 225). Thus the pressure from the extractions in the first stages is not sufficient for all applications. In those cases the much more valuable air from the latter stages in the compressor is needed to ensure the flow.

The SAS is crucial to the performance of the gas turbine. If the SAS fails, the cooling of the turbine will fail causing severe damages. If the SAS requires too much air, the performance will decrease since too much of the mass flow is used for cooling making the main mass flow too

small. The turbine efficiency will also decrease as the amount of cooling air increases since the mixing of this cool air disturbs the main flow leading to losses.

3 The studied gas turbines

In this thesis focus will be on two of SIT's gas turbines; SGT-700 and SGT-750. The gas turbines are constantly improved to meet higher demands and reduce costs. Both engines belong to the segment that SIT refers to as industrial gas turbines, gas turbines with a power between 5 and 50 MW. Both engines have two rows of VGVs, IGV included, that are controlled by one actuator.

3.1 SGT-700

SGT-700, shown in Fig. 3-1, is a twin-shaft gas turbine that delivers 33 MW shaft power at an efficiency of 37.8%. The compressor has a pressure ratio of 18.7:1, consists of 11 stages and is equipped with two rows of VGVs. It has extractions for the SAS at stage 2, stage 6 and stage 11 which is used to cool an air-cooled two-stage CT (Tageman, 2014). The power is delivered by a two stage PT. SGT-700 is designed to be able to run on both gaseous and liquid fuels. It is also designed to match the criteria set in an Ex-environment and to meet offshore codes and standards (Siemens AG, 2009a, p. 1).

Fig. 3-1 The left picture shows a schematic view of the SGT-700. The right picture shows SGT-700 during assembly (Siemens AG, 2009b, pp. 1-2)

3.2 SGT-750

SGT-750, shown in Fig. 3-2, is the newest product in SIT's gas turbine portfolio. It is a twin-shaft engine that delivers 38.2 MW shaft power at an efficiency of 40.7% (Tageman, 2014). The compressor consists of 13 stages and is equipped with two rows of VGVs. The compressor has a pressure ratio of 24:1. It is driven by an air-cooled two-stage CT and the power is generated in a counter-rotating PT consisting of two stages (Siemens AG, 2010, p. 8). The cooling air for the CT is taken from extraction points at stage 3, stage 6, stage 9 and stage 13 (Tageman, 2014). The combustion takes place in eight can-burners (Siemens AG, 2010, p. 9).

Fig. 3-2 The left picture shows a schematic view of SGT-750. The right picture shows a model of SGT-750 (Siemens AG, 2014)

4 Mapping of potential

There is no available tool to quickly calculate how the gas turbine will respond to a change in VGV-position. Therefore every component is modelled individually. The performance of the entire gas turbine is then acquired through an iterative process between the different programs. In this study GTPerform and HT0300 have been used.

Six different cases have been tested. The 75% load cases are by default calculated from the 100% load results. Therefore these results will be affected if the 100% load case reaches any limitations even though that might not be the case in reality. This thesis focuses on high ambient temperatures but for this chapter 15°C is also tested for comparison.

The figures in this chapter show the results as variations from design cases. The figures display the variation in CT polytropic efficiency as a function of the variation in physical shaft-speed.

4.1 SGT-700

To allow higher physical shaft-speed, the physical shaft-speed limitation has been disabled during these tests. This implies that even though a potential is possible, the raised physical shaft-speed might endanger the solidity of the rotating parts. The solidity depends on many parameters and the physical shaft-speed might exceed the chosen limit without endangering the solidity. Nevertheless great care has to be taken to ensure the lifespan of the engine. In the case of an ambient temperature of both 15°C and 30°C there are three points where the physical shaft-speed is higher than the original limit. In the case where the ambient temperature is 45°C there are four points where the physical shaft-speed is higher than the original limit.

At 45°C the exhaust temperature limit is reached leading to a reduced TIT. The impact of this limitation is further discussed in section 4.1.3 on p. 31.

4.1.1 15°C

When the ambient temperature is 15°C there is a positive correlation between CT polytropic efficiency and physical shaft-speed. The impact on the CT polytropic efficiency when the physical shaft-speed is altered is presented in Fig. 4-1.

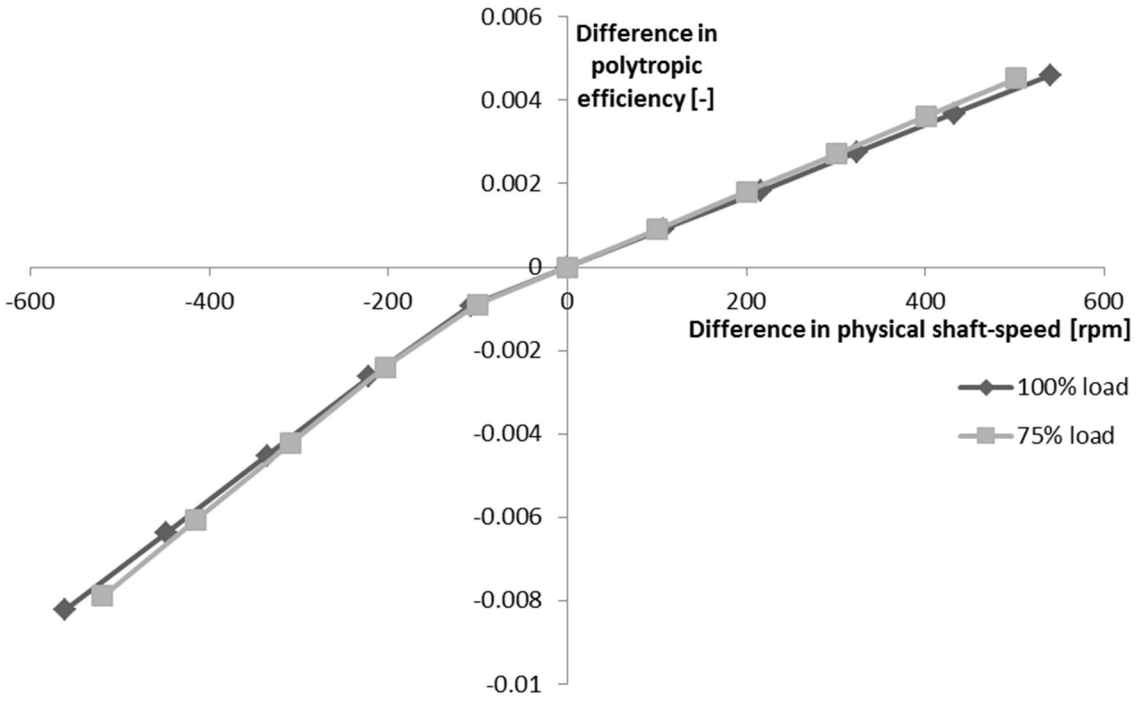

Fig. 4-1 Variation in CT polytropic efficiency as a function of variation in physical shaft-speed at an ambient temperature of 15°C for SGT-700

4.1.2 30°C

For an ambient temperature of 30°C the results show a positive correlation between CT polytropic efficiency and physical shaft-speed. The impact on the CT polytropic efficiency when the physical shaft-speed is altered is presented in Fig. 4-2.

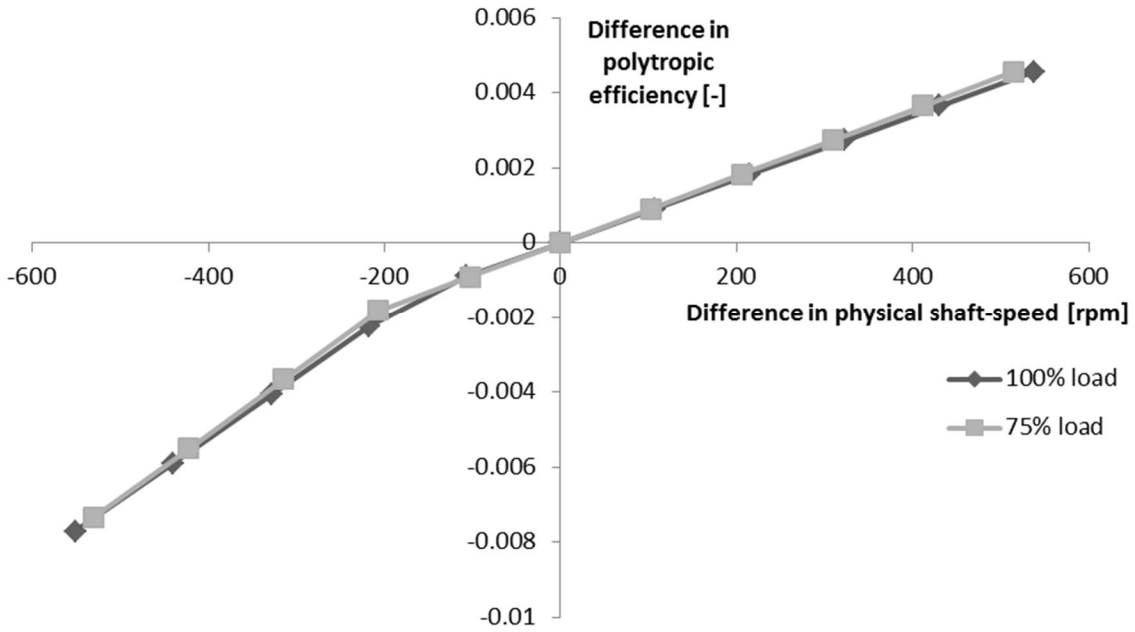

Fig. 4-2 Variation in CT polytropic efficiency as a function of variation in physical shaft-speed at an ambient temperature of 30°C for SGT-700

4.1.3 45°C

When the ambient temperature is increased to 45°C the results show a positive correlation between CT polytropic efficiency and physical shaft-speed. All test points in this simulation are limited by the exhaust temperature leading to a limit of the TIT. The exhaust temperature limit is set to ensure the solidity of the outlet components such as housing, bearings and outlet duct. The impact of limiting the TIT is that the engine will not be reaching its highest temperature i.e. the engine will not be used to its maximum. Due to the nature of the calculations the results at 75% are also limited. The impact on the CT polytropic efficiency when the physical shaft-speed is altered is presented in Fig. 4-3.

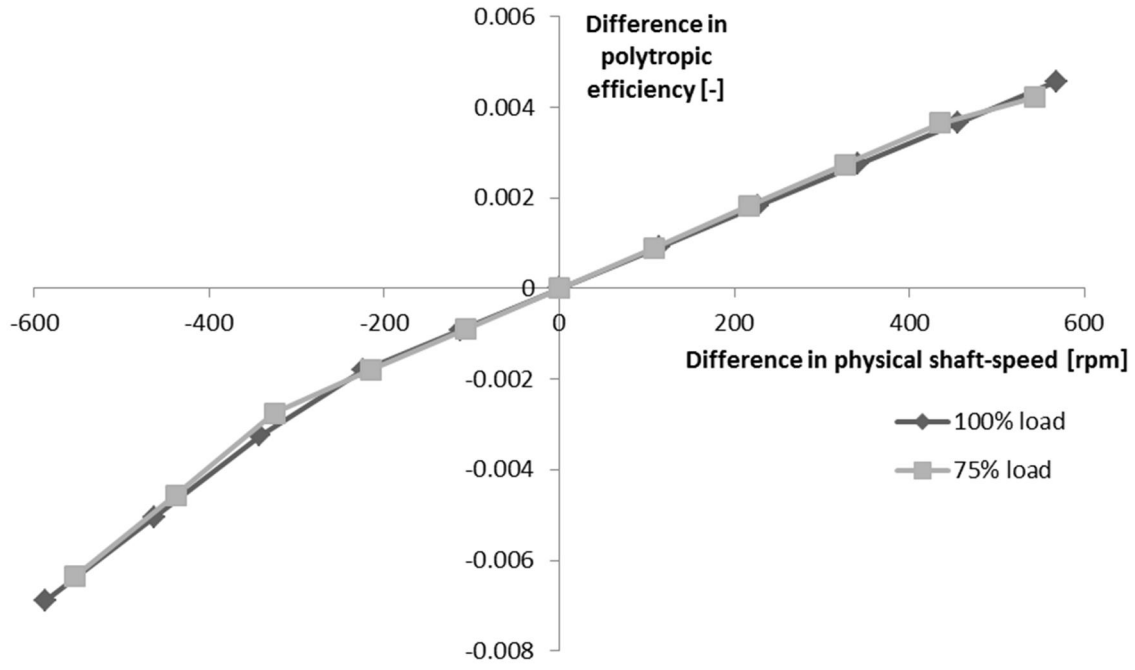

Fig. 4-3 Variation in CT polytropic efficiency as a function of variation in physical shaft-speed at an ambient temperature of 45°C for SGT-700

4.2 SGT-750

During the test neither the physical shaft-speed limit nor the temperature limit of the exhaust gas for SGT-750 was reached.

4.2.1 15°C

When the ambient temperature is 15°C there is a positive correlation between CT polytropic efficiency and physical shaft-speed. When the load is 75% the efficiency reaches its maximum faster than for 100% load and at lower absolute level. This implies that the potential for higher efficiency is lower at part load. The impact on the CT polytropic efficiency when the physical shaft-speed is altered is presented in Fig. 4-4.

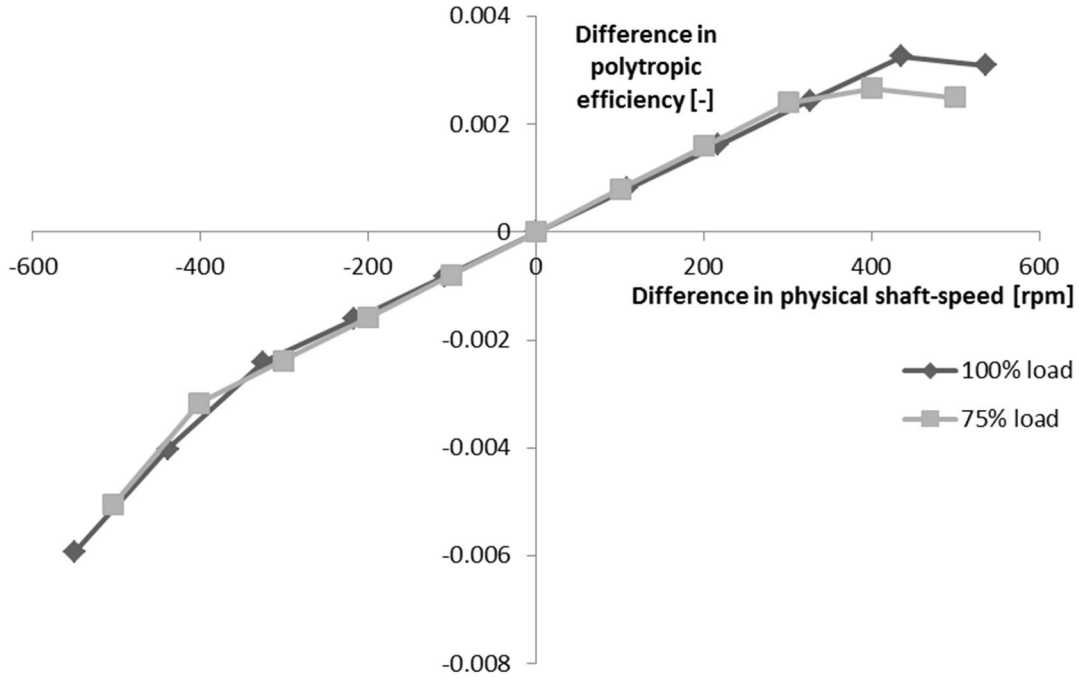

Fig. 4-4 Variation in CT polytropic efficiency as a function of variation in physical shaft-speed at an ambient temperature of 15°C for SGT-750

4.2.2 30°C

For an ambient temperature of 30°C the results show a positive correlation between CT polytropic efficiency and physical shaft-speed. When the load is 75% the efficiency reaches its maximum faster than for 100% load and at lower absolute level. This implies that the potential of higher efficiency gets lower at part load. On the other hand the part load case does not get a steep decrease in efficiency as the physical shaft-speed is lowered implying that the CT efficiency is more sensitive to an opening of the VGVs at full load. The impact on the CT polytropic efficiency when the physical shaft-speed is altered is presented in Fig. 4-5.

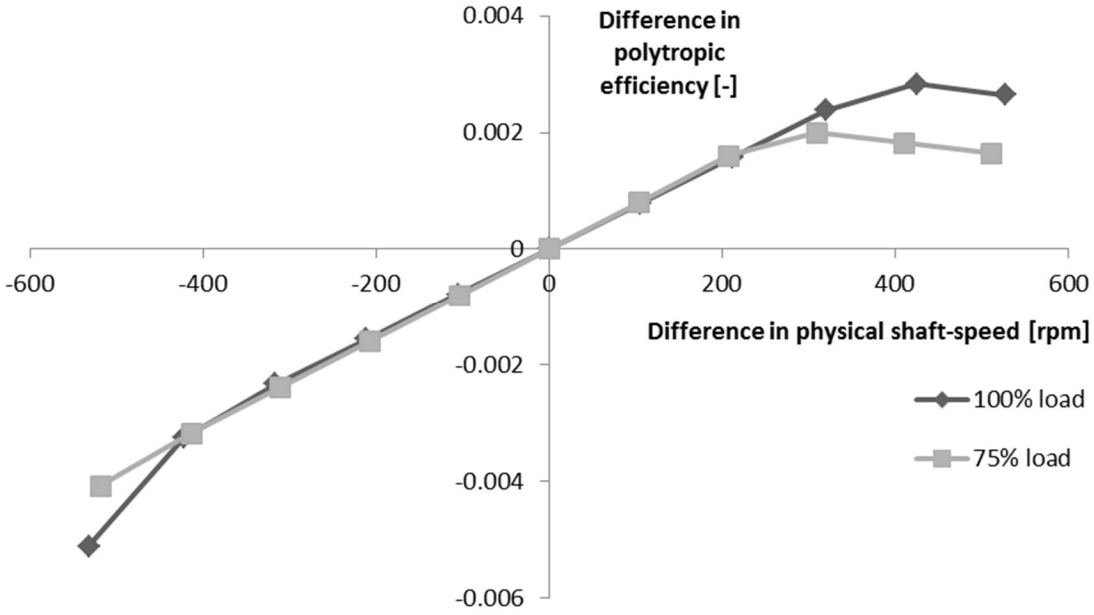

Fig. 4-5 Variation in CT polytropic efficiency as a function of variation in physical shaft-speed at an ambient temperature of 30°C for SGT-750

4.2.3 45°C

When the ambient temperature increases to 45°C, there is a positive correlation between CT polytropic efficiency and physical shaft-speed. When the load is 75% the efficiency reaches its maximum faster than for 100% load and at lower absolute level. This implies that the potential gets lower at part load. The impact on the CT polytropic efficiency when the physical shaft-speed is altered is presented in Fig. 4-6.

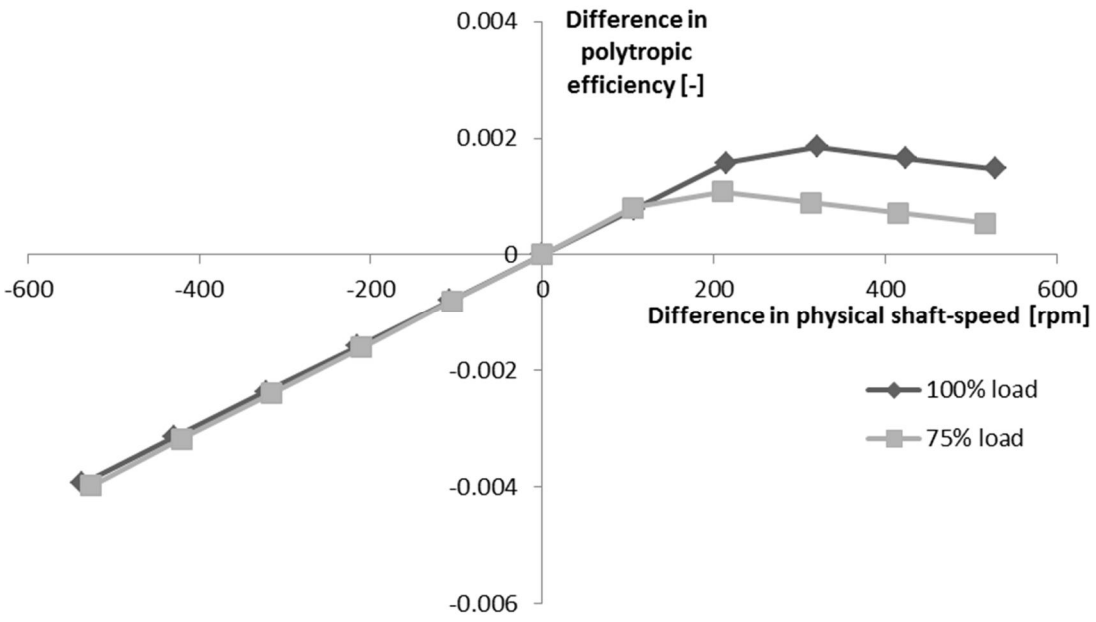

Fig. 4-6 Variation in CT polytropic efficiency as a function of variation in physical shaft-speed at an ambient temperature of 45°C for SGT-750

4.3 Summary

A comparison of the test results shows that the potential of improving the CT polytropic efficiency is larger for SGT-700 than for SGT-750 even though it is still minor. It can also be seen that the CT polytropic efficiency varies more with load for SGT-750 than for SGT-700 where hardly any differences were detected. The physical shaft-speed could be either increased or decreased without making major effects on the CT polytropic efficiency for both SGT-700 and SGT-750.

One thing that did change with load for SGT-750 was the relative physical shaft-speed at which the peak in efficiency occurred. At part load the peak in efficiency occurred at lower relative physical shaft-speed than at full load for the same ambient conditions. The absolute improvement in efficiency was also higher for the full load case.

Another thing that changes is that the efficiency suddenly starts to drop faster when the relative physical shaft-speed decreases below a certain level. The point where this drop occurs is at higher shaft-speed for full load compared with part load. This behaviour is more significant for SGT-750 and implies that the engine can tolerate a larger drop in physical shaft-speed at part load before dropping steeply in CT efficiency. These changes will also occur on the SGT-700 but outside the explored interval of physical shaft-speed. In this thesis the physical shaft-speed interval is limited since the gas turbine performance will be affected negative if the physical shaft-speed is too far away from its design point.

Even though the effects on CT efficiency might be small it can still be valuable as long as no other component is negatively affected to such extent that the total efficiency is reduced. Since the cost of reprograming the VGV-controller is low the improvement might be economically viable as long as it is only a matter of different control algorithms.

At the same time the loss in CT efficiency when opening the VGVs might be acceptable if the efficiency of other components are affected in such extent that the total performance of the engine is enhanced. An opening of the VGVs may also lead to an increase in lifespan due to lower stress levels in the rotating parts. Since no major loss in CT efficiency is detected it is interesting to further investigate the possibility to open the VGVs.

It is necessary to keep investigating both the hypothesis of closing to gain CT efficiency and the hypothesis of opening to gain compressor efficiency and enhance engine lifespan. Further investigation is needed in a compressor program to see how the compressor responds to the variation in VGV-position, physical shaft-speed and aerodynamic shaft-speed.

Due to the small differences in results between the cases with different loads the cases with 75% load will not be further investigated. The small difference in results is not sufficient to justify the time consumption needed for further investigation of the part load cases. The hypotheses that are no longer tested are denoted with a dash (-) and will not appear in future hypothesis matrix. The hypothesis matrix is presented in Table 4-1.

Table 4-1 Hypothesis matrix showing the progress for each hypothesis. Hypothesis under investigation is denoted u.i. Hypothesis no longer investigated is marked with a dash (-). No hypothesis has been proven true or false

	30°C/100%	45°C/100%	30°C/75%	45°C/75%
SGT-750/Open	u.i.	u.i.	-	-
SGT-750/Close	u.i.	u.i.	-	-
SGT-700/Open	u.i.	u.i.	-	-
SGT-700/Close	u.i.	u.i.	-	-

5 Analysis of effects from ambient temperature

GTPerform is used in Finspång to calculate gas turbine performance. As have been discussed in chapter 2.4 on p.11 the characteristics changes when the VGV-position is altered. In SIT's twin-shaft gas turbines the VGVs are controlled as a function of aerodynamic shaft-speed, i.e. the VGV-position is determined by the aerodynamic shaft-speed and for a given aerodynamic shaft-speed the VGVs will always have the same position. This simplifies the characteristics since one characteristic is sufficient to calculate the performance of the engine as long as the regulation of the VGVs is not altered.

It is commonly known at SIT how the gas turbines will behave as the ambient temperature is altered, given that the VGVs are controlled the way they are today. Due to the fact that the VGV-position is a part of the characteristics it is hard to distinguish the effects that are coupled to the change in ambient temperature from the effects that results from the controlling of the VGVs.

By keeping the VGV-position fixed at a constant angle using HT0300 and thereafter changing the parameters in GTPerform to match the results from HT0300 an operational point can be found. The process is iterative since a change of input data in GTPerform may lead to a change of input data for HT0300. Once an operating point is found that matches the results in both programs the effects of the ambient temperature without the interference from the existing control algorithm for the VGVs is revealed.

This thesis focuses on how the VGVs can be used to get a higher performance at high ambient temperatures. It is therefore important to first distinguish what is caused by pure physics and what can be related to the controlling of the VGV-position to see the effects without the influence of existing modifications. This since the goal is to find an improved control algorithm for the VGVs.

In these tests the ambient temperature has been altered using 15, 30 and 45°C at 60% humidity. 15°C has been tested to be used as a comparison. The results have been normalized to the case of 30°C. To estimate the effects of the water content in the air an additional point has been tested at 45°C where the relative humidity has been adjusted to keep the composition of the air at 30°C. For 45°C this is achieved with a relative humidity at 27%. This is relevant since the relative humidity normally decreases when the temperature increases.

In the figures the results are compared with those retrieved from GTPerform where the VGVs are automatically controlled as a function of the aerodynamic shaft-speed to show the effects of the existing control algorithm. When the VGV-position is fixed it is at the angle the gas turbine would have at 30°C if it was tropical matched. Thus the VGVs are more closed at 15°C and more open at 45°C than for the existing control algorithm.

5.1 SGT-700

Fig. 5-1 shows the aerodynamic shaft-speed as a function of the ambient temperature. As can be seen in the figure the aerodynamic shaft-speed decreases as the ambient temperature rises. The existing control algorithm counteracts these effects and keeps the aerodynamic shaft-speed at a higher level at higher ambient temperatures. The results also show that the aerodynamic shaft-speed is almost independent of the relative humidity for SGT-700.

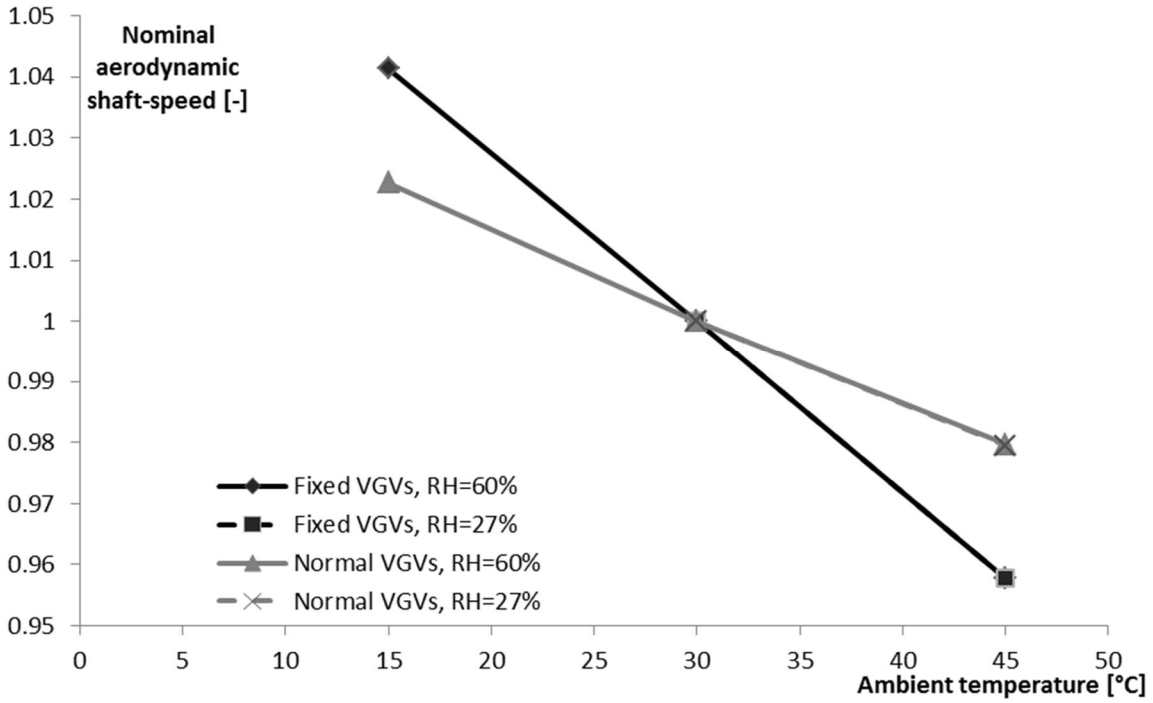

Fig. 5-1 Aerodynamic shaft-speed as a function of ambient temperature, VGV-position and relative humidity for SGT-700

As mentioned in section 2.9.1 on p. 22 the impact of a decreased aerodynamic shaft-speed is lowered corrected mass flow and lower pressure ratio along with a variation in efficiency. Since a higher ambient temperature leads to a decreased aerodynamic shaft-speed, these phenomena are expected to occur. This is confirmed by the results shown in Fig. 5-2, Fig. 5-3 and Fig. 5-4. The results show that an opening of the VGVs will result in lower mass flow, lower pressure ratio and lower CT efficiency but higher compressor efficiency. These parameters also seem to be close to independent of relative humidity for SGT-700.

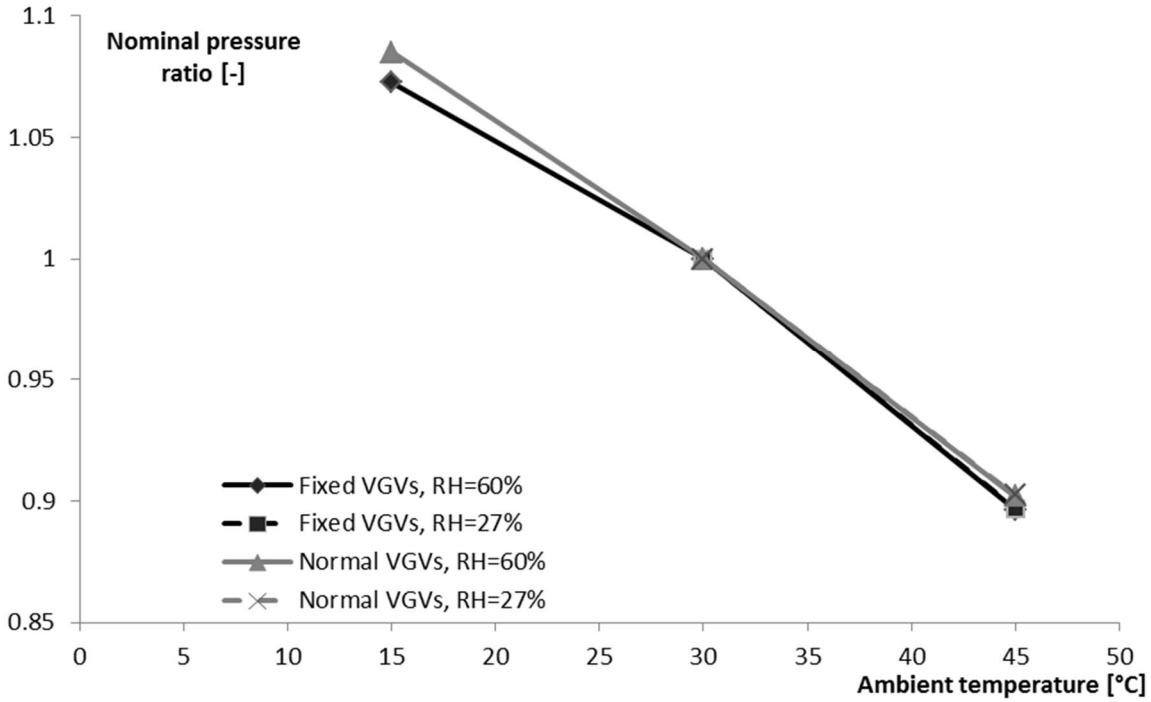

Fig. 5-2 Pressure ratio as a function of ambient temperature, VGV-position and relative humidity for SGT-700

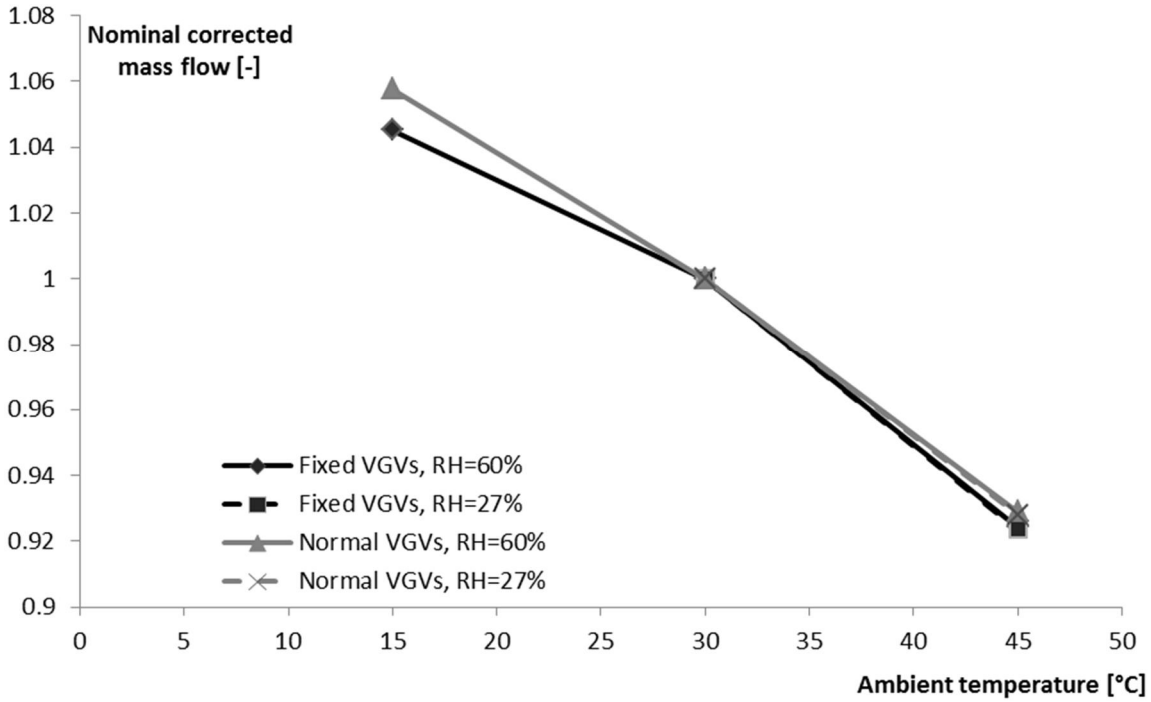

Fig. 5-3 Corrected mass flow as a function of ambient temperature, VGV-position and relative humidity for SGT-700

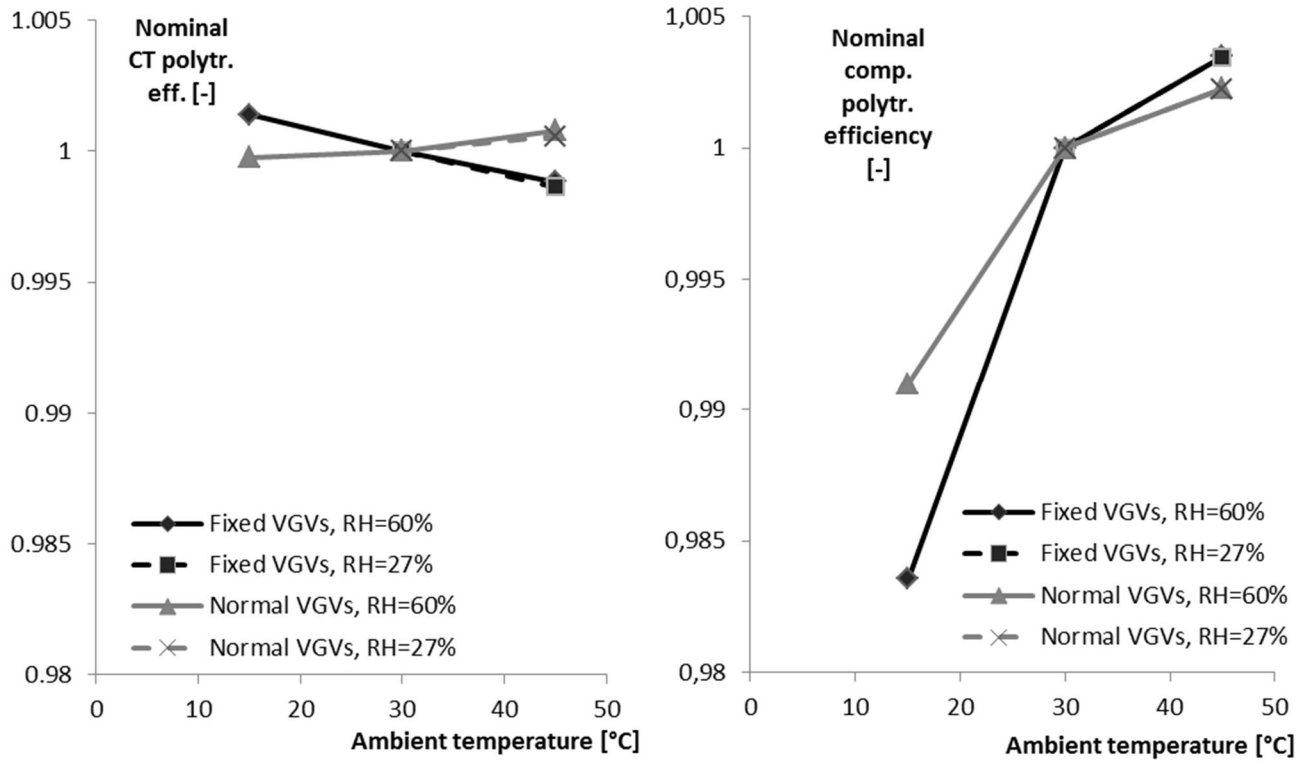

Fig. 5-4 To the left: CT polytropic efficiency as a function of ambient temperature, VGV-position and relative humidity. To the right: compressor polytropic efficiency as a function of ambient temperature, VGV-position and relative humidity. Both figures are for SGT-700

Fig. 5-5 shows how the physical shaft-speed varies with the ambient temperature. There is a distinct difference between the controlled and the uncontrolled VGVs. For the existing VGV control algorithm the physical shaft-speed increases when the ambient temperature increases whereas for the case without a control algorithm for the VGVs the opposite behaviour occurs.

As mentioned in section 2.9.4 on p 24 the centrifugal stresses are proportional to the square of the physical shaft-speed. The existing control algorithm brings up the physical shaft-speed when the temperature rises to keep up the aerodynamic shaft-speed. This will cause higher centrifugal stresses.

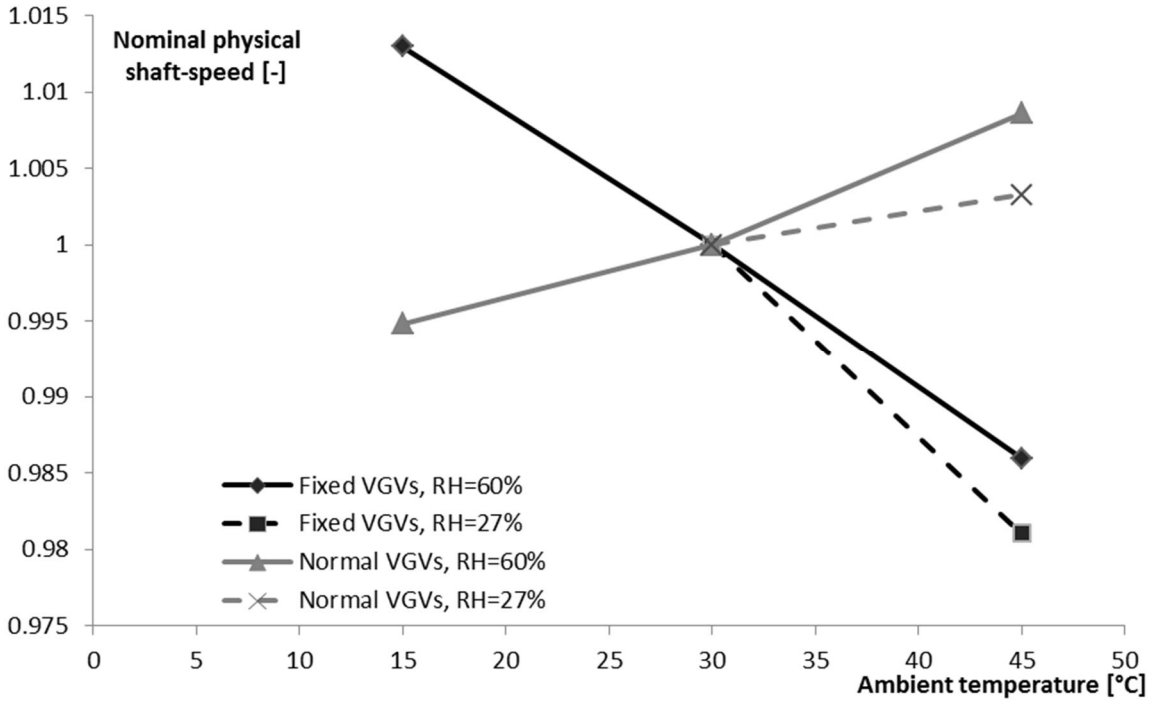

Fig. 5-5 Physical shaft-speed as a function of ambient temperature, VGV-position and relative humidity for SGT-700

Fig. 5-6 and Fig. 5-7 show how shaft power and thermal efficiency varies with the ambient temperature. Both shaft power and thermal efficiency decreases when the ambient temperature increases for both controlled and fixed VGVs. When the ambient temperature is 45°C, both shaft power and thermal efficiency is lower for fixed VGVs than for today's existing VGV-position.

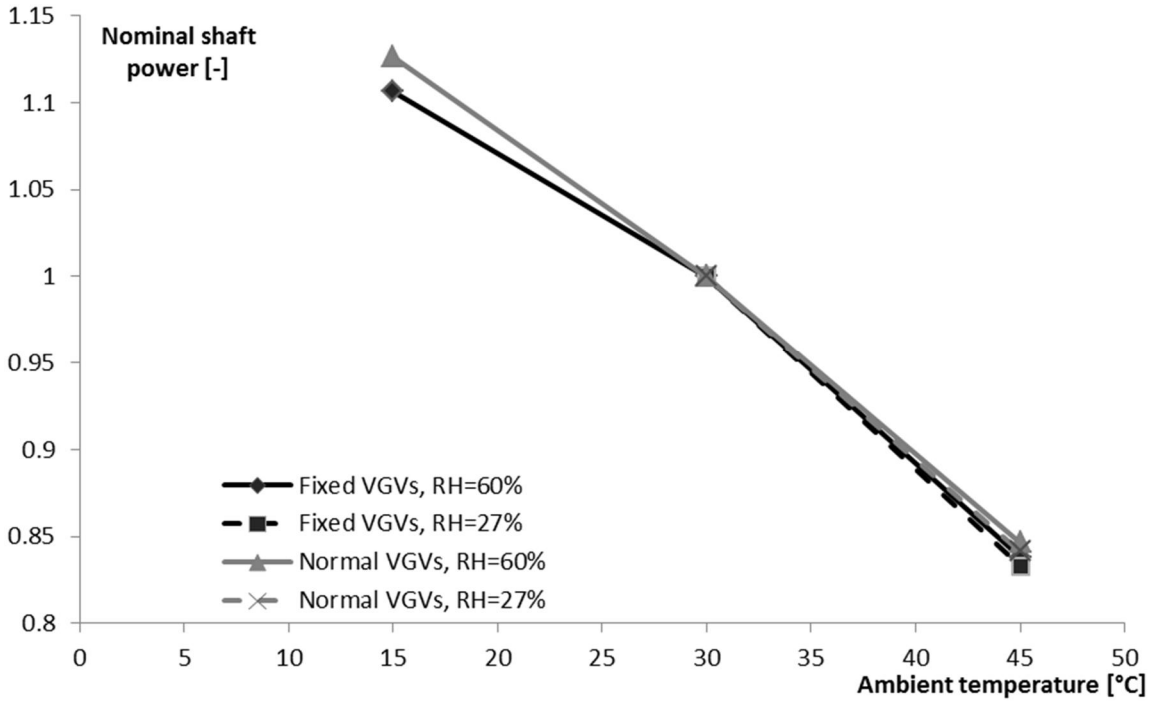

Fig. 5-6 Shaft power as a function of ambient temperature, VGV-position and relative humidity for SGT-700

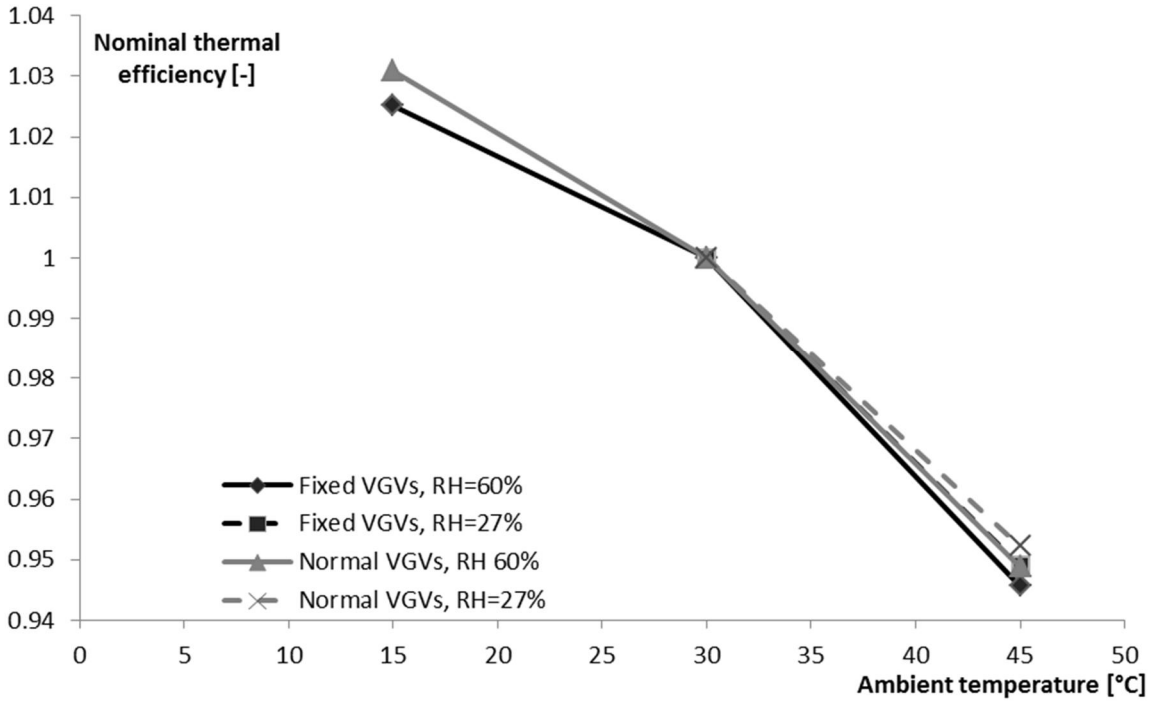

Fig. 5-7 Thermal efficiency as a function of ambient temperature, VGV-position and relative humidity for SGT-700

5.2 SGT-750

Fig. 5-8 shows the aerodynamic shaft-speed as a function of the ambient temperature. As can be seen in the figure the aerodynamic shaft-speed decreases as the ambient temperature rises. The existing control algorithm counteracts these effects and keeps the aerodynamic shaft-speed at a higher level at higher ambient temperatures.

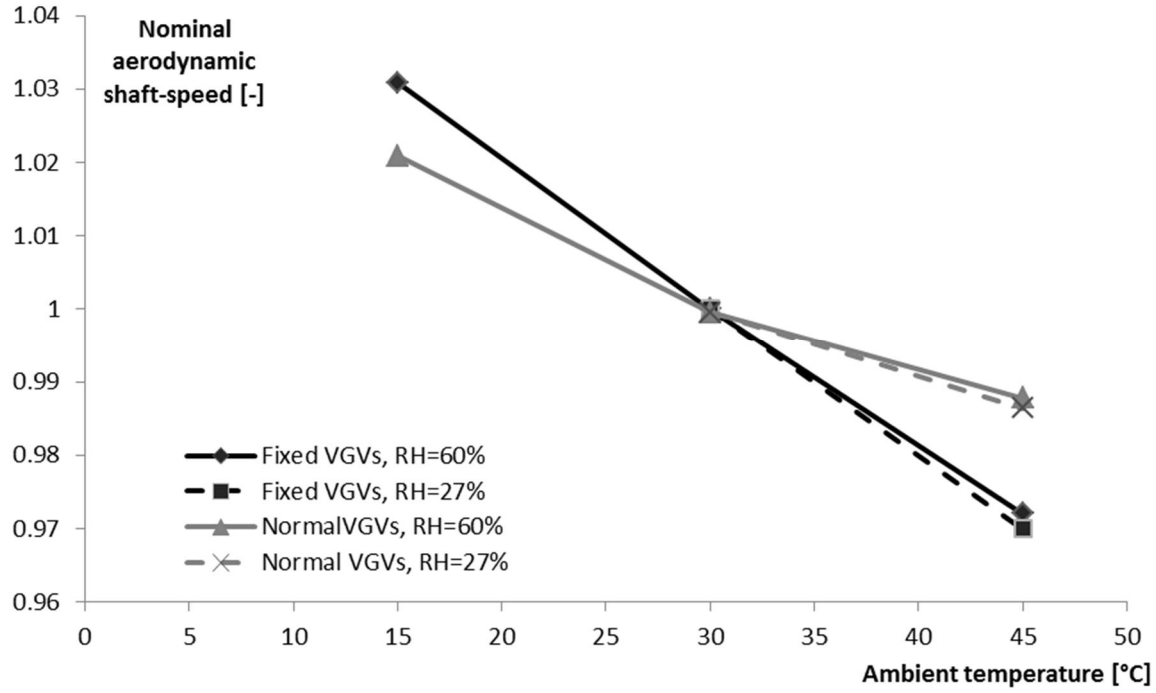

Fig. 5-8 Aerodynamic shaft-speed as a function of ambient temperature, VGV-position and relative humidity for SGT-750

As mentioned in section 2.9.1 on p. 22 the impact of a decreased aerodynamic shaft-speed is lowered corrected mass flow and lower pressure ratio along with a variation in efficiency. Since a higher ambient temperature leads to a decreased aerodynamic shaft-speed these phenomena are expected to occur. This is confirmed by the results shown in Fig. 5-9, Fig. 5-10 and Fig. 5-11. As the control algorithm closes the VGVs to increase the aerodynamic shaft-speed, the intake area will decrease thereby decreasing the corrected mass flow and pressure ratio. That is why the results in Fig. 5-9 and Fig. 5-10 show that the mass flow and pressure ratio is lower for the controlled VGVs than for the fixed VGVs at 45°C.

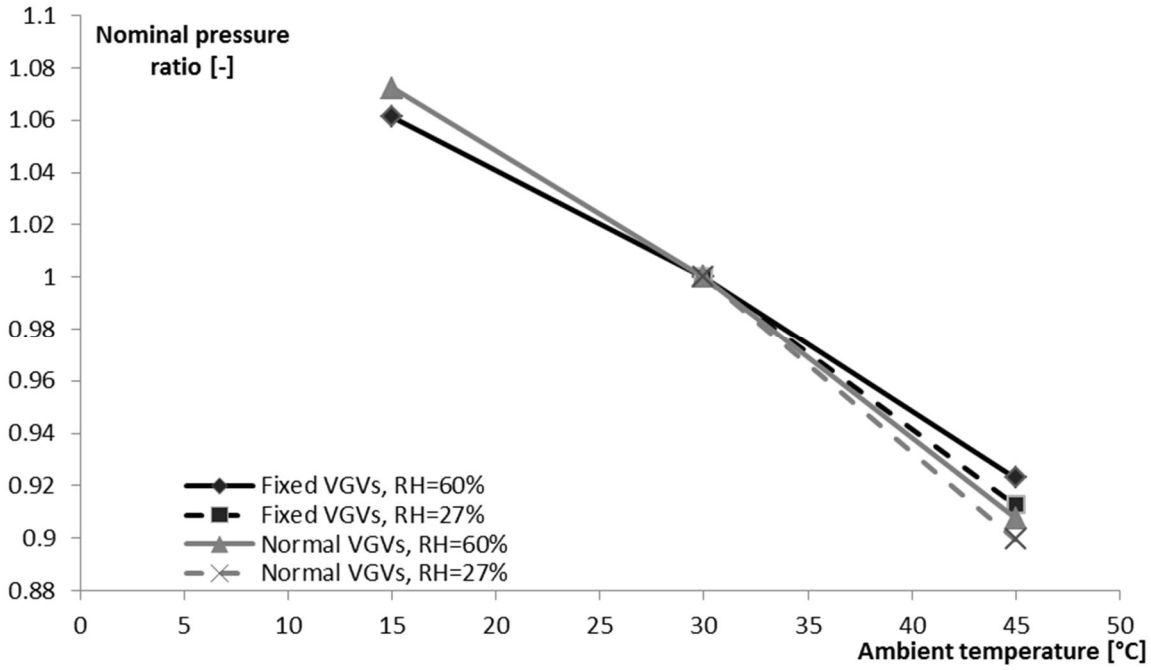

Fig. 5-9 Pressure ratio as a function of ambient temperature, VGV-position and relative humidity for SGT-750

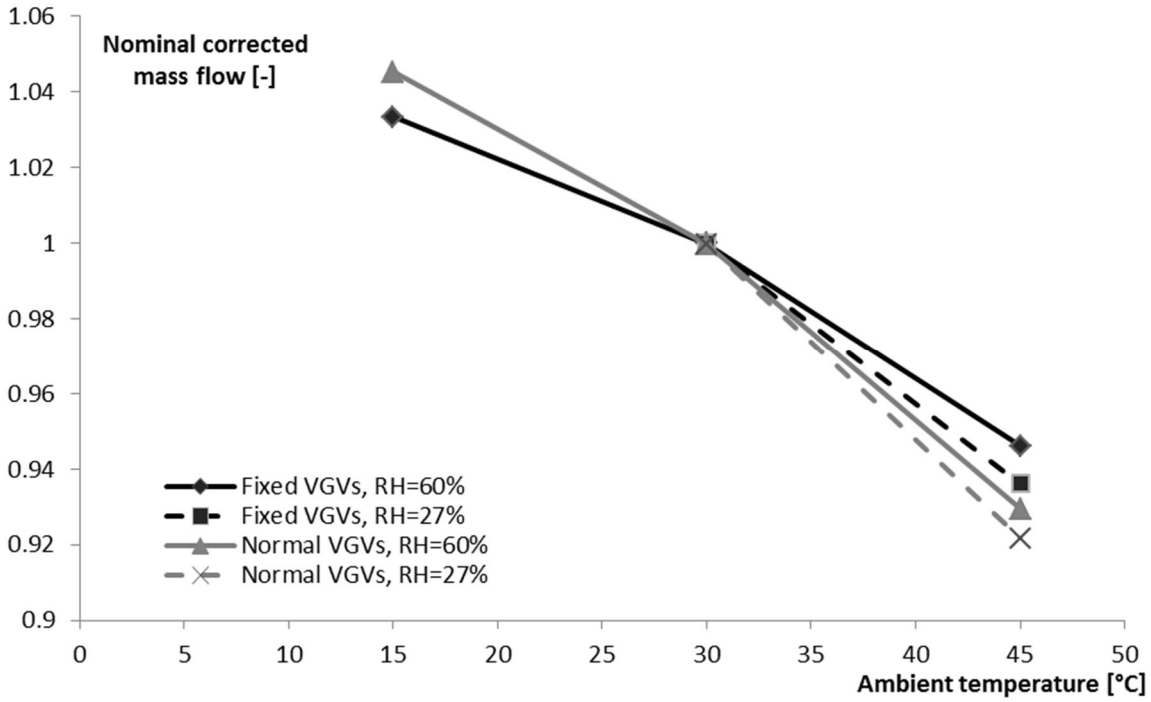

Fig. 5-10 Corrected mass flow as a function of ambient temperature, VGV-position and relative humidity for SGT-750

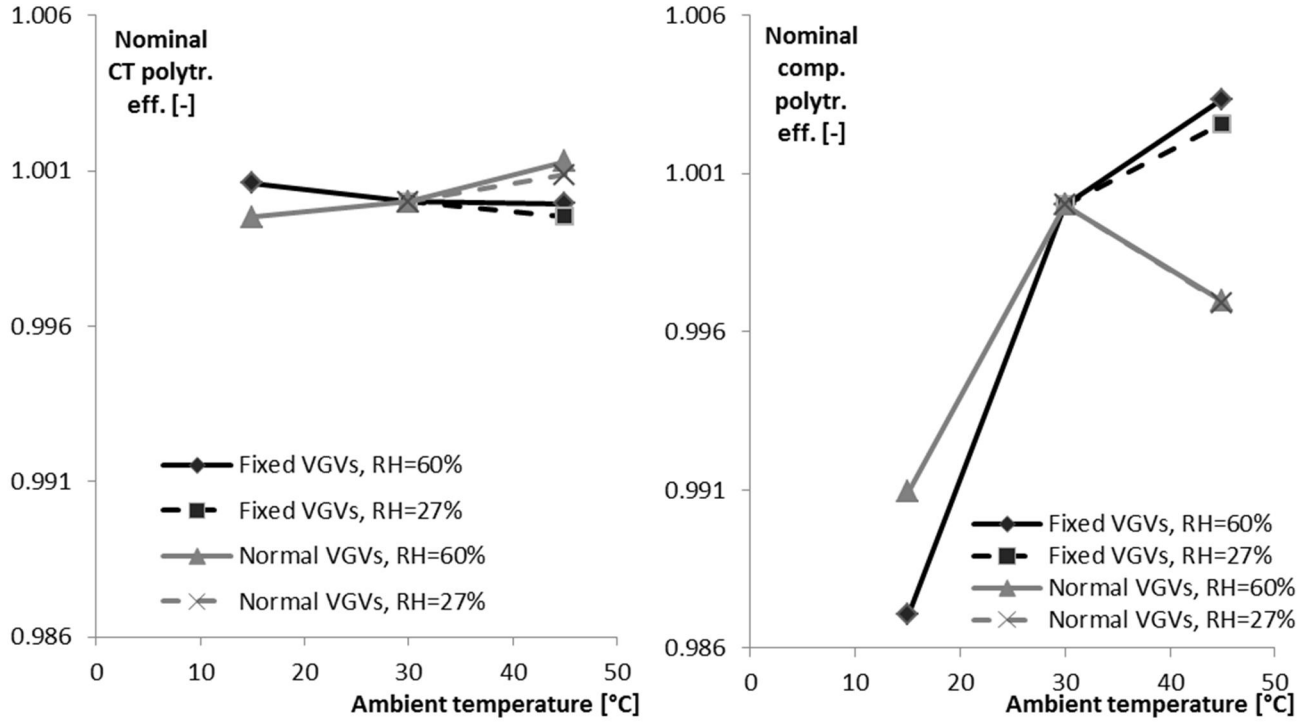

Fig. 5-11 To the left: CT polytropic efficiency as a function of ambient temperature, VGV-position and relative humidity. To the right: compressor polytropic efficiency as a function of ambient temperature, VGV-position and relative humidity. Both figures are for SGT-750

Fig. 5-12 shows how the physical shaft-speed varies with the ambient temperature. There is a distinct difference between the controlled and the uncontrolled VGVs. For the existing VGV control algorithm, the physical shaft-speed increases when the ambient temperature increases whereas for the case without a control algorithm for the VGVs, the physical shaft-speed is almost constant or even decreases if the relative humidity is low.

As mentioned in section 2.9.4 on p 24 the centrifugal stresses are proportional to the square of the physical shaft-speed. The existing control algorithm brings up the physical shaft-speed when the temperature rises to keep up the aerodynamic shaft-speed. This will cause higher centrifugal stresses and lower compressor efficiency in exchange for higher CT efficiency and a higher surge margin due to lower mass flow and lower pressure ratio.

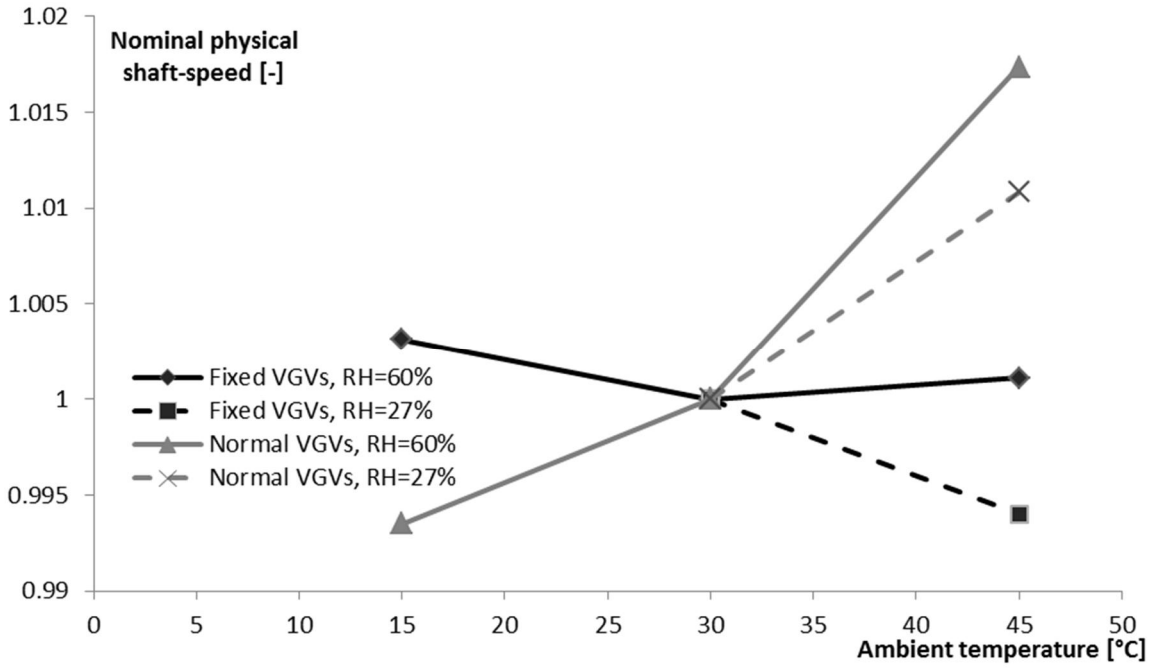

Fig. 5-12 Physical shaft-speed as a function of ambient temperature, VGV-position and relative humidity for SGT-750

Fig. 5-13 and Fig. 5-14 presents how shaft power and thermal efficiency varies with the ambient temperature. Both shaft power and thermal efficiency decreases when the ambient temperature increases for both controlled and fixed VGVs. When the ambient temperature is 45°C, both shaft power and thermal efficiency is higher for fixed VGVs than for controlled VGVs. This implies that it could be possible to gain efficiency and power by opening the VGVs.

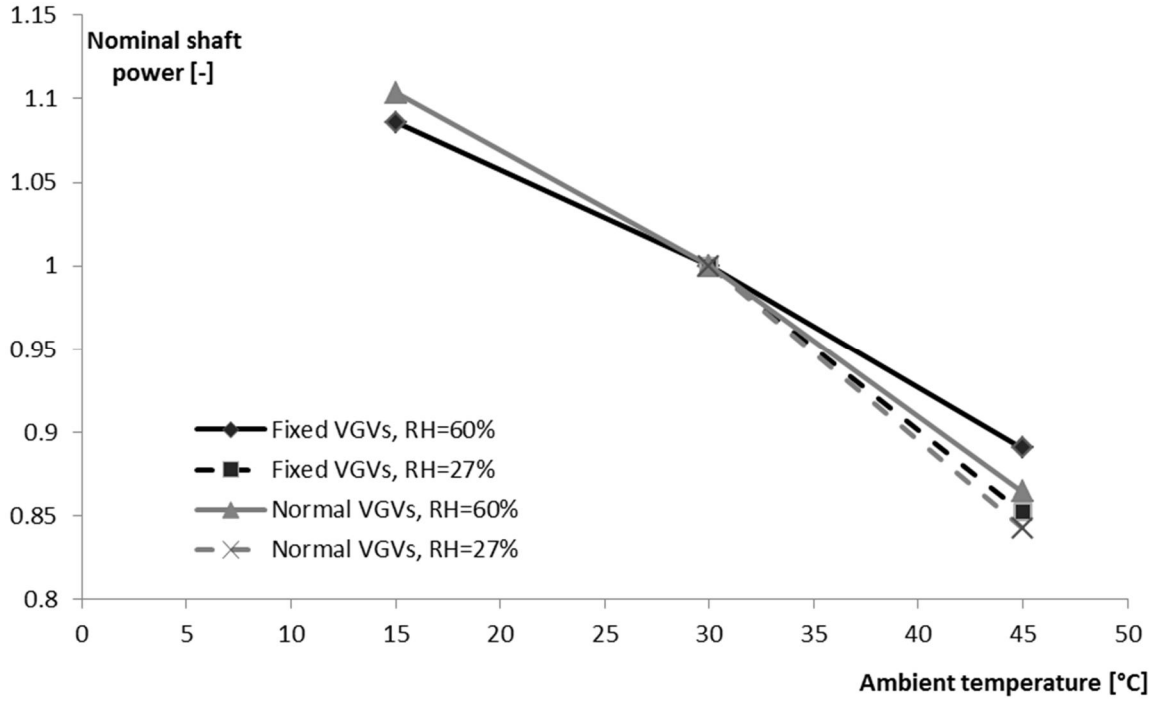

Fig. 5-13 Shaft power as a function of ambient temperature, VGV-position and relative humidity for SGT-750

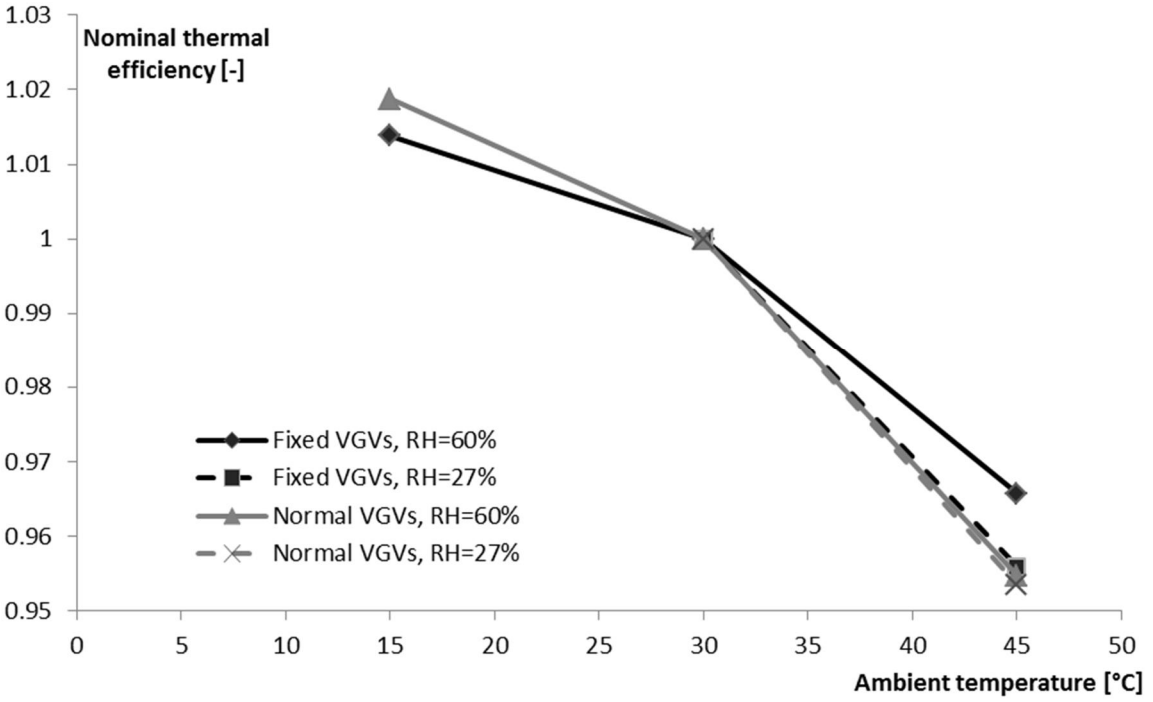

Fig. 5-14 Thermal efficiency as a function of ambient temperature, VGV-position and relative humidity for SGT-750

5.3 Summary

The aim of this chapter was to distinguish the effects of high ambient temperature from the effects of the control algorithm. The study shows that the physical shaft-speed is reduced due to an increase in ambient temperature but the control algorithm will try to keep up the physical shaft-speed to ensure surge margin. This holds true for both engines. As previously discussed less surge margin is needed at full load since no rapid increase in load can occur. It can therefore be possible to reduce the surge margin as long as the engine is running at full load. All the results in this chapter are based on keeping the VGVs fixed. It is therefore not possible to determine how an opening or closing would affect the performance since only one new VGV-position is tested.

In this study the VGVs were kept at a more opened position at 45°C and a more closed position at 15°C compared to today's existing position. The results showed some similar trends for both engines. The CT efficiency benefits from more closed VGVs whereas the compressor efficiency is higher at a more opened position. The variation in CT efficiency is smaller than the variation in compressor efficiency implying that a potential increase in CT efficiency due to higher aerodynamic shaft-speed will be counteracted by a greater decrease in compressor efficiency.

At 45°C the more opened position gave a decrease in performance along with lower physical shaft-speed for SGT-700. For SGT-750 more opened VGVs resulted in higher corrected mass flow and higher pressure ratio but lower aerodynamic shaft-speed at 45°C. The more opened position gave an increase in performance and a lower physical shaft-speed. Since only one angle is tested it is too soon to prove any of the hypotheses true or false. Additional VGV-positions need to be tested and the effects on the SAS need to be investigated.

For SGT-750 the relative humidity gives more significant difference to the result than for SGT-700. This is coupled to iterative loops between the programs used in this chapter and the used convergence criteria. For SGT-700 the relative humidity did affect the performance but it was within the convergence criteria thus the results does not differ as much as for SGT-750 where several iteration were needed before the result converged.

The hypothesis matrix shown in Table 5-1 shows the progress of each hypothesis. This chapter has focused on the temperature's effects and has not proven any hypothesis true or false.

Table 5-1 Hypothesis matrix showing the progress for each hypothesis. Hypothesis under investigation is denoted u.i. No hypothesis has been proven true or false

	30°C/100%	45°C/100%
SGT-750/Open	u.i.	u.i.
SGT-750/Close	u.i.	u.i.
SGT-700/Open	u.i.	u.i.
SGT-700/Close	u.i.	u.i.

6 Analysis of effects from different VGV-positions

To further investigate the possibilities of enhanced performance alternatively lowered physical shaft-speed the VGV-position has been altered for the cases of 30 and 45°C. Existing armature has been used for this study. Thus the IGV and first stator row are mechanically coupled forcing the first stator row to follow the IGV with a predefined gear ratio. An opening represents a decrease in IGV-angle and a closing represents an increase in IGV-angle. For some cases the data is retrieved from the test performed in chapter 5 on p. 37.

The data for the tested VGV-positions are collected through an iterative process between GTPerform and HT0300. The VGV-position is given as input to HT0300 and the two programs are then matched together to find a new operational point. This point represents the operational point where the gas turbine would be running if the VGV-position was altered.

Since the relative humidity is often lower at higher ambient temperatures the 45°C cases will from here on be tested with a relative humidity at 27% to keep the water mass fraction in the air at the same level as at 30°C.

6.1 SGT-700

6.1.1 30°C

For an ambient temperature of 30°C the IGV-angle have been altered from -7° to +5° relative today's existing position.

Table 6-1 presents how different parameters vary with VGV-position. Fig. 6-1 shows the nominal values of the shaft power, thermal efficiency and physical shaft-speed as a function of IGV-angle relative today's existing position.

Table 6-1 Gas turbine performance for different VGV-positions at 30°C for SGT-700

Parameters	Nominal values				
IGV-angle rel. today's existing angle [˚]	5	2.5	-2.5	-5	-7
Shaft power	0.976	0.989	1.004	1.003	0.992
GT shaft thermal eff.	0.991	0.996	1.001	1.001	0.996
Compressor isentr. eff.	0.991	0.996	1.002	1.003	1.000
CT isentr. eff.	1.002	1.001	0.999	0.998	0.997
PT isentr. eff.	0.999	1.000	1.000	1.000	1.000
Pressure ratio	0.986	0.994	1.002	1.001	0.994
Corr. mass flow	0.986	0.994	1.002	1.001	0.994
Shaft-speed	1.022	1.011	0.990	0.981	0.975
Aerodyn. shaft-speed	1.022	1.011	0.990	0.981	0.975

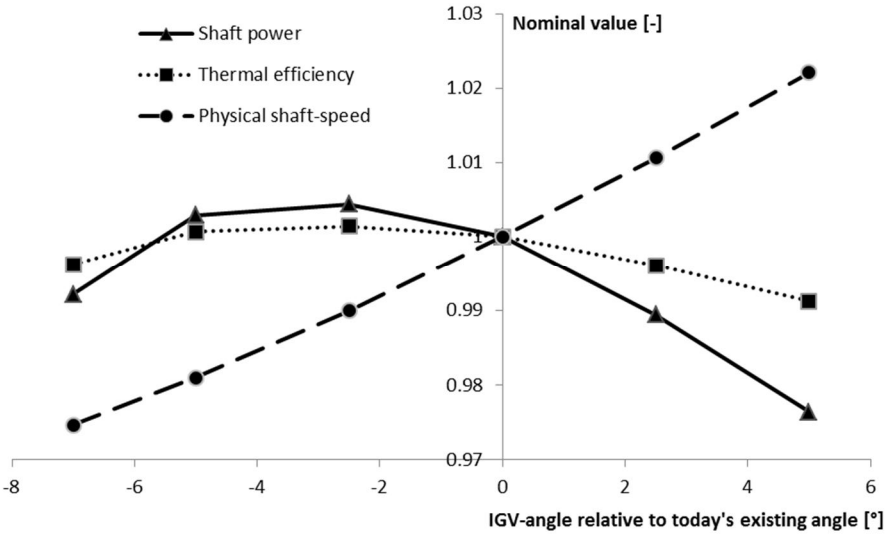

Fig. 6-1 Shaft power, thermal efficiency and physical shaft-speed as a function of IGV-angle relative today's existing position at 30°C for SGT-700

The results show a possible improvement of performance and a decrease in physical shaft-speed when the IGVs are opened, up to 5°. When the VGVs are opened even more the performance is reduced as well as the physical shaft-speed. The highest performance was calculated at an IGV-angle of -2.5° relative today's existing position. Fig. 6-1 indicates that there is an optimum of performance in the interval of 0° to -5° relative to the existing control algorithm. The results also show that there is no potential in closing the VGVs, it will increase physical shaft-speed and reduce engine performance.

6.1.2 45°C

For ambient temperature of 45°C the IGV-angle has been altered between -5 to +5.1 degrees relative today's existing position.

Table 6-2 shows how different parameters vary with VGV-position. The results show that both an opening and a closing of 2.5° leads to an increase in performance. An opening also leads to a reduced physical shaft-speed and is therefore considered more favourable. The results for the largest opening of the VGVs are taken from the analysis made in chapter 5 on p. 37. That is why the IGV-angle is set at -5.1° relative to today's existing position. Fig. 6-2 shows the nominal values of the shaft power, thermal efficiency and physical shaft-speed as a function of IGV-angle relative today's existing position.

Table 6-2 Gas turbine performance for different VGV-positions at 45°C for SGT-700

Parameters	Nominal values			
IGV-angle rel. today's existing angle [˚]	5	2.5	-2.5	-5.1
Shaft power	0.980	1.001	1.010	0.990
GT shaft thermal eff.	0.993	1.000	1.003	0.997
Compressor isentr. eff.	0.994	0.999	1.003	1.001
CT isentr. eff.	1.002	1.001	0.999	0.998
PT isentr. eff.	1.000	1.000	1.000	1.000
Pressure ratio	0.990	1.001	1.005	0.994
Corr. mass flow	0.990	1.001	1.005	0.995
Shaft-speed	1.019	1.008	0.988	0.978
Aerodyn. shaft-speed	1.019	1.008	0.988	0.978

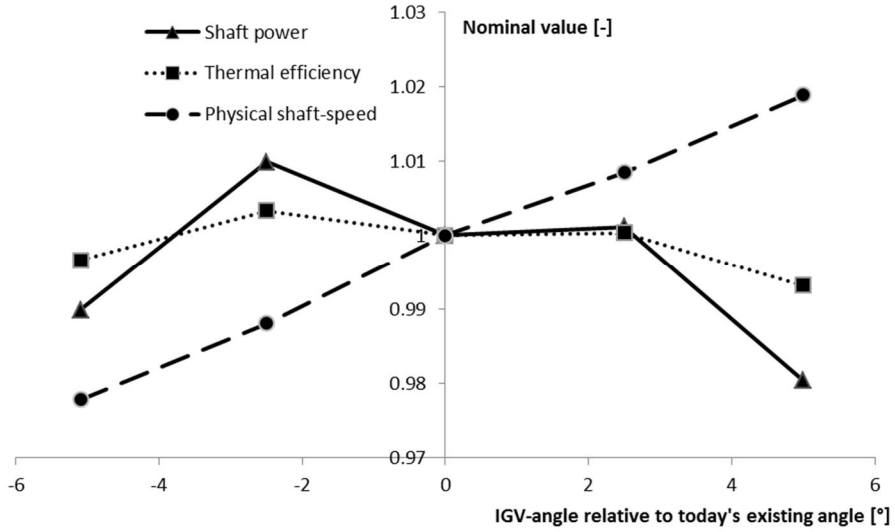

Fig. 6-2 Shaft power, thermal efficiency and physical shaft-speed as a function of IGV-angle relative today's existing position at 45°C for SGT-700

6.2 SGT-750

For SGT-750 an opening of 5° at 30°C was not possible to test due to problems with convergence in the calculations. Calculations show that the problem occurs in the front stages where the stage loading gets to high resulting in detachment of the boundary layers.

6.2.1 30°C

For ambient temperature of 30°C the IGV-angle have been altered between -5 to +5 degrees relative today's existing position. Because of problems with convergence the results for opening 5 degrees will not be presented.

Table 6-3 shows how different parameters vary with VGV-position. The results show that an opening of the IGVs of 2.5 degrees gives a potential increase along with reduced physical shaft-speed. A closing of the VGVs leads to a decrease in performance and higher physical shaft-speed for both tested angles. Fig. 6-3 shows the nominal values of the shaft power, thermal efficiency and physical shaft-speed as a function of IGV-angle relative today's existing position.

Table 6-3 Gas turbine performance for different VGV-positions at 30°C for SGT-750

Parameters	Nominal values		
IGV-angle rel. today's existing angle [°]	5	2.5	-2.5
Shaft power	0.974	0.988	1.007
GT shaft thermal eff.	0.991	0.996	1.003
Compressor isentr. eff.	0.991	0.996	1.003
CT isentr. eff.	1.001	1.001	1.000
PT isentr. eff.	1.000	1.000	1.000
Pressure ratio	0.983	0.992	1.005
Corr. mass flow	0.983	0.992	1.005
Phys. shaft-speed	1.015	1.007	0.993
Aerodyn. shaft-speed	1.015	1.007	0.993

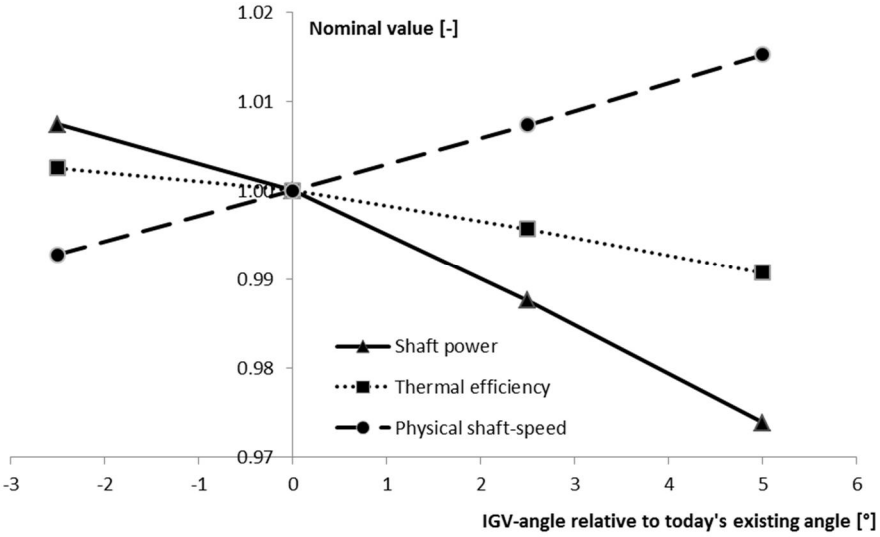

Fig. 6-3 Shaft power, thermal efficiency and physical shaft-speed as a function of IGV-angle relative today's existing position at 30°C for SGT-750

6.2.2 45°C

For ambient temperature of 45°C the IGV-angle has been altered between -7.77 to +5 degrees relative today's existing position.

Table 6-4 presents the variation in performance as the VGV-position was altered. The results for the largest opening of the VGVs are taken from the analysis made in chapter 5 on p. 37. That is why the IGV-angle is set at -7.77° relative to today's existing position for that case. Fig. 6-4 shows the nominal values of the shaft power, thermal efficiency and physical shaft-speed as a function of IGV-angle relative today's existing position.

Table 6-4 Gas turbine performance for different VGV-positions at 45°C for SGT-750

Parameters	Nominal values					
IGV-angle rel. today's existing angle [°]	5	2.5	-2	-4	-6	-7.77
Shaft power	0.983	1.000	1.026	1.033	1.032	1.030
GT shaft thermal eff.	0.994	1.000	1.011	1.013	1.013	1.012
Compressor isentr. eff.	0.994	0.999	1.008	1.010	1.010	1.009
CT isentr. eff.	1.001	1.001	1.000	0.999	0.999	0.999
PT isentr. eff.	1.000	1.000	1.001	1.001	1.001	1.001
Pressure ratio	0.991	1.001	1.016	1.020	1.019	1.017
Corr. mass flow	0.991	1.001	1.016	1.020	1.019	1.017
Phys. shaft-speed	1.020	1.011	0.996	0.991	0.986	0.984
Aerodyn. shaft-speed	1.020	1.011	0.996	0.991	0.986	0.984

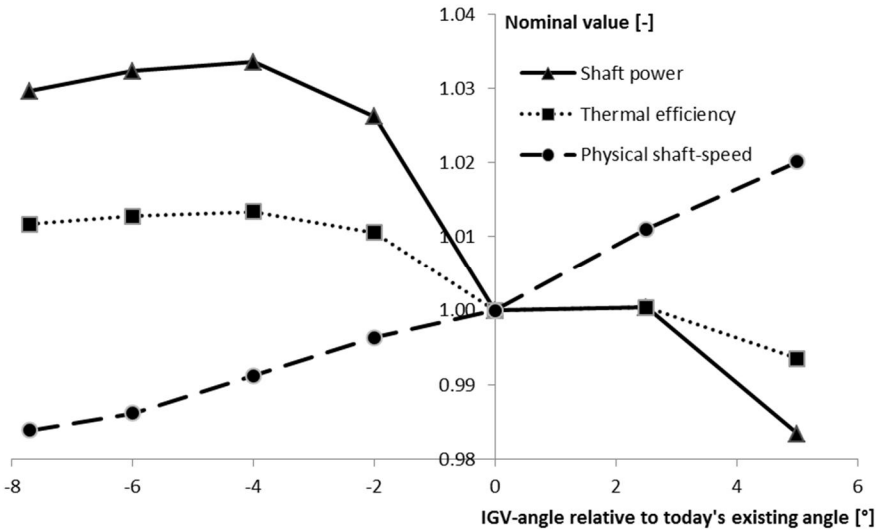

Fig. 6-4 Shaft power, thermal efficiency and physical shaft-speed as a function of IGV-angle relative today's existing position at 45°C for SGT-750

The result shows that an opening of the VGVs leads to an increase in performance and reduced physical shaft-speed. A closing of the VGVs gives different results depending on how much the angle is altered. For a closing of 2.5° the performance is almost constant but for a closing of 5° the performance decreases. As a closing of the VGVs also increases the physical shaft-speed while an opening results in lower physical shaft-speed, an opening is favourable.

The highest performance was calculated at an IGV-angle of -4° relative to today's existing position. According to the results there is an optimum in the interval of -2° to -6° relative to today's existing position.

6.3 Summary

In this chapter the approach was to open and close the VGVs to investigate how the gas turbine performance was affected for SGT-700 and SGT-750. The study was performed for ambient temperatures of 30 and 45°C.

For SGT-700 an opening of the VGVs at 30°C resulted in an increase in performance as well as lowered shaft-speed as long as the IGV was opened no more than 5°. When the VGVs were opened even more the performance was reduced. The highest performance was calculated at an IGV-angle of -2.5° relative to today's existing position. According to the results there is an optimum in the interval of 0° to -5° relative to today's existing position.

A closing of the VGVs at 30°C gave the opposite behaviour with a decrease in performance at a higher shaft-speed. The conclusion is therefore that the hypothesis of closing the VGVs at 30°C for SGT-700 is proven false since the increase in CT efficiency is not sufficient to enhance the total performance.

At 45°C both an opening and a closing resulted in enhanced performance as long as the angle alteration was small. Opening the VGVs increased the performance more than closing. As a closing of the VGVs also increases the physical shaft-speed while an opening results in lower physical shaft-speed the opening is favourable. The hypothesis of closing the VGVs at 45°C for SGT-700 is considered proven false since it is not a suitable solution, even though it does enhance performance. An opening increases the performance more and reduces the physical shaft-speed and is therefore more suitable.

For SGT-750 a closing of the VGVs at 30°C gave a decrease in performance at higher physical shaft-speed. The hypothesis of closing the VGVs at 30°C for SGT-750 is considered proven false since the increase in CT efficiency is not sufficient to enhance the total performance.

It was impossible to model how SGT-750 would react to an opening of 5° at 30°C due to problems with convergence. The front stages were too heavily loaded resulting in detached boundary layers and steep pressure losses. A real engine might be able to run on these harsh conditions but the modelling fails due to the restrictions, set to cover phenomena like fouling and manufacturing differences, in the program. Even though a real engine could be able to run on

these conditions the performance would be severely lowered. As the IGV was opened up only 2.5° an increase in performance at lower physical shaft-speed was detected.

At 45°C an opening of the VGVs gave an increase in performance as well as a decrease in physical shaft-speed. The highest performance was calculated at an IGV-angle of -4° relative to today's existing position. According to the results there is an optimum in the interval of -2° to -6° relative to today's existing position. At the same time the physical shaft-speed decreased along with the opening of the VGVs. Further investigation is needed to decide where the optimum is considering both performance and lifespan.

A closing of the VGVs resulted in higher physical shaft-speed. Opening the VGVs increased the performance more than closing. As a closing of the VGVs also increases the physical shaft-speed while an opening results in lower physical shaft-speed opening is favourable. The hypothesis of closing the VGVs at 45°C for SGT-750 is considered proven false since it is not a suitable solution, even though it does enhance performance. An opening increases the performance more and reduces the physical shaft-speed and is therefore more suitable.

The hypothesis matrix in Table 6-5 shows the progress of each hypothesis. 4 hypotheses have been proven false and are denoted by an F. The conclusion is that a more closed position of the VGVs is not a suitable way to increase performance at high ambient temperatures for the two investigated gas turbines. No hypothesis has been proven true yet since the effects on the SAS and surge margin needs to be evaluated.

Table 6-5 Hypothesis matrix showing the progress for each hypothesis. Hypothesis under investigation is denoted u.i. No hypothesis has been proven true. Hypotheses proven false are denoted by an F

	30°C/100%	45°C/100%
SGT-750/Open	u.i.	u.i.
SGT-750/Close	F	F
SGT-700/Open	u.i.	u.i.
SGT-700/Close	F	F

7 Evaluation of how physical shaft-speed affects lifespan

To evaluate the effects from the reduced physical shaft-speed on the lifespan, interviews have been held with Johan Kling and Jonas Gustafsson at SIT. The information gathered at those interviews is summarized in this chapter.

7.1 SGT-700

SGT-700's lifespan is limited by creep damages at the second rotor of the CT. As discussed in section 2.9.4 on p. 24 the centrifugal stresses are proportional to the annulus area and to the square of the physical shaft-speed, hence a reduction in physical shaft-speed leads to lower stress levels and less creep damages. Lower stress levels also increase the resistance to cyclic fatigue.

Table 6-2 on p. 51 presents that a 5° opening of the IGVs at 45°C leads to a reduction in physical shaft-speed with roughly 2.2%. A reduction by 2.2% would lead to a tension reduction by around 4% which results in an increased lifespan (Kling, 2014).

The tension reduction would be beneficial for the engine but not enough to increase the time between the service intervals for the second rotor of the CT (Kling, 2014).

7.2 SGT-750

SGT-750's lifespan is limited by cyclic fatigue damages at the CT rotor (Gustafsson, 2014). As mentioned in the previous section a reduction in physical shaft-speed leads to lower stress levels resulting in less cyclic fatigue and creep damages.

Table 6-4 on p. 53 presents that a 7.77° opening of the IGVs at 45°C leads to a reduction in physical shaft-speed with roughly 1.6%. A reduction by 1.6% would lead to a tension reduction by around 3%. The reduction in stress levels is positive but too small to increase the time between the service intervals. Such low reductions in stress levels do not counterweight loss in performance (Gustafsson, 2014). Comparing the case of opening 7.77° and opening 4° the latter case is a more suitable way to control the VGVs.

7.3 Summary

The decrease in physical shaft-speed gained from altered VGV-positions reduces the centrifugal stresses thereby increasing the lifespan of the components. The level of reduction is too small however, to increase the service intervals as it is today. The decreases in centrifugal stresses are positive but at such small levels the performance should be optimized without considering the physical shaft-speed.

The hypothesis matrix in Table 7-1 shows the progress of each hypothesis. 4 hypotheses have been proven false and are denoted by an F.

Table 7-1 Hypothesis matrix showing the progress for each hypothesis. Hypothesis under investigation is denoted u.i. No hypothesis has been proven true. Hypotheses proven false are denoted by an F

	30°C/100%	45°C/100%
SGT-750/Open	u.i.	u.i.
SGT-750/Close	F	F
SGT-700/Open	u.i.	u.i.
SGT-700/Close	F	F

8 Analysis of effects from altered pressure levels in the SAS

When the VGV-position is altered the pressure ratio over the compressor is changed, thereby altering the pressure levels in the extractions for the SAS. A more opened VGV-position gives higher pressure levels in the compressor. Thus the pressures in the extractions are higher possibly leading to higher SAS flow. As described in section 2.11 on p. 25 this air will induce losses in performance.

In this chapter the effects from SAS on gas turbine performance, due to altered VGV-position, will be evaluated. For this study Merlin has been used in an iterative process with GTPerfom. The most promising VGV-positions from chapter 6 are evaluated in this analysis. The aim of this analysis is to include the effects of the SAS to get a more realistic comparison of the performance at different VGV-positions. Today's existing position, denoted by 0°, is still based on the calculations from GTPerform with standard reference values.

During these tests the compressor pressure profile has been assumed to be constant for a set IGV-angle. This way Merlin and GTPerform can be used in an iterative process without including HT0300 to get the extraction pressures at each iteration. When the iterative loop between Merlin and GTPerform is finished HT0300 is used once more to evaluate the assumption. The static pressures in all extractions are assumed to vary as much as the total pressure in the last extraction. This pressure is available from GTPerform.

In the last extraction the air is often taken directly from the stream thus the kinetic component is not lost. It is therefore common to use the total pressure in the last extraction point for SAS calculations. For simplicity all other extraction pressures are taken as the static pressure in this thesis since these SAS flows are often taken from cavities or wedges where the kinetic part of the pressure is small. In reality the geometry of the extraction decides how much of the kinetic energy in the extraction pressure that is preserved (Rabal Carerra, 2014).

The assumption requires starting values for the static pressures in the extractions. These starting values are taken from calculations from chapter 6 where the GTPerform calculations for today's existing VGV-position have been matched with HT0300. The matching is done to ensure that the operational point is the same in the two programs. These matched calculations are only used for receiving the static pressures in the extractions.

8.1 SGT-700

There was no existing calculation model for SGT-700 with correct CT flow number. The ones that were available had too large CT flow number leading to a too large expansion in the CT thus giving wrong pressure ratios over the separate turbines. A new model was made by modifying an old model to bring down the flow number closer to the one used in GTPerform to allow matching between the two programs. The model had convergence problems when MAC1 was used but worked well with Beta2. Therefore Beta2 was used in these calculations.

8.1.1 30°C

Two different IGV-angles, -2.5° and -5° relative to today's existing position, have been analysed for SGT-700 at 30°C since the optimum seemed to be located in the span of -5° to 0°. In Table 8-1 and Table 8-2 the SAS mass flows from the extractions are shown. The results show that the mass flow increases at the early stages while decreasing at the final stages.

The ratio between SAS flow and total flow is almost constant for the different VGV-positions. The physical shaft-speed is reduced when the VGV-position is more open due to lower turbine efficiency. Thus also the total flow is reduced. This will counteract the reduced SAS flow resulting in almost constant ratios. The cooling of the components is therefore not endangered.

Table 8-1 SAS mass flow from different compressor stages for different VGV-positions at 30°C for SGT-700

Parameters	Nominal values	
IGV angle rel. today's existing angle[°]	-2.5	-5
Mass flow at stage 2	1.010	1.039
Mass flow at stage 6	1.008	1.029
Mass flow at stage 11	0.984	0.980

Table 8-2 The ratio between the SAS flow and the compressor inlet flow, stage 2 and 6, and the SAS flow and the turbine inlet flow, stage 11 at 30°C for SGT-700 compared to today's existing position

Parameters	Nominal value of ratio between SAS flow and total flow	
IGV angle rel. today's existing angle[°]	-2.5	-5
Mass flow at stage 2	1.025	1.059
Mass flow at stage 6	1.022	1.049
Mass flow at stage 11	0.998	1.000

In Table 8-3 the results from chapter 6 have been updated to include the changes in the SAS. If the parameters in Table 8-3 are compared to the parameters in Table 6-1on p. 49 where the calculations are without consideration to the effects from SAS, it could be seen that the values are reduced.

There is no longer any potential in opening the VGVs. The increased SAS flow leads to lower turbine efficiencies thus reducing the physical shaft-speed and mass flow. The gain in compressor efficiency is not large enough to counteract the losses thus the thermal efficiency of the engine decreases due to the altered SAS flow.

Table 8-3 Gas turbine performance for different IGV-angles after considering the effects from changes in SAS at 30°C for SGT-700

Parameters	Nominal values	
IGV angle rel. today's existing angle[°]	-2.5	-5
Shaft power	0.982	0.974
GT shaft thermal eff.	0.991	0.987
Compressor isentr. eff.	1.003	1.004
CT isentr. eff.	0.990	0.988
PT isentr. eff.	1.000	0.999
Pressure ratio	0.985	0.979
Corr. mass flow	0.986	0.981
Physical shaft-speed	0.985	0.975
Aerodyn. shaft-speed	0.985	0.975

8.1.2 45°C

For SGT-700 at 45°C the most promising VGV-position was an IGV-angle of -2.5° relative to today's position. In Table 8-4 and Table 8-5 the SAS mass flows from the extractions are shown. The results show that the mass flow increases at the early stages while decreasing at the final stage.

The ratio between the SAS flow and the total flow is almost constant. The physical shaft-speed has been reduced for the tested VGV-position due to lower turbine efficiency, therefore the lowered SAS flow from the last stages is counteracted by the lower total flow into the turbine resulting in almost constant ratios. Thus the cooling of the components is not endangered.

Table 8-4 SAS mass flow from different compressor stages for different VGV-positions at 45°C for SGT-700

Parameters	Nominal values
IGV angle rel. today's existing angle[°]	-2.5
Mass flow at stage 2	1.032
Mass flow at stage 6	1.005
Mass flow at stage 11	0.982

Table 8-5 The ratio between the SAS flow and the compressor inlet flow, stage 2 and 6, and the SAS flow and the turbine inlet flow, stage 11 at 45°C for SGT-700 compared to today's existing position

Parameters	Nominal value of ratio between SAS flow and total flow
IGV angle rel. today's existing angle[°]	2.5
Mass flow at stage 2	1.051
Mass flow at stage 6	1.024
Mass flow at stage 11	1.001

In Table 8-6 the results from chapter 6 have been updated to include the changes in the SAS. If the parameters in Table 8-6 are compared to the parameters in Table 6-2 on p. 51 where the calculations are without consideration to the effects from SAS, it could be seen that the values are reduced due to the new SAS flow.

Table 8-6 Gas turbine performance for different IGV-angles after considering the effects from changes in SAS at 45°C for SGT-700

Parameters	Nominal values
IGV angle rel. today's existing angle[°]	-2
Shaft power	0.974
GT shaft thermal eff.	0.992
Compressor isentr. eff.	1.004
CT isentr. eff.	0.994
PT isentr. eff.	1.002
Pressure ratio	0.982
Corr. mass flow	0.986
Physical shaft-speed	0.983
Aerodyn. shaft-speed	0.983

There is no longer any potential in opening the VGVs. The increased SAS flow leads to lower CT efficiency thus reducing the physical shaft-speed and mass flow. The gain in compressor and PT efficiency is not large enough to counteract the losses thus the thermal efficiency of the engine decreases.

8.2 SGT-750

A sufficient calculation model of SGT-750, needed for the calculations in Merlin, already existed so there was no need for adjusting the model. MAC1 was used for the calculations since it reduces the calculation time compared to using Beta2. The accuracy is sufficient using MAC1 so there is no incentive for using Beta2 in this case.

SGT-750 has extractions at stage 3, 6, 9 and 11. The first extraction, at stage 3, has been left out of this study due to the small mass flows through that extraction. The cooling flow from stage 3 does increase but the impact is so small that it was left out of the study to save time.

8.2.1 30°C

For SGT-750 at 30°C the only IGV-angle that showed an improved performance was an IGV-angle of -2.5° relative to today's position. In Table 8-7 and Table 8-8 the SAS mass flows from the extractions are shown. The results show that the mass flow increases at all extractions indicating increased losses. Meanwhile the mass flow through the engine has increased keeping the ratios between SAS flow and inlet flow almost constant.

Table 8-7 SAS mass flow from different compressor stages for different VGV-positions at 30°C for SGT-750

Parameters	Nominal values
IGV angle rel. today's existing angle[°]	-2.5
Mass flow at stage 6	1.020
Mass flow at stage 9	1.020
Mass flow at stage 13	1.002

Table 8-8 The ratio between the SAS flow and the compressor inlet flow, stage 6 and 9, and the SAS flow and the turbine inlet flow, stage 13 at 30°C for SGT-750 compared to today's existing position

Parameters	Nominal value of ratio between SAS flow and total flow
IGV angle rel. today's existing angle[°]	-2.5
Mass flow at stage 6	1.017
Mass flow at stage 9	1.017
Mass flow at stage 13	0.999

In Table 8-9 the results from chapter 6 have been updated to include the changes in the SAS. If the parameters in Table 8-9 are compared to the parameters in Table 6-3 on p. 52 where the calculations are without consideration to the effects from SAS, it could be seen that the values are reduced due to the increased SAS flow.

Table 8-9 Gas turbine performance for different VGV-positions after considering the effects from changes in SAS at 30°C for SGT-750

Parameters	Nominal values
IGV angle rel. today's existing angle[°]	-2.5
Shaft power	1.005
GT shaft thermal eff.	1.001
Compressor isentr. eff.	1.003
CT isentr. eff.	0.998
PT isentr. eff.	1.000
Pressure ratio	1.002
Corr. mass flow	1.003
Physical shaft-speed	0.992
Aerodyn. shaft-speed	0.992

The results still show a possible improvement in performance as the IGVs are opened 2.5° at 30°C. An opening of the IGV-angle of 2.5° compared to today's existing position would have the potential to increase the shaft power by 0.5% and reducing the physical shaft-speed by 0.8%.

8.2.2 45°C

Three different IGV-angles have been analysed for SGT-750 at 45°C since the optimum seemed to be located within the span of these IGV-angles. In Table 8-10 and Table 8-11 the SAS mass flows from the extractions are shown. The results show that the mass flow increases at all extractions for all cases indicating increased losses. Meanwhile the mass flow through the engine has increased keeping the ratios between SAS flow and inlet flow almost constant. Thus the cooling of the components is not endangered.

Table 8-10 SAS mass flow from different compressor stages for different VGV-positions at 45°C for SGT-750

Parameters	Nominal values		
IGV angle rel. today's existing angle[°]	-2	-4	-6
Mass flow at stage 6	1.007	1.034	1.045
Mass flow at stage 9	1.002	1.028	1.037
Mass flow at stage 13	1.015	1.015	1.013

Table 8-11 The ratio between the SAS flow and the compressor inlet flow, stage 6 and 9, and the SAS flow and the turbine inlet flow, stage 13 at 45°C for SGT-750 compared to today's existing position

Parameters	Nominal value of ratio between SAS flow and total flow		
IGV angle rel. today's existing angle[°]	-2	-4	-6
Mass flow at stage 6	0.994	1.017	1.031
Mass flow at stage 9	0.988	1.012	1.023
Mass flow at stage 13	1.001	0.999	1.000

In Table 8-12 the results from chapter 6 have been updated to include the changes in the SAS. Opening the VGVs still shows an improved performance, with both higher shaft power and thermal efficiency. An opening of the IGV-angle by 4° showed a potential of increasing the shaft power by 2.9% and increasing the thermal efficiency by 1.1% as well decreasing the physical shaft-speed by 0.9%.

Table 8-12 Gas turbine performance for different IGV-angles after considering the effects from changes in SAS at 45°C for SGT-750

Parameters	Nominal values		
IGV angle rel. today's existing angle[°]	-2	-4	-6
Shaft power	1.025	1.029	1.025
GT shaft thermal eff.	1.010	1.011	1.009
Compressor isentr. eff.	1.008	1.010	1.010
CT isentr. eff.	0.999	0.998	0.997
PT isentr. eff.	1.001	1.001	1.001
Pressure ratio	1.015	1.016	1.012
Corr. mass flow	1.014	1.016	1.014
Physical shaft-speed	0.996	0.991	0.985
Aerodyn. shaft-speed	0.996	0.991	0.985

If the parameters in Table 8-12 are compared to the parameters in Table 6-4 on p. 53 where the calculations are without consideration to the effects from SAS, it could be seen that the values are reduced, confirming that the increased SAS flow has led to a small reduction in performance. The results show a steeper gradient between the cases of an IGV-angle of -4° and -6° due to the fact that the latter case has a bigger increase in SAS mass flow and therefore more performance losses occur.

8.3 Summary

The aim of this chapter was to evaluate how the different VGV-positions affected the SAS and the differences this made to the cycle. The study was made through an iterative process between GTPerform and Merlin. To simplify the time consuming process the compressor pressure profile was assumed to be fixed for a set IGV-angle thus excluding HT0300 from the iterative process. In the end HT0300 was used to evaluate how the new operational point affected the compressor and to evaluate the accuracy of the assumption.

The results show that there is no potential in opening the VGVs for SGT-700 at high ambient temperatures. For both 30 and 45° the new SAS flow decreased the CT efficiency leading to lower physical shaft-speed and lower mass flow. This affected the cycle negatively and resulted in lower thermal efficiency and lower shaft power compared to using today's existing VGV-position.

The evaluation using HT0300 showed that the compressor was affected by the new operational points and that the assumption made of constant compressor pressure profile was not accurate for SGT-700. HT0300 predicted that the compressor would operate at lower efficiency but at higher mass flow due to the new operational points. It also predicted that the pressure profile would change towards higher pressures in the first stages but the same pressures in the last stages. This would lead to increased SAS flow from the first extractions inducing more losses while keeping the SAS flow from the last stages nearly constant.

If the new data from HT0300 were to be used it would have led to lower compressor efficiency due to the new operational points and lower turbine efficiency due to the increase in SAS flow from the early extractions. Since the results already showed no potential the tests were not repeated to ensure more accurate results. The new results would only confirm that SGT-700 does not benefit from a more opened VGV at 30 or 45°C. The hypothesis of opening the VGVs at 30 and 45°C for SGT-700 is therefore considered proven false.

The results were more optimistic for SGT-750. Improved performance is possible at both 30 and 45°C if the VGVs are opened. For 30°C and an opening of 2.5° the results show a possible increase of the thermal efficiency by 0.1% and the shaft power could increase 0.5%. Further investigation is needed to ensure surge margin. At 45°C an opening led to higher performance with higher thermal efficiency and higher shaft power. The highest performance was still calculated at an IGV-angle of -4° relative today's existing position with a potential improvement of thermal efficiency by 1.1% and shaft power by 2.9%. Further investigation is needed to ensure surge margin.

The iteration process with Merlin and GTPerform led to slightly different operational points for SGT-750 compared to the ones from chapter 6. HT0300 was used to see how the differences affected the compressor. The results showed no significant differences and the decision was

therefore to not repeat the iteration loop between HT0300 and GTPerform for the new operational points.

The HT0300 calculation also showed that the assumption that the compressor pressure profile was constant for a set IGV-angle was not entirely correct but the errors encountered were small. A more correct way would have been to use slightly higher pressures in the first stages. The assumption was accurate for the last compressor stages. Still the results are considered reliable since the errors encountered were in the order of tenths of bar.

The hypothesis matrix in Table 8-13 shows the progress of each hypothesis. 6 hypotheses have been proven false and are denoted by an F. The conclusion is that no possible improvements can be achieved by adjusting the VGVs for the SGT-700 at full load and high ambient temperatures. Opening the VGVs for SGT-750 at full load is the only option that still has potential to increase the performance at high ambient temperatures. No hypothesis has been proven true yet since the effects on the surge margin needs to be evaluated.

Table 8-13 Hypothesis matrix showing the progress for each hypothesis. Hypothesis under investigation is denoted u.i. No hypothesis has been proven true. Hypotheses proven false are denoted by an F

	30°C/100%	45°C/100%
SGT-750/Open	u.i.	u.i.
SGT-750/Close	F	F
SGT-700/Open	F	F
SGT-700/Close	F	F

9 Analysis of surge margin

As discussed in section 2.10 on p. 24 the surge margin can be calculated according to Equ. (2-16) where the changes in mass flow are neglected or according to Equ. (2-17) where the changes in mass flow are taken into account. In this chapter both types of surge margin will be analysed. When the VGV-position is adjusted the corrected mass flow and the pressure ratio will be affected thereby affecting the surge margin. In this chapter the effects on the surge margin, due to the altered VGV-position, will be evaluated. The analysis will only be performed for SGT-750 since the result from the previous chapter showed that there are no potential for enhanced performance in adjusting the VGV-position for SGT-700.

As the VGVs are altered both the running line and the surge line will be affected. Today the surge margin during operation of SIT's gas turbines is measured by measuring the angle of the fuel valve, thus measuring the fuel mass flow entering the combustion chamber and from there calculating how the pressure ratio is affected. A better way would be to measure the pressure ratio directly but until now the measurement has been assumed too slow (Axelsson, 2014). New calculations indicate that this assumption is no longer valid. This is further discussed in Appendix A.

9.1 Numerical surge margin

Surge margin can be calculated with measured values from tests but also from calculated values. When the surge margin is based on calculated values it is referred to as numerical surge margin. The method used is to set the aerodynamic shaft-speed in HT0300 and then increase the pressure ratio until the program does not converge. The last point that is able to converge is used as surge point. This is an effective way to estimate the surge margin without having the need to run the test rig. This chapter is based on the numerical surge margin.

The results in this chapter are presented as relative differences from the existing surge margin according to Equ. (9-1). In this chapter the case with the today's existing VGV-position is based on calculations where GTPerform has been matched with HT0300. The matching is done to ensure that the operational point is the same in the two programs. This since the pressure ratios needed to calculate the surge margin are gathered from HT0300.

$$\frac{SM_{new} - SM_{existing}}{SM_{existing}} \qquad (9\text{-}1)$$

The method used is not sufficiently accurate and the surge margin should be measured in test rigs to be fully evaluated. Still the results can be used to see trends and evaluate if the performance is endangering the surge margin.

9.1.1 30°C

The only IGV-angle that showed an improved performance at 30°C was an IGV-angle of -2.5° relative to today's position. In Fig. 9-1 the nominal surge margin for the two tested IGV-angles is presented.

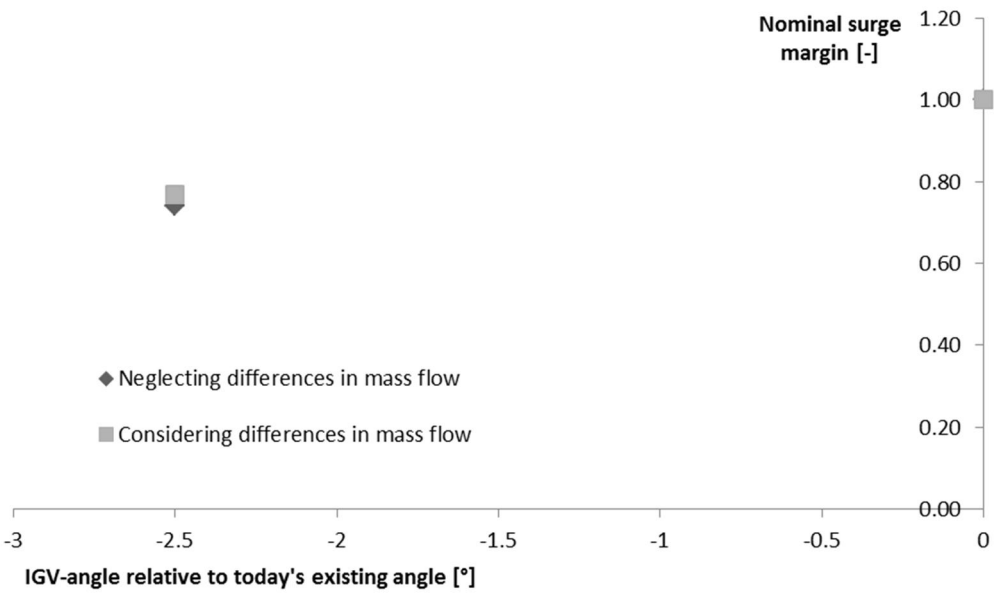

Fig. 9-1 Numerical surge margin for different VGV-positions at 30°C

The results show that when the IGV-angle is altered -2.5° the surge margin decreases with roughly 25%. The reduction in surge margin is lower if the differences in mass flow are considered during the calculations. Since the surge margin decreases the gas turbine will be closer to surge. The surge margin therefore needs to be further investigated to ensure that the gas turbine never encounters surge even as the running conditions changes. The big decrease in surge margin implies that testing may be needed to confirm if the increase in performance is possible without the risk of running into surge.

Fig. 9-2 shows how the pressure ratios in the different stages of the compressor are affected, as the VGV-position is altered. As can be seen in the figure an opening of the VGVs leads to a higher pressure ratio in the front stage while the pressure ratios of the last stages are close to unaffected. Thus the risk of surge will be coupled to the front stage where pressure ratio will be higher than normal if the VGVs are opened.

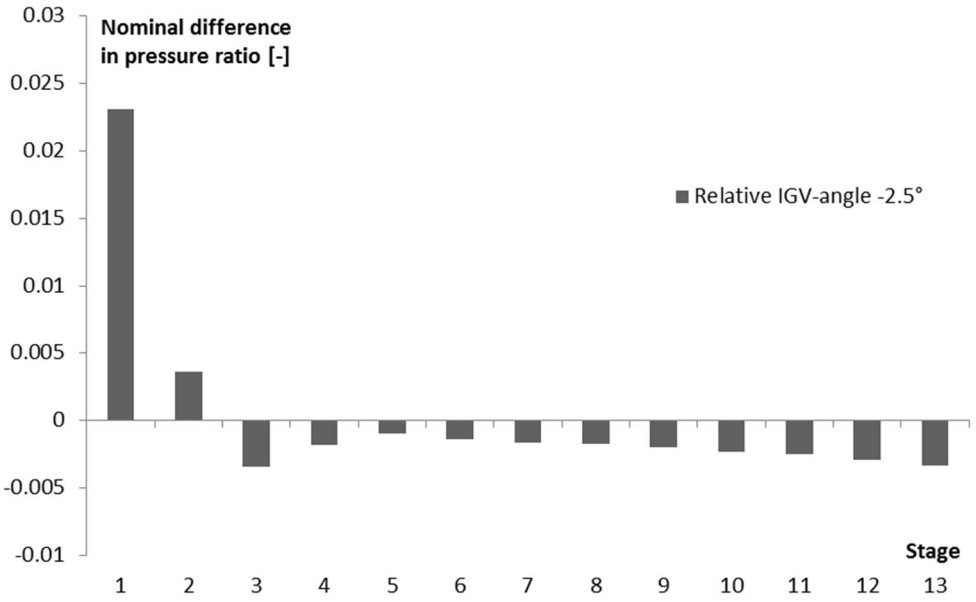

Fig. 9-2 Relative pressure ratio in the compressor stages for a 2.5° more open VGV-position at 30°C compared to today's position

9.1.2 45°C

Three different IGV-angles have been evaluated at 45°C. Fig. 9-3 shows nominal surge margin for the tested cases.

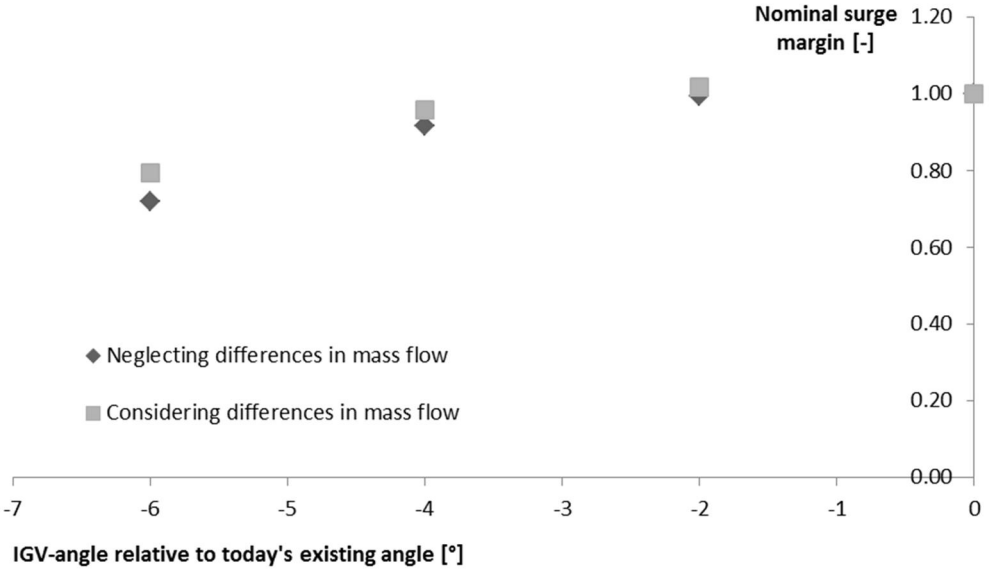

Fig. 9-3 Nominal surge margin for different VGV-positions at 45°C

The results show that all tested angles give a decrease in surge margin if the differences in mass flow are neglected. If the differences in mass flow are considered the surge margin does increase slightly at an IGV-angle of -2° relative today's angle before dropping as the VGV-position is

more opened. Since the surge margin decreases the gas turbine will be closer to surge. The surge margin therefore needs to be further investigated to ensure that the gas turbine never encounters surge even as the running conditions changes.

For the best case, when the IGV-angle is opened 4° compared to today's existing position, the surge margin decreases by less than 10 % for both tested calculation methods. Considering that no margin is needed for sudden increases in load, as the engine is assumed running at full load, the improvement may be possible without the risk of running into surge.

Fig. 9-4 shows how the pressure ratios in the different stages of the compressor are affected, as the VGV-position is altered. As can be seen in the figure an opening of the VGVs leads to a higher pressure ratio in the front stage while the pressure ratio of the last stages decrease slightly. Thus the risk of surge will be coupled to the front stage where pressure ratio will be higher than normal if the VGVs are opened. An opening of 6° gives the highest pressure ratio for the first stage and it can be seen that the pressure ratio increases as the opening angle increases. Thus the risk for surge in the first stage increases as the VGV-position is opened.

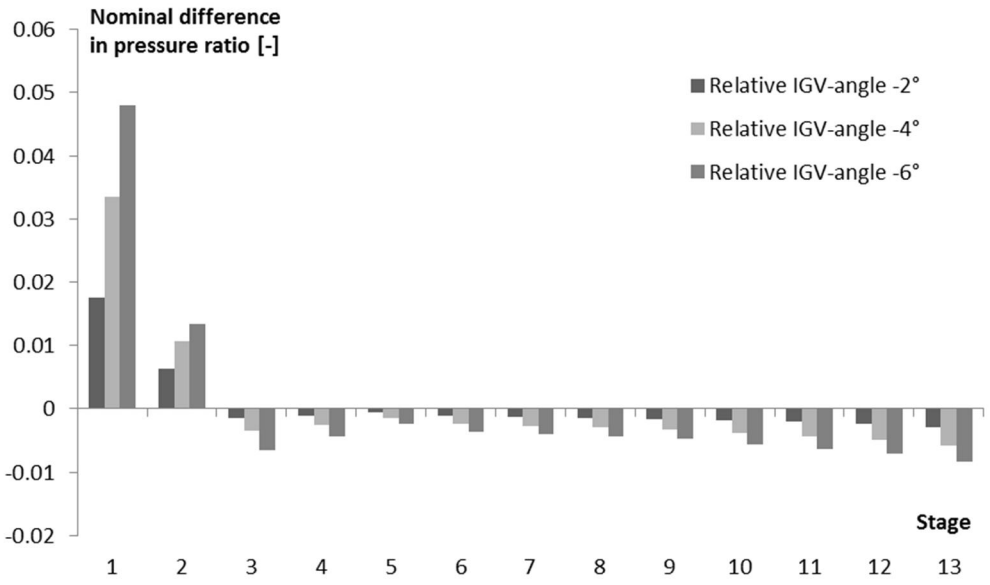

Fig. 9-4 Relative pressure ratio in the compressor stages for different VGV-positions at 45°C

9.2 Summary

When the VGV-position is altered to a more opened position the pressure ratio over the compressor and the corrected mass flow are altered thereby affecting the surge margin. The more opened VGV-position gives a reduced surge margin indicating that the gas turbine would be closer to surge. This confirms the findings by Razak (2007, pp. 246-248) earlier described in section 2.10 on p. 24.

The more opened VGV-position gives a higher pressure ratio in the front stage while the pressure ratios of the last stages decrease slightly. Thus the risk of surge will be coupled to the front stage.

At full load there is no risk that the load will increase and the surge margin does therefore not need to be as large as at part load. Since these calculations are performed for full load the smaller surge margin could be within accepted limits. To fully evaluate the surge margin and the potential of our calculations experimental tests have to be performed in test-rig.

It is difficult to evaluate how much the surge margin can decrease before the limit is reached. The results show that an opening of the IGVs of 4° relative to today's existing position at 45°C could improve the performance without having a big impact on the surge margin. At 30°C an opening of the IGVs of 2.5° relative today's existing position also showed enhanced performance but at the same time the surge margin was reduced by roughly 25%. Assuming that a big part of the surge margin is used to protect the engines at rapid increases in load this reduction might be acceptable. The hypotheses regarding an opening of the VGVs for SGT-750 at both 30 and 45°C are considered proven true.

The hypothesis matrix in Table 9-1 shows the progress of each hypothesis. 6 hypotheses have been proven false and are denoted by an F and 2 hypotheses have been proven true and are denoted by a T. The conclusion is that no possible improvements can be achieved by adjusting the VGVs for the SGT-700 at full load and high ambient temperatures. Opening the VGVs for SGT-750 at full load is the only option that has potential to increase the performance at high ambient temperatures.

Table 9-1 Hypothesis matrix showing the progress for each hypothesis. Hypothesis under investigation is denoted u.i. Hypotheses proven true are denoted by a T. Hypotheses proven false are denoted by an F

	30°C/100%	45°C/100%
SGT-750/Open	T	T
SGT-750/Close	F	F
SGT-700/Open	F	F
SGT-700/Close	F	F

10 Analysis of the performance at part load

Today SIT controls the VGVs as a function of aerodynamic shaft-speed, without considering the reason for reaching a specific aerodynamic shaft-speed. This is beneficial since it minimizes the number of input parameters to the control algorithm thus limiting the need of computational time and number of measurement probes. It would therefore be beneficial if a new control algorithm based on the results from chapter 8 can be used without having to increase the number of input parameters.

To test this, the proposed settings for the VGV-positions for SGT-750 at full load have been tested for other ambient temperatures and part load. The load has been chosen to give the same aerodynamic shaft-speed thus giving the ability to test if the proposed VGV-position still improves the performance independent of load and ambient temperature. This would imply that a new control algorithm based on the proposed VGV-position can still operate with only the aerodynamic shaft-speed as input parameter.

This analysis is only performed for SGT-750 since the earlier results showed that SGT-700 seem to be running at optimum VGV-settings. GTPerform and Merlin have been used to perform this analysis. The compressor pressure profile is assumed constant as the load varies, i.e. the pressure profile is assumed to match earlier results for the same VGV-position. The input parameters for the compressor are taken from earlier calculations involving HT0300 and GTPerform.

The first step is to find the correct load that gives the same aerodynamic shaft-speed at the new ambient temperature. The shaft power is then locked while Merlin and GTPerform are used in an iterative process to evaluate the new SAS flow and the impact on the turbines. The results are then compared to the performance at that shaft power if today's existing control algorithm at that ambient temperature is used. The results from the comparison are then compared to the improvement found in chapter 8. If these match it implies that the proposed control algorithm gives the same improvement at a specific aerodynamic shaft-speed independent of the load and ambient temperature.

This chapter is divided into three sections. The first two sections contain the results for the two tested aerodynamic shaft-speeds and the third section contains a summary and a comparison of the results from the two earlier sections. The two tested aerodynamic shaft-speeds are 99.2% of aerodynamic shaft-speed at design point, from the proposed VGV-position at 30°C, and 97.7%, from the proposed VGV-position at 45°C.

10.1 99.2% of aerodynamic shaft-speed at design point

According to the results in chapter 8 the full load performance of SGT-750 would increase at 30°C if the VGV-position was opened 2.5° relative today's existing position. The new operational point would then correspond to an aerodynamic shaft-speed of 99.2% of design speed. To see if the increase in performance is independent of load two part loads that correspond to the same aerodynamic shaft-speed but different inlet temperatures are tested.

The results are compared to the performance for the existing VGV-position at the same shaft power and ambient temperature. In Fig. 10-1 the results from the two part load tests are presented together with the performance for full load from chapter 8. The results are presented as nominal differences from the existing VGV-position. Since the shaft power is locked for the part load cases the nominal difference is zero.

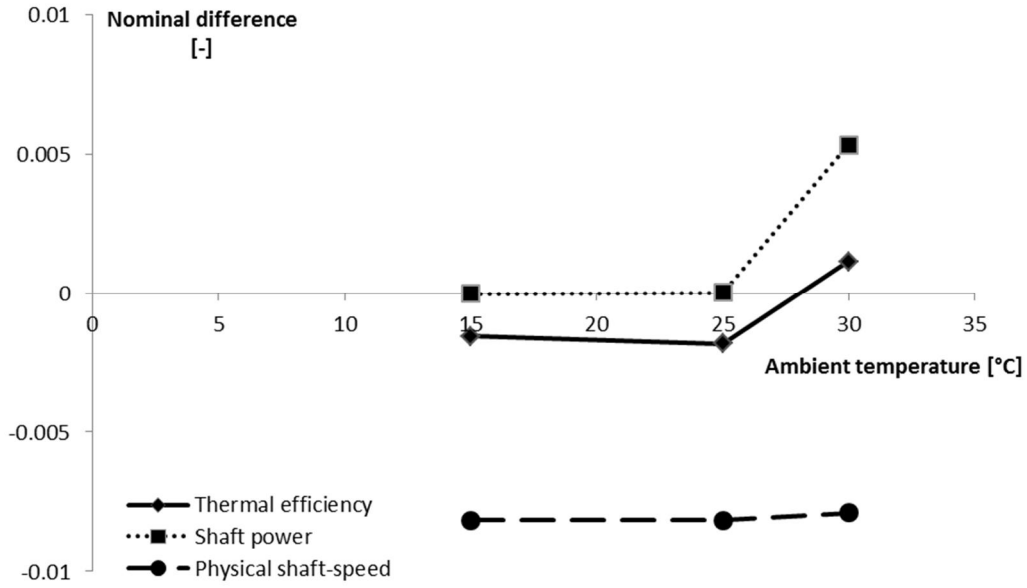

Fig. 10-1 Nominal difference in thermal efficiency, shaft power and physical shaft-speed as a function of ambient temperature for two part loads and the full load case at 99.2% of design speed

Fig. 10-1 shows that the increase in thermal efficiency seen in chapter 8, see Table 8-9 on p.63, has been replaced by a decrease. The result implies that the thermal efficiency is nearly constant for part load and increases at full load. The physical shaft-speed is reduced slightly more at part load than at full load implying that the centrifugal stresses will decrease even further.

At full load the increased compressor efficiency gives the opportunity to acquire a higher temperature rise in the combustion chamber. This is not possible when the shaft power is kept at a constant value. At part load the SAS flow as percentage of total flow increases which decreases the CT and PT efficiencies.

10.2 97.7% of aerodynamic shaft-speed at design point

According to the results in chapter 8 the full load performance of SGT-750 would increase at 45°C if the VGV-position was opened 4° relative today's existing position. The new operational point would then correspond to an aerodynamic shaft-speed of 97.7% of design speed. This aerodynamic shaft-speed also corresponds to running the engine at the three part loads.

The results are compared to the performance for the existing VGV-position at the same shaft power and ambient temperature. In Fig. 10-2 the result from the three part load tests are presented together with the performance for full load from chapter 8. The results are presented as nominal differences from the existing VGV-position. Since the shaft power is locked for the part loads the nominal difference is zero.

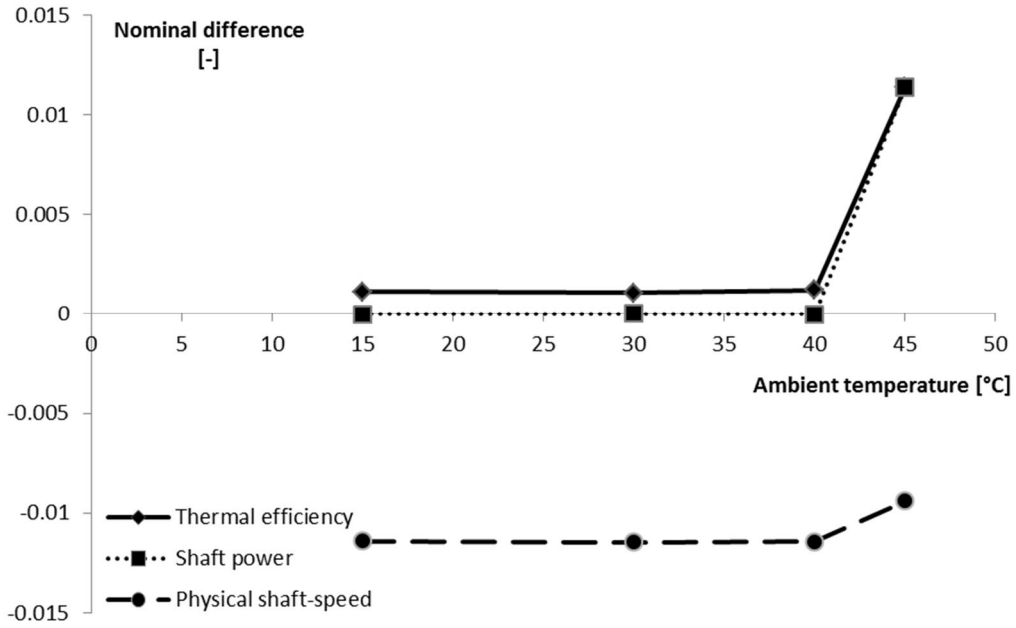

Fig. 10-2 Nominal difference in thermal efficiency, shaft power and physical shaft-speed as a function of ambient temperature for three part loads and the full load case at 97.7% of design speed

Fig. 10-2 shows that the improvement seen in chapter 8, see Table 8-12 on p.64, has been reduced. The thermal efficiency still increases for the part load cases if the VGV-position is more opened but the increase is less than in chapter 8. The result implies that the thermal efficiency is constant for part load and increases at full load. The physical shaft-speed is reduced slightly more at part load than at full load implying that the centrifugal stresses will decrease even further.

At full load the increased compressor efficiency gives the opportunity to acquire a higher temperature rise in the combustion chamber. This is not possible when the shaft power is kept at a constant value. At part load the SAS flow as percentage of total flow increases which decreases the CT and PT efficiencies.

10.3 Summary

The aim of this chapter was to evaluate if the control algorithm proposed in chapter 8 could be used with aerodynamic shaft-speed as the only input. The analyses were performed for both the VGV-position proposed to be used at 30°C and the VGV-position proposed to be used at 45°C for SGT-750. The proposed VGV-positions were in this chapter tested for the same aerodynamic

shaft-speed but at part load and different ambient temperatures to evaluate if the performance was still improved.

The result shows that at 99.2% of design speed the increase in performance gained in chapter 8 is now lost. At part load the new VGV-position instead gives a reduced performance. At 97.7% of design speed the results shows that the performance still increases but compared to the result in chapter 8 the increase is less. At part load the mass flow of cooling air is larger at all extraction leading to increased cooling and inducing losses. Thus the performance for both tested aerodynamic shaft-speeds is reduced. At full load the increased compressor efficiency gives the opportunity to acquire a larger temperature rise in the combustion chamber which increases the thermal efficiency.

The analysis in this chapter implies that the proposed control algorithm in chapter 8 is not only dependent on aerodynamic shaft-speed. The control algorithm could still be used with only the aerodynamic shaft-speed as input but then the gained performance at full load will be lost. Further discussion concerning which control algorithms that can be used could be found in Appendix B.

The results also imply that the enhanced performance seen in chapter 8 is mainly due to the possibility to require a larger temperature rise in the combustion chamber. As the compressor efficiency is increased the temperature into the combustion chamber will decrease. With a fixed TIT this gives the opportunity to increase the temperature rise in the combustion chamber.

As this is not possible at part load where the shaft power is kept at a constant level this phenomena will not occur. At part load it is only the behavior of the individual components that affects the cycle performance. The results show that the gain in performance at part load is much lower than the gain at full load. This implies that the pure effects from the components are only a minor part of the total increase.

11 Analysis of effects from separate controlling of IGV and first stator

In previous studies the IGV and S1 have been assumed to follow the existing gear ratio for the gas turbines. In this chapter the IGV and S1 will be moved separately to investigate which gear ratio that is the most suitable. The study will be performed for SGT-700 at 30°C since SGT-700 showed no improvement in performance in the previous studies. The IGV will be kept at the previous investigated angles -2.5, 0, 2.5 and 5° compared to today's existing position. Meanwhile S1 will be adjusted to different angles at each IGV-position to evaluate performance and influence on the SAS.

From chapter 6 it was clear that the changes in SAS flow led to a reduction in performance as the VGV-positions were more opened. It is therefore interesting not only to vary S1 to try to counterweight these effects but also to test a closing of the VGVs to see how the SAS flow affects the performance.

This chapter is divided into three sections. In the first section the effects on the compressor as the VGV-positions are varied are evaluated. In the second section the effects on the SAS and thus the effects on the CT due to changed SAS flow are evaluated. Each section is further divided into four subsections, one for each tested IGV-angle. The last section is a summary where the results are compared and summarized.

11.1 Evaluation of effects from different angles

The results in this section are first shown as absolute values and then compared to the values for today's existing position, here marked as IGV-angle 0° and S1-angle 0°. The S1-angle is marked as 0° if it adjusted according to today's existing gear ratio thus the S1-angle can be noted as 0° more than once in each table even though these angles are not the same. The S1-angle is adjusted as long as the performance increases in comparison with performance for the existing S1-angle at that IGV-angle.

11.1.1 IGV-angle -2.5°

In Table 11-1 the result for when the IGV-angle is closed 2.5° compared to today's existing position is presented. Here the S1-angle has been adjusted to five different positions.

Table 11-1 Gas turbine performance for today's existing position and for different S1-angles when the IGV-angle is altered -2.5°

Parameters	Nominal values				
IGV-angle rel. today's existing angle [°]	-2.5	-2.5	-2.5	-2.5	-2.5
S1-angle rel. today's existing S1-angle [°]	-1.89	-1.26	-0.63	0	0.63
Shaft power	1.006	1.006	1.005	1.004	1.004
GT shaft thermal eff.	1.002	1.002	1.002	1.001	1.001
Comp. isentr. eff.	1.003	1.003	1.003	1.002	1.002
CT isentr. eff.	0.999	0.999	0.999	0.999	0.999
PT isentr. eff.	1.000	1.000	1.000	1.000	1.000
Pressure ratio	1.003	1.003	1.002	1.002	1.002
Corr. mass flow	1.003	1.004	1.003	1.002	1.002
Physical shaft-speed	0.986	0.987	0.988	0.990	0.990
Aerodyn. shaft-speed	0.986	0.987	0.988	0.990	0.990

Table 11-1 shows that all tested S1- angles give an increase in shaft power and thermal efficiency when the IGV-angle is opened 2.5° compared to the performance for today's existing positions. The highest performance is gained when the S1-angle is opened 1.89 and 1.26°. The increase is small however, for all tested S1-angles.

11.1.2 IGV-angle 0°

In Table 11-2 the results for when the IGV-angle is adjusted 0° compared to today's existing position are presented. Here the S1-angle has been adjusted to three different positions.

Table 11-2 Gas turbine performance for today's existing position and for different S1-angles when the IGV-angle is altered 0°

Parameters	Nominal values		
IGV-angle rel. today's existing angle [°]	0	0	0
S1-angle rel. today's existing S1-angle [°]	-0.63	0.62	1.25
Shaft power	1.000	1.000	0.998
GT shaft thermal eff.	1.000	1.000	0.999
Comp. isentr. eff.	1.000	1.000	0.999
CT isentr. eff.	1.000	1.000	1.000
PT isentr. eff.	1.000	1.000	1.000
Pressure ratio	1.000	1.000	0.999
Corr. mass flow	1.000	1.000	0.999
Physical shaft-speed	0.998	1.002	1.003
Aerodyn. shaft-speed	0.998	1.002	1.003

Table 11-2 shows that the performance is almost constant for when the S1-angle is altered -0.63° and 0.62° compared to the performance for today's existing positions. The small differences that can be observed are within the error margin. When the S1-angle is altered 1.25° a small decrease can be observed.

11.1.3 IGV-angle 2.5°

In Table 11-3 the results for when the IGV-angle is closed 2.5° compared to today's existing position are presented. Here the S1-angle has been adjusted to six different positions.

Table 11-3 Gas turbine performance for today's existing position and for different S1-angles when the IGV-angle is altered 2.5°

Parameters	Nominal values					
IGV-angle rel. today's existing angle [°]	2.5	2.5	2.5	2.5	2.5	2.5
S1-angle rel. today's existing S1-angle [°]	-2.51	-1.88	-1.25	-0.62	0	0.63
Shaft power	0.992	0.993	0.992	0.991	0.989	0.989
GT shaft thermal eff.	0.997	0.998	0.997	0.997	0.996	0.996
Comp. isentr. eff.	0.997	0.997	0.997	0.996	0.996	0.995
CT isentr. eff.	1.000	1.001	1.001	1.001	1.001	1.001
PT isentr. eff.	1.000	1.000	1.000	1.000	1.000	1.000
Pressure ratio	0.995	0.996	0.995	0.995	0.994	0.993
Corr. mass flow	0.995	0.996	0.995	0.995	0.994	0.993
Physical shaft-speed	1.005	1.006	1.008	1.009	1.011	1.013
Aerodyn. shaft-speed	1.005	1.006	1.008	1.009	1.011	1.013

Table 11-3 shows that all tested S1- angles give a decrease in shaft power and thermal efficiency when the IGV-angle is closed 2.5° compared to the performance for today's existing positions.

11.1.4 IGV-angle 5°

In Table 11-4 and Table 11-5 the results for when the IGV-angle is closed 5° compared to today's existing position are presented. Here the S1-angle has been adjusted to ten different positions. The results are divided into two tables to make the results more lucid.

Table 11-4 Gas turbine performance for today's existing position and for different S1-angles when the IGV-angle is altered 5°

Parameters	Nominal values				
IGV-angle rel. today's existing angle [°]	5	5	5	5	5
S1-angle rel. today's existing S1-angle [°]	-5.06	-4.43	-3.8	-3.17	-2.51
Shaft power	0.983	0.984	0.982	0.981	0.980
GT shaft thermal eff.	0.994	0.994	0.993	0.993	0.993
Comp. isentr. eff.	0.994	0.994	0.993	0.993	0.992
CT isentr. eff.	1.001	1.001	1.001	1.001	1.002
PT isentr. eff.	1.000	1.000	1.000	1.000	1.000
Pressure ratio	0.990	0.990	0.989	0.989	0.988
Corr. mass flow	0.990	0.990	0.989	0.988	0.988
Physical shaft-speed	1.011	1.013	1.013	1.014	1.017
Aerodyn. shaft-speed	1.011	1.013	1.013	1.014	1.017

Table 11-5 Gas turbine performance for today's existing position and for different S1-angles when the IGV-angle is altered 5°

Parameters	Nominal values				
IGV-angle rel. today's existing angle [°]	5	5	5	5	5
S1-angle rel. today's existing S1-angle [°]	-1.88	-1.25	-0.63	0.00	0.63
Shaft power	0.980	0.978	0.978	0.976	0.974
GT shaft thermal eff.	0.993	0.992	0.992	0.991	0.991
Comp. isentr. eff.	0.992	0.991	0.991	0.991	0.990
CT isentr. eff.	1.002	1.002	1.002	1.002	1.002
PT isentr. eff.	1.000	0.999	0.999	0.999	0.999
Pressure ratio	0.988	0.987	0.987	0.986	0.985
Corr. mass flow	0.988	0.987	0.987	0.986	0.985
Physical shaft-speed	1.017	1.019	1.020	1.022	1.024
Aerodyn. shaft-speed	1.017	1.019	1.020	1.022	1.024

Table 11-4 and Table 11-5 show that all tested S1- angles reduce the performance when the IGV-angle is opened 5° compared to the performance for today's existing positions.

11.2 Evaluation of effects from the secondary air system

When the VGV-position is altered the pressure ratio over the compressor will change, as mentioned in chapter 8 on p. 58. This will affect the SAS and must therefore be further investigated. In this study GTPerform and Merlin are used in an iterative process as in chapter 8.

Here the most promising opened and closed S1-angle for each tested IGV-angle will be further investigated. For an IGV angle of 2.5 and 5° the cases with S1 controlled according to today's existing gear ratio will also be further investigated since these angles were not investigated in chapter 8.

The compressor pressure profile has been assumed to be constant as in chapter 8, this time for each combination of IGV- and S1- angle. The calculation model made for the study in chapter 8 is used in this chapter as well.

11.2.1 IGV-angle -2.5°

In Table 11-6 the mass flows from the extractions in the compressor are shown for the two tested S1-angles when the IGV-angle is opened 2.5° compared to today's existing position. The results show that the SAS mass flow at all extractions increases when the IGV-angle is altered -2.5° for all tested S1-angles.

Table 11-6 SAS mass flow from different compressor stages for different S1-angles when the IGV-angle is altered -2.5°

Parameters	Nominal values	
IGV angle rel. today's existing angle [°]	-2.5	-2.5
S1-angle rel. today's existing S1-angle [°]	-1.26	0.63
Mass flow at stage 2	1.030	1.031
Mass flow at stage 6	1.037	1.036
Mass flow at stage 11	1.002	1.000

The ratio between the SAS flow and the total flow is almost constant for the different VGV-positions. When the VGV-position is more open the total flow is increased. This will counteract the increased SAS flow resulting in almost constant ratios. Thus the cooling of the components is not endangered.

In Table 11-7 the performance results from the previous section have been updated to include effects from changes in SAS. If the parameters in Table 11-7 are compared to the parameters in Table 11-1 on p. 77, where the calculations are without consideration to the effects from SAS, it could be seen that the thermal efficiency decreases for all tested S1-angles due to the increase in SAS flow. The shaft power decrease for S1-angle 0.63° but a small improvement was found for S1-angle -1.26°.

Table 11-7 Gas turbine performance, after considering the effects from changes in the SAS, for today's existing position and different S1-angles when the IGV-angle is altered -2.5°

Parameters	Nominal values	
IGV angle rel. today's existing angle [°]	-2.5	-2.5
S1-angle rel. today's existing S1-angle [°]	-1.26	0.63
Shaft power	1.001	0.999
GT shaft thermal eff.	1.000	0.999
Compressor isentr. eff.	1.004	1.002
CT isentr. eff.	0.997	0.998
PT isentr. eff.	1.000	1.000
Pressure ratio	0.999	0.999
Corr. mass flow	1.001	1.000
Physical shaft-speed	0.986	0.990
Aerodyn. shaft-speed	0.986	0.990

11.2.2 IGV-angle 0°

In Table 11-8 the SAS mass flows from the extractions are shown for the two tested S1-angles when the IGV-angle is altered 0° compared to today's existing position.

Table 11-8 SAS mass flow from different compressor stages for different S1-angles when the IGV-angle is altered 0°

Parameters	Nominal values	
IGV angle rel. today's existing angle [°]	0	0
S1-angle rel. today's existing S1-angle [°]	-0.63	0.62
Mass flow at stage 2	1.010	1.000
Mass flow at stage 6	1.010	1.002
Mass flow at stage 11	0.998	1.000

The results in Table 11-8 show that the SAS mass flow is constant when the S1 angle is altered 0.62° and increases at stage 2 and 6 while it decreases at stage 11 when the S1-angle is altered -0.63°. The ratio between the SAS flow and the total flow is almost constant for the different VGV-positions thus the cooling of the components is not endangered.

In Table 11-9 the results from the previous section have been updated to include the effects from changes in SAS. If the parameters in Table 11-9 are compared to the parameters in Table 11-2 on p. 77, where the calculations are without consideration to the effects from SAS, no significant increases are detected for the shaft power and thermal efficiency for all tested S1-angles due to the increase in SAS flow.

Table 11-9 Gas turbine performance, after considering the effects from changes in the SAS, for today's existing position and different S1-angles when the IGV-angle is altered 0°

Parameters	Nominal values	
IGV angle rel. today's existing angle [°]	0	0
S1-angle rel. today's existing S1-angle [°]	-0.63	0.62
Shaft power	0.997	1.000
GT shaft thermal eff.	0.999	1.000
Compressor isentr. eff.	1.000	1.000
CT isentr. eff.	0.999	1.000
PT isentr. eff.	1.000	1.000
Pressure ratio	0.998	1.000
Corr. mass flow	0.998	1.000
Physical shaft-speed	0.998	1.002
Aerodyn. shaft-speed	0.998	1.002

11.2.3 IGV-angle 2.5°

In Table 11-10 the SAS mass flows from the extractions are shown for the three tested S1-angles when the IGV-angle is closed 2.5° compared to today's existing position. The results show that the mass flow decrease at all stages for all tested S1-angles.

Table 11-10 SAS mass flow from different compressor stages for different S1-angles when the IGV-angle is altered 2.5°

Parameters	Nominal values		
IGV angle rel. today's existing angle [°]	2.5	2.5	2.5
S1-angle rel. today's existing S1-angle [°]	-1.88	0	0.63
Mass flow at stage 2	0.980	0.980	0.971
Mass flow at stage 6	0.985	0.972	0.966
Mass flow at stage 11	0.997	0.995	0.994

The ratio between the SAS flow and the total flow is almost constant for the different VGV-positions. The total mass flow is reduced when the VGV-position is more closed. This will counteract the reduced SAS flow resulting in almost constant ratios. Thus the cooling of the components is not endangered.

In

Table 11-11 the results from the previous section have been updated to include the effects from changes in SAS. If the parameters

Table 11-11 are compared to the parameters in Table 11-3 on p. 78, where the calculations are without consideration to the effects from SAS, it could be seen that shaft power and thermal

efficiency are reduced for all tested angles. The CT efficiency increases for all tested S1-angles but the increase is too small to counterweight the reduction in compressor efficiency, pressure ratio and corrected mass flow.

Table 11-11 Gas turbine performance, after considering the effects from changes in the SAS, for today's existing position and different S1-angles when the IGV-angle is altered 2.5°

Parameters	Nominal values		
IGV angle rel. today's existing angle [°]	2.5	2.5	2.5
S1-angle rel. today's existing S1-angle [°]	-1.88	0	0.63
Shaft power	0.994	0.992	0.991
GT shaft thermal eff.	0.998	0.997	0.997
Compressor isentr. eff.	0.997	0.996	0.995
CT isentr. eff.	1.001	1.002	1.002
PT isentr. eff.	0.999	0.999	1.000
Pressure ratio	0.998	0.997	0.995
Corr. mass flow	0.997	0.996	0.994
Physical shaft-speed	1.007	1.011	1.013
Aerodyn. shaft-speed	1.007	1.011	1.013

11.2.4 IGV-angle 5°

In Table 11-12 the SAS mass flows from the extractions are shown for the three tested S1-angles when the IGV-angle is closed 5° compared to today's existing position. The results show that the mass flow decrease at all stages for all tested S1-angles.

Table 11-12 SAS mass flow from different compressor stages for different S1-angles when the IGV-angle is altered 5°

Parameters	Nominal values		
IGV angle rel. today's existing angle [°]	5	5	5
S1-angle rel. today's existing S1-angle [°]	-4.43	0	0.63
Mass flow at stage 2	0.971	0.940	0.940
Mass flow at stage 6	0.964	0.930	0.929
Mass flow at stage 11	0.992	0.988	0.987

The ratio between the SAS flow and the total flow is almost constant for the different VGV-positions. The total mass flow is reduced when the VGV-position is more closed. This will counteract the reduced SAS flow resulting in almost constant ratios. Thus the cooling of the components is not endangered.

In Table 11-13 the performance results from the previous section have been updated to include the effects from changes in SAS. If the parameters in Table 11-13 are compared to the parameters in Table 11-4 on p. 79 and Table 11-5 on p 79, where the calculations are without consideration to the effects from SAS, it could be seen that the shaft power and thermal efficiency are reduced for all tested angles. The CT efficiency increases for all tested S1-angles but the increase is too small to counterweight the reduction in compressor efficiency, pressure ratio and corrected mass flow.

Table 11-13 Gas turbine performance, after considering the effects from changes in the SAS, for today's existing position and different S1-angles when the IGV-angle is altered 5°

Parameters	Nominal values		
IGV angle rel. today's existing angle [°]	5	5	5
S1-angle rel. today's existing S1-angle [°]	-4.43	0	0.63
Shaft power	0.987	0.982	0.979
GT shaft thermal eff.	0.995	0.993	0.992
Compressor isentr. eff.	0.994	0.990	0.990
CT isentr. eff.	1.002	1.003	1.004
PT isentr. eff.	0.999	0.999	0.999
Pressure ratio	0.993	0.991	0.990
Corr. mass flow	0.992	0.989	0.988
Physical shaft-speed	1.013	1.023	1.025
Aerodyn. shaft-speed	1.013	1.023	1.025

11.3 Summary

The aim of this chapter was to evaluate if another gear ratio between the IGV and first stator could increase the performance for SGT-700 at 30°C. First a study was made through an iterative process between GTPerform and HT0300 to predict the potential of different gear ratios. Secondly an additionally study was made through an iterative process between GTPerform and Merlin to include the effects from SAS. To simplify the time consuming process the compressor pressure profile was assumed to be fixed for a set IGV-angle thus excluding HT0300 from the iterative process.

The result from the first study show that when the IGV-angle was set to -2.5° compared to today's existing position, all S1-angles gave an increased performance. For all other tested combination of IGV- and S1-angles the shaft power and thermal efficiency was constant or decreased.

The most promising combinations of IGV- and S1-angles from the first study were further investigated in the next study. Here the effects from the altered pressure ratio in the compressor and thereby the SAS was taken under consideration. For the case where the IGV was adjusted to

a more opened position the effects from the SAS decreased the CT efficiency whereas for the case with a more closed position the effects from the SAS increased the CT efficiency. Even though the CT efficiency increased the efficiency, pressure ratio and corrected mass flow for the compressor decreased thereby reducing the thermal efficiency.

To control the IGV and stator 1 individually would demand separate actuators which could be implemented but at a higher cost. A great increase in performance would have to be obtained to motivate this change. From the studies in this chapter no tested combination of IGV- and S1-angle indicates that this is possible. Therefore a new way to control the VGVs for SGT-700 will no longer be investigated.

12 Conclusions

The overall objective of this thesis was to investigate how an altered VGV-position would affect performance and lifespan at high ambient temperatures. The study showed no possible improvements for SGT-700 while a more opened VGV-position showed both enhanced performance and reduced physical shaft-speed for SGT-750.

For SGT-700 at 30°C an analysis of how separated controlling of IGV and S1 affected the performance was also made. The study showed a very small possible improvement for an IGV settings at -2.5° and S1 setting at 0°. The increase was too small however, to counterweigh for the increased cost with separate actuators. SGT-700 seems to be running on the best possible VGV-setting.

The most promising case for SGT-750 at full load and 30°C was an opening of the IGVs of 2.5° relative today's existing position. This resulted in an increase in shaft power of nearly 0.5% and an increase in thermal efficiency of 0.1% while reducing physical shaft-speed by 0.8%. The most promising case at 45°C was an opening of the IGVs of 4° relative today's existing position. This resulted in an increase in shaft power of 2.9% and an increase in thermal efficiency of 1.1% while reducing physical shaft-speed by nearly 0.9%. Based on our studies we recommend further studies or tests in test-rig to confirm and possibly apply these new VGV-positions at full load.

A numerical surge margin evaluation was made but to truly assure the surge margin tests in test-rig needs to be performed. If the VGVs are set at an more opened position it will be the first stage that has the highest increase in pressure ratio thus having the largest risk of running into surge.

The VGV-position was also tested at part load to see if the new control algorithm can be used with the aerodynamic shaft-speed as the only input. These tests showed that the potential improvement decreased compared to the cases at full load. At low aerodynamic shaft-speed an opening resulted in enhanced performance compared to using today's VGV-position while at a higher aerodynamic shaft-speed today's VGV-position is more beneficial.

To benefit from the gained performance with a more opened VGV-position at full load it could be interesting to investigate the possibility to use a more complex control algorithm with more input parameters. Based on the results in this master thesis three different ways to control the VGVs have been created. These suggestions can work as a foundation to start off the work with an improved control algorithm for SGT-750. The three suggestions are presented in Appendix B.

During our studies many iterative loops have been used and several programs have been matched using simple correlations. This is a source of error since the simple correlations cannot describe the behaviour of the programs to full extent. The iteration loops have all introduced small errors since the solution is assumed converged before the results are identical. The differences are considered negligible but may in the end add up to an error too large to be neglected.

GTPerform and Merlin gave slightly different results when calculating the turbine efficiencies. The absolute values differed and the difference in PT efficiency varied with ambient temperature at part load. As the ambient temperature changed Merlin often calculated a bigger loss in PT efficiency than GTPerform. This is coupled to the incidence losses discussed in section 2.3 on p.8 and is further discussed in Appendix C. The result is less accurate results from GTPerform. The difference is minor for all normal purposes but in a study like this it contributes to the uncertainty.

The programs used for these analyses are all intended to model the gas turbine in reality. Normally within SIT these programs are not operated as one unit but rather as individual design tools. None of the programs we used calculate in 3D. Therefore some complex effects may have been left out but the programs used were assumed to give reliable results with enough accuracy for this thesis. The errors introduced by using more basic programs and not fully knowing how to integrate the programs together are hard to estimate and that is why we strongly recommend that our results are confirmed by rig tests.

13 Future developments at Siemens Industrial Turbomachinery AB

This chapter aims to discuss possibilities for SIT to further investigate areas that we found interesting but did not fit under the purpose of this thesis. The problems have been encountered during our work but left unsolved.

In chapter 11 the proposed VGV-position was tested at part load to see if the new control algorithm can be used with the aerodynamic shaft-speed as the only input. These tests showed that the potential improvement decreased compared to full load. At low aerodynamic shaft-speed an opening resulted in enhanced performance compared to using today's VGV-position while at a higher aerodynamic shaft-speed today's VGV-position is more beneficial. In this thesis only two aerodynamic shaft-speeds have been tested for one VGV-position each. We recommend that the subject is further investigated to find the optimum VGV-position at part load for several aerodynamic shaft-speeds to use in an improved control algorithm.

It would be interesting to investigate if the control algorithm can be built with more than one input parameter. This would give the opportunity to control the VGV-position according to today's control algorithm until the gas turbine is close to full load where the VGV can be adjusted to a more opened position. Three suggestions on foundations to build an improved control algorithm around are presented in Appendix B. We recommend that time and resources are devoted to develop this new control algorithm.

During the work with this thesis a lot of iterations have been made between different programs. One tool that would have been useful is a correlation between the programs since there is an offset between the results. When HT0300 was matched with GTPerform the difference in results from the two programs varied with ambient temperature, relative humidity and type of engine. Other parameters affecting the difference might exist but has not been encountered during this thesis. We recommend that time and resources are devoted to find a suitable correlation to interpret and compare the results from different programs.

14 Bibliography

Axelsson, S., 2014. [Interview] (12 03 2014).

Brun, K. & Kurz, R., 2000. *Introduction to Gas Turbine Theory.* 2nd ed. San Diego: Solar Turbines.

Flydalen, K., 2011. *Iteration Interface Merlin RT_GRCTA_020_11,* Finspång: Siemens Industrial Turbomachinery (Proprietary).

Gustafsson, J., 2014. [Interview] (25 02 2014).

Kling, J., 2014. [Interview] (24 02 2014).

Moustapha, H., Zelesky, M. F., Baines, N. C. & Japikse, D., 2003. *Axial and Radial Turbines.* Vermont: Concepts NREC.

Rabal Carerra, S., 2014. [Interview] (12 03 2014).

Razak, A., 2007. *Industrial gas turbines.* Cambridge: Woodhead Publishing Limited.

Saravanamuttoo, H. I. H., Rogers, G. F. C., Cohen, H. & Straznicky, P. V., 2009. *Gas Turbine Theory.* 6th ed. Essex: Pearson Education Limited.

Siemens AG, 2009a. *SGT-700 Gas Turbine for Mechanical Drive.* [Online]
Available at: http://www.energy.siemens.com/hq/pool/hq/power-generation/gas-turbines/SGT-700/Brochure_Siemens_Gas-Turbine_SGT-700_MD.pdf
[Accessed 28 01 2014].

Siemens AG, 2009b. *SGT-700 Gas Turbine for Power Generation.* [Online]
Available at: http://www.energy.siemens.com/hq/pool/hq/power-generation/gas-turbines/SGT-700/E50001-W430-A104-X-4A00_SGT-700_GB_LR.pdf
[Accessed 28 01 2014].

Siemens AG, 2010. *SGT-750 Siemens Gas Turbine.* [Online]
Available at: http://www.energy.siemens.com/hq/pool/hq/power-generation/gas-turbines/sgt-750/SGT-750_brochure.pdf
[Accessed 28 01 2014].

Siemens AG, 2013. *Siemens Gas Turbines.* [Online]
Available at: http://www.energy.siemens.com/hq/en/fossil-power-generation/gas-turbines/#content=Output%20Overview
[Accessed 15 01 2014].

Siemens AG, 2014. *Gas Turbine SGT-750.* [Online]
Available at: http://www.energy.siemens.com/hq/en/fossil-power-generation/gas-turbines/sgt-

750.htm
[Accessed 12 02 2014].

Siemens Industrial Turbomachinery AB, 2009. *SIT Homepage.* [Online]
Available at: http://www.sit-ab.se/
[Accessed 15 01 2014].

Siemens Industrial Turbomachinery AB, 2013. *En historia om drivkraft.* [Online]
Available at: http://sit-ab.leon.se/
[Accessed 15 01 2014].

Sjödin, M., 2013. *SIT Performance Model Definition RT RP 01/13 Edition B*, Finspång: Siemens Industrial Turbomachinery (Proprietary).

Sjödin, M., 2014. [Interview] (29 01 2014).

Tageman, K., 2014. [Interview] (27 01 2014).

Walsh, P. P. & Fletcher, P., 2004. *Gas Turbine Performance.* 2nd ed. Oxford: Blackwell Science Ltd.

Appendix A Evaluation of surge margin during operation

The surge margin is one of the hardest parameters to measure and evaluate since the surge line is so hard to estimate. Since experimental tests are expensive and rarely done for full load and full-sized engines the surge margin for each individual engine is hard to evaluate.

Today the surge margin during operation is evaluated by measuring the fuel mass flow into the combustion chamber. The energy sent into the combustion chamber is then used to evaluate the pressure ratio to assure surge margin. One problem with this method is that it is indirect and it can be influenced by other parameters such as the heating value of the fuel. The surge margin is therefore often bigger than needed.

A direct measurement of the pressure ratio would be much better but until recently the measurement devices has been too slow. The risk of having slow measurements is that once the risk of surge is detected it is too late to save the engine from running into surge. At SIT surge is considered to be very dangerous thus this risk is not acceptable.

New calculations indicates that there are new devices on the market that are capable of measuring the pressure ratio fast enough to guarantee that the control system will have time to prevent the engine from running into surge. Using this new devices and measuring the pressure ratio directly would remove a level of uncertainty that is otherwise introduced as the fuel mass flow is converted into pressure ratio.

Being more certain of the instant pressure ratio of the engine gives the opportunity to lower the surge margin. As showed in this study the performance of the engine can sometimes be improved by running closer to surge. Having a direct way of measuring the pressure ratio thus having the ability to lower the surge margin would therefore be beneficial.

Appendix B Suggestions for improved controlling of the VGVs

Today the VGVs are controlled as a function of aerodynamic shaft-speed. The results in this master thesis show that there is potential of increased performance if the controlling algorithm is modified to a more opened VGV-position at high ambient temperatures, primary at full load. In this appendix three different ways of controlling is presented. The actual VGV-position for every position in the matrixes is not presented but rather the trends and the parameters that can be used for controlling.

B - 1 Alternative 1

Table B - 1 shows a schematic view of a control algorithm that could be used to enhance performance at high ambient temperatures. Here the aerodynamic shaft-speed and the compressor intake temperature (T_{1200}) form two matrixes. The left matrix represent today's way of controlling the VGV-position while the right matrix represent a new VGV-position. At high ambient temperatures we suggest that b is a more opened VGV-position than a. The right hand matrix is primary used at high TIT, i.e. full load.

Since the biggest increase in performance was reached at full load the TIT will be used to evaluate when to use which matrix. To get a smooth transition between the two matrixes a coefficient based on TIT (k) can be used. If the TIT equals $TIT_{Base\ load}$, k would equal 1 and at $TIT << TIT_{Base\ load,}$ k would equal 0. The VGVs would then be controlled according to Equ. (B - 1), where a_{ij} is the VGV-position gathered from the left matrix in Table B - 1 and b is the VGV-position gathered from the right matrix.

$$VGV = a_{ij} * (1 - k) + b_{ij} * k \qquad (B - 1)$$

This way of controlling would require two separate matrixes and the coefficient k would have to be carefully estimated to get the best performance at all loads without getting an unstable system. The benefit with this system is that the coefficient k ensures that the engine is running close to full load before adjusting the VGVs, i.e. no other phenomena can trick the system into opening up the VGVs as the engine is running at part load.

Table B - 1 VGV matrixes with aerodynamic shaft-speed and compressor intake temperature as input. a is the VGV-position used today and b is a new VGV-position

Aerodyn. shaft-speed / T_{1200}	-60	0	20	30	45
2000	A	a	a	a	a
-	A	a	a	a	a
-	A	a	a	a	a
-	a	a	a	a	a
-	a	a	a	a	a
10000	a	a	a	a	a

Aerodyn. shaft -speed / T_{1200}	-60	0	20	30	45
2000	b	b	b	b	b
-	b	b	b	b	b
-	b	b	b	b	b
-	b	b	b	b	b
-	b	b	b	b	b
10000	b	b	b	b	b

B - 2 Alternative 2

Under the assumption that an engine running at full load and low aerodynamic shaft-speed will only do so at a high ambient temperature, i.e. no other phenomena such as fouling or dysfunctional VGVs will cause this behavior, the two matrixes in alternative 1 can be reduced into one matrix as shown in Table B - 2. Here the aerodynamic shaft-speed and the difference between TIT and $TIT_{Base\ load}$ are used to find the right VGV-position. As the TIT gets close to $TIT_{Base\ load}$ and the aerodynamic shaft-speed gets lower the VGVs are set at a more opened position. Here a is the VGV-position used at part load and x is the change in VGV-position at high ambient temperatures. This is a much simpler solution than alternative 1 since only one matrix is used and no correlation is needed to calculate the VGV-position.

Table B - 2 VGV matrix with aerodynamic shaft-speed and ΔTIT as input. a is the VGV-position used at part load and x is the change in VGV-position at high ambient temperatures

Aerodyn. shaft-speed / ΔTIT	-500	-25	-5	0	5
2000	a	a	a	a	a
-	a	a	a	a	a
-	a	a	a	a	a
-	a	a	a	a	a
-	a	a	a	a	a
-	a	a	a	a	a
-	a	a	a	a	a
-	a	a-x	a-x	a-x	a
-	a	a	a-x	a-x	a
10000	a	a	a	a-x	a

B - 3 Alternative 3

Both alternative 1 and 2 focuses on the improvement at full load and aims at using existing VGV-position at part load. Alternative 3 presents a more straightforward solution. According to the results from chapter 10 there are no significant losses in performance at part load when the VGVs are set at a more opened position as long as the ambient temperature is within certain values. This implies that today's control algorithm can be used and just be modified to a more opened position for certain aerodynamic shaft-speeds. A schematic view of this is shown in Table B - 3.

Table B - 3 VGV table with aerodynamic shaft-speed as input. a is the VGV-position used at part load and x is the change in VGV-position at high ambient temperatures

Aerodyn. shaft-speed	VGV-position
2000	a
-	a
-	a
-	a
-	a
-	a
-	a
-	a-x
-	a-x
10000	a-x

The simplicity of this alternative is its biggest advantage. The disadvantage is that the simple solution may lead to that the engine runs at a more opened position at part load even though the performance does not benefit until the engine reaches full load.

Appendix C Evaluation of turbine efficiency in different programs

In this master thesis different programs have been used to evaluate the CT-efficiency. To get better understanding of the behavior of the different programs the CT-efficiency as a function of physical shaft-speed and ambient temperature has been evaluated using both GTPerform and Merlin. This way it is possible to evaluate how usage of the different programs affects the results.

Merlin generally predicts a higher CT-efficiency than GTPerform. In this chapter the results has been normalized to see the gradients rather than absolute values. The aim is not to prove that Merlin predicts higher CT-efficiency than GTPerform but rather to evaluate how the CT-efficiency varies in the different programs as the physical shaft-speed and ambient temperature varies.

Fig. C - 1 shows how the CT-efficiency varies as a function of ambient temperature using GTPerform and Merlin for the calculations at full load. The results show that the two programs estimate the variation in CT-efficiency almost similar. Here the results from Merlin are dependent on an iterative process using input data from GTPerform. The iterative process explains why the results from Merlin do not form such as smooth trend as the results from GTPerform. The results indicate that as long as the relative differences are used, the programs will estimate the CT-efficiency as a function of ambient temperature in a similar way.

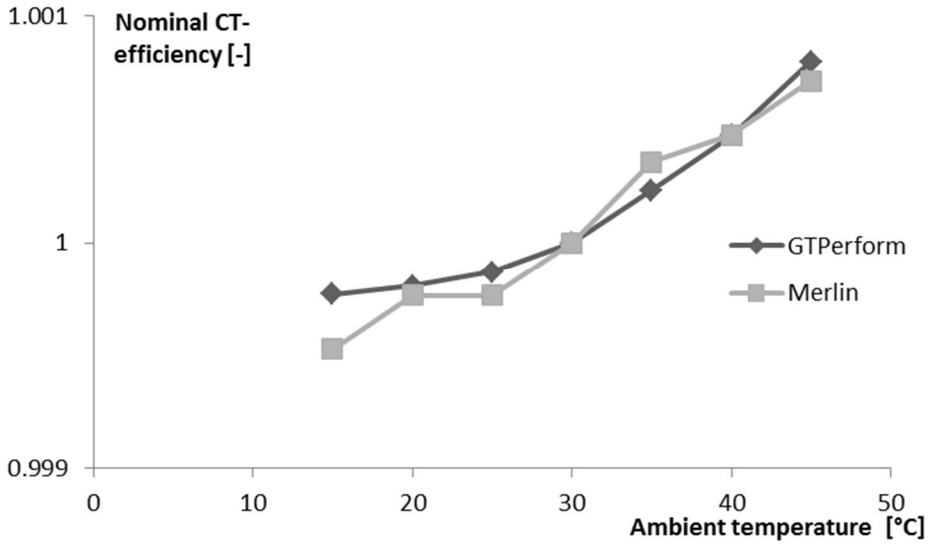

Fig. C - 1 Nominal CT-efficiency as a function of ambient temperature calculated in GTPerform and Merlin

At part load the difference between the programs is bigger. As the ambient temperature changes Merlin often calculates a bigger loss in PT efficiency than GTPerform. This is coupled to the incidence losses discussed in section 2.3 on p. 8. The lower ambient temperature results in lower

velocities for the same Mach numbers. Since the rotational speed is not equally lowered the flow angles in and out from the rotor will change thus changing the incidence which introduces losses. These effects are taken into account by Merlin since the flow angles and velocities of each stage are calculated. GTPerform on the other hand only do a mean line analysis using the characteristics to capture these effects. The existing PT characteristic does not seem to be able to fully capture these effects resulting in less accurate results from GTPerform.

Fig. C - 2 shows how the CT-efficiency varies as a function of physical shaft-speed using GTPerform and Merlin for the calculations. The result shows that the programs estimate the CT-efficiency almost similar as long as the shaft-speed is not altered too much. In our calculations the shaft-speed alteration is within this area which implies that as long relative differences are used the programs estimate the CT-efficiency in a similar way.

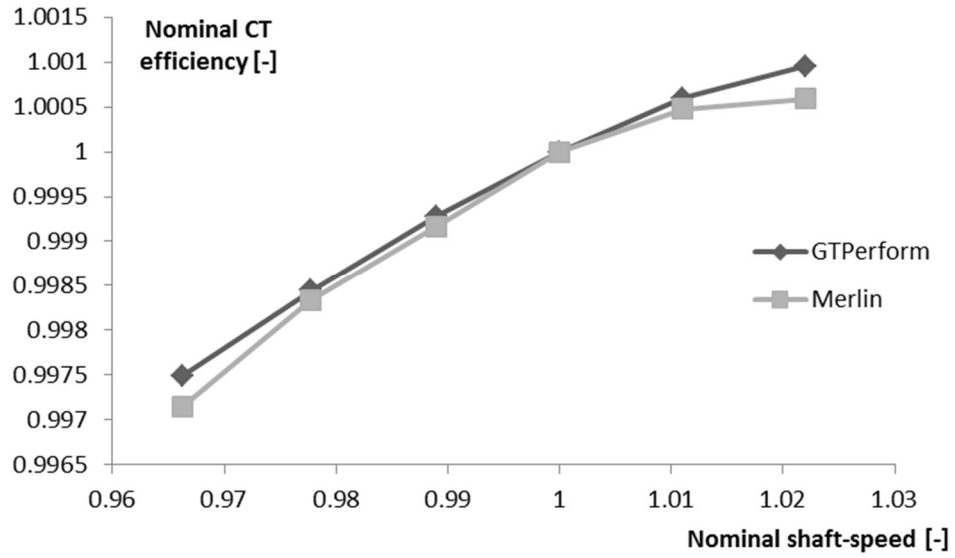

Fig. C - 2 Nominal CT-efficiency as a function of nominal shaft-speed calculated in GTPerform and Merlin

The results show that the programs estimate the CT efficiency almost similar for both variations in ambient temperature and physical shaft-speed at full load. The results indicate that as long as the relative differences are used, the programs will estimate the CT-efficiency in a similar way. At part load the programs evaluate PT-efficiency different because GTPerform is not able to fully estimate the losses due to changes in Mach number. This contradicts the theory in section 2.6 on p.13 where the ambient temperature is assumed to not affect the Mach numbers to such extent that it affects the results. The results imply that there is an effect at part load.